CHARACTERISTICS AND MINERALISATION OF PLATINUM-GROUP ELEMENTS (PGE) IN THE UPPER GROUP 2 CHROMITITE (UG2) AND MERENSKY REEFS AT THE BUFFELSHOEK FARM, TWO RIVERS PLATINUM MINE: IMPLICATIONS FOR PLATINUM-GROUP ELEMENTS RECOVERY

by

LESETJA CHARLES PHEEHA

[redacted]

DISSERTATION

Submitted in fulfilment of the requirements for the degree of

MASTERS OF SCIENCE

in

GEOLOGY

in the

FACULTY OF SCIENCE AND AGRICULTURE

(School of Physical and Mineral Sciences)

at the

UNIVERSITY OF LIMPOPO

SUPERVISOR: Prof. NQ Hammond

2022

I dedicate this dissertation to my late Granny

Mokgaetsi Caroline Legodi

Thank you for raising me and always understanding, supporting and encouraging my dreams

DECLARATION

I declare that "*CHARACTERISTICS AND MINERALISATION OF PLATINUM-GROUP ELEMENTS (PGE) IN THE UPPER GROUP 2 CHROMITITE (UG2) AND MERENSKY REEFS AT THE BUFFELSHOEK FARM, TWO RIVERS PLATINUM MINE: IMPLICATION FOR PLATINUM-GROUP ELEMENTS RECOVERY"* is my own work and that all the sources that I have used or quoted have been clearly indicated and acknowledged by means of complete references and that this work has not been submitted before for any other degree at any other institution.

LESETJA CHARLES PHEEHA **31 AUGUST 2021**

ACKOWLEDGEMENTS

I want to thank the following persons and organisations for their respective contributions to this dissertation:

- A special thank you to my supervisor, Prof. Napoleon Hammond, for going above and beyond in making sure that I do not only do what is required but I understand the mineralisation styles of my study area, his words of encouragements, guidance beyond the dissertation and support in all aspects of funding, research and writing.
- Two Rivers Platinum Mine's Management and the Geology Department, in particular Chief Geologist Mr. Jabu Khumalo and Senior Geologist Mr. Juan Coetzee for their support in relation to samples collections, ease to access mine facilities and providing requested internal data.
- The Geology and Mining Department of University of Limpopo, in particular Prof. John Dunlevey for his encouragements and acceptance into the master's program.
- The Faculty of Sciences and Agriculture Research Division of the University of Limpopo, the Geological Society of South Africa and North-West University's School of Geo- and Spatial Sciences for their support (funding) towards the success of the research.
- The Central Analytical Facility of the Faculty of Science of the University of Johannesburg for their continued support when requesting to use their analytical facilities, in particular the Instruments Scientists Dr Christian Reinke (Electron Microprobe Analyser) for assisting with procedures to use the electron microprobe and Dr Bradley Guy (Mineral Liberation Analyser) for analysing some of the samples.

ABSTRACT

The Two Rivers Platinum Mine (TRP) located in the Eastern Bushveld Igneous Complex is currently exploiting platinum-group elements (PGE) in the Upper Group 2 chromitite (UG2) Reef at the Dwarsrivier Farm. TRP has acquired a new prospect (at the Buffelshoek Farm) and is currently planning to mine the UG2 Reef and potentially also the Merensky Reef (MR). Three drill-cores which intersected the UG2 Reef and MR at the Buffelshoek Farm made available by TRP were sampled for mineralogical studies using complementary techniques including reflected light microscopy, mineral liberation analyser and electron microprobe. The platinum group minerals (PGM) which host the PGE exhibit variability in their flotation rates and consequently variable PGE recoveries that is mostly attributed to the not so well understood PGM distributions and characteristics.

The purpose of the study was to investigate the PGE process mineralogical characteristics such as the PGM phases, their modal abundances and mineral associations, as well as the grain size distributions within the UG2 Reef and MR at the Buffelshoek Farm. The observed PGM phases are broadly grouped into PGE sulphides, PGE arsenides, PGE bismuth-tellurides, PGE antimonides and PGE alloys. The PGM phases are largely dominated by PGE-sulphides (average of 80%) in the UG2 Reef and PGE-arsenides (average of 39%) in the MR. Although the UG2 Reef and MR are mineralogically different, the PGM observed are similar in composition, but vary in their proportions. The PGM are mostly associated with base metal sulphides typically, pentlandite in the UG2 Reef and silicates, which are dominated by amphiboles in the MR. The PGM grain sizes generally range between 2 and 22 microns in the UG2 Reef and range between 2 and 32 microns in the MR.

The concentrations of platinum are the highest in both the UG2 Reef and MR, and with the platinum largely deported in PGE-sulphides (about 69 - 84.9%) in the UG2 Reef and PGE-arsenides in the MR. Palladium is mostly deported in the PGE-sulphides (about 52.3 - 69.2%) in the UG2 Reef and mostly deported in PGE antimonides (about 43%) and PGE bismuth-tellurides (about 37%) in the MR. Rhodium (Rh) is entirely deported in the PGE sulphides in the UG2 Reef and deported in PGE sulphides (about 86.5%) and PGE bismuth-tellurides (about 13.5%) in the MR. Expected recoveries of PGM ranges from 76 to 89% for PGE sulphides and arsenides in the UG2 Reef and 61.3% in the MR, which is considered good. PGE bismuth-tellurides, PGE antimonides and PGE alloys are expected to be variably to poorly recovered, requiring suitable reagents to be well recovered both in the UG2 Reef and MR.

Keywords: *Platinum group elements; Upper Group 2 chromitite; Merensky Reef; Two Rivers Platinum Mine; Process Mineralogy.*

TABLE OF CONTENTS

LIST OF FIGURES

LIST OF TABLES

LIST OF ABBREVIATIONS

Au	Gold
BC	Bushveld Complex
Bi-Te	Bismuth-Tellurides
BMS	Base Metal Sulphides
BSE	Back Scattered Electron
Co	Cobalt
Cp	Chalcopyrite
Chr	Chromite
Cu	Copper
CZ	Critical Zone
EDS	Energy Dispersive Spectrometers
EMPA	Electron Microprobe Analyser (Electron Microprobe)
GSD	Grain Size Distribution
g/t	Grams Per Ton (equivalent of ppm)
GXMAP	General or Grain X-ray mapping
IPGE	Iridium Platinum-Group Elements
Ir	Iridium
LZ	Lower Zone
MarZ	Marginal Zone

Mt	Magnetite
MG	Middle Group Chromitites
MLA	Mineral Liberation Analyser
MR	Merensky Reef
MZ	Main Zone
Ni	Nickel
Pd	Palladium
PGE	Platinum-Group Elements
PGM	Platinum Group Mineral
PPGE	Palladium Platinum-Group Elements
PPL	Plane Polarised Light
ppm	Part Per Million
Pn	Pentlandite
Po	Pyrrhotite
Pt	Platinum
Py	Pyrite
Rh	Rhodium
RLS	Rustenburg Layered Suite
Ru	Ruthenium
SACS	South African Committee for Stratigraphy

SPL_Lt	Sparse Phase Liberation Lite
TRP	Two Rivers Platinum Mine
UG2	Upper Group 2 Chromitites
UZ	Upper Zone
XBSE	Extended Backscattered Image
WDS	Wavelength Dispersive Spectrometers
Wt%	Weight Percentage

CHAPTER 1 INTRODUCTION AND BACKGROUND

1.1. The Two Rivers Platinum Mine's Buffelshoek prospect

The Two Rivers Platinum Mine (TRP) is located about 35 km south-west of the town Burgersfort in the Limpopo Province, South Africa (in the past the mine used to fall under the Mpumalanga Province). The mine currently mines platinum-group elements (PGE), and chromium as by-product hosted in the Upper Group 2 chromitite (UG2) on the farm Dwarsrivier 372 KT (Figure 1.1) in the Eastern Bushveld Complex. Recent work (Rose, 2016) indicated studies of the PGE hosting Merensky Reef (MR) which also occurs at the TRP, but no official mining of the MR was established at the time. However, evaluation of potentially mining the MR was underway.

The TRP at the time of this study was managed by African Rainbow Minerals (ARM) which owns 51% of the operation and with 49% owned by Implats. The mine operation comprised two decline shafts and a flotation concentrator plant (TRP, 2016). The mine had two prospects for a potential mine expansion on the adjacent farms Kalkfontein 367 KT and Buffelshoek 368 KT, which presented the opportunity for this study. The Buffelshoek prospect (Buffelshoek 368 KT Farm) on which this study is based was the most recent acquisition located south-west of the TRP (Figure 1.1). Three boreholes were drilled at the Buffelshoek prospect to initiate a 10 to 20 years ahead life-of-mine expansion plan. Borehole data indicate the occurrence of PGE hosting UG2 and MR with grades up to 29 g/t total PGE at the Buffelshoek prospect.

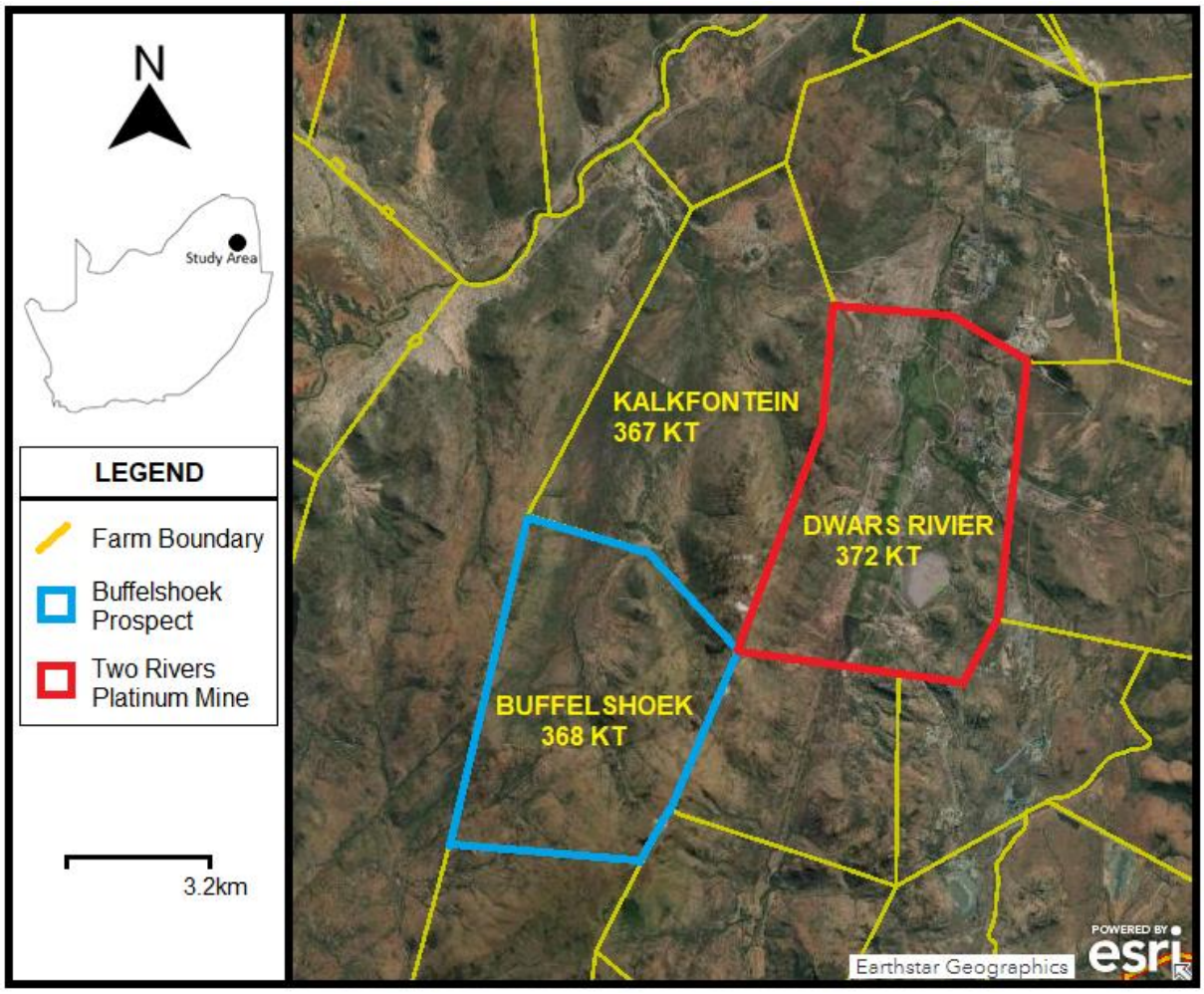

Figure 1.1: Location of the Buffelshoek prospect (Buffelshoek 368 KT) in relation to the operating Two Rivers Platinum Mine site at the farm Dwarsrivier 372 KT. Map data obtained from the Chief Surveyor General of South Africa data (2021).

1.2. Rationale and motivation of the study

The largest concentration of platinum-group elements (platinum (Pt), palladium (Pd), rhodium (Rh), ruthenium (Ru), osmium (Os) and iridium (Ir)) resources in the world are hosted within the Critical Zone (CZ) of the Bushveld Igneous Complex or Bushveld Complex (BC) in South Africa (Cawthorn et al., 2002; Holwell et al., 2006). Within the CZ the platinum-group elements (PGE) are hosted in the chromitite layer

known as the Upper Group 2 Chromitite (UG2) Reef as well as the Merensky Reef (MR) in the Western and Eastern Limb and the Platreef and Flatreef in the Northern Limb (Cawthorn *et al.,* 2002; Bye, 2003; Grobler *et al*., 2018; Langa *et al*., 2020).

Each of these platiniferous Reefs has its distinctive mineralogy and requires different approaches to metallurgical processing for PGE recoveries. For example, the PGE in the UG2 Reef are hosted in an oxide (chromite) rich lithology and in the MR are hosted in a silicate (pyroxene) rich lithology. Historically, the MR was the first to be targeted during the initial exploitation of the PGE in the BC due to easier metallurgical constraints for PGE recoveries (Cawthorn, 1999). However, the UG2 Reef contains the largest known reserves of PGE in the BC (Vermaak, 2005).

In the UG2 and MR reefs, the PGE occur mostly as discrete platinum-group minerals (PGM) and as solid-solutions in the base-metal sulphides (BMS) (Penberthy *et al.,* 2000; Cawthorn *et al.,* 2002; Godel *et al.,* 2008; Godel *et al*., 2010). The PGM can be broadly grouped into sulphides, arsenides, bismuth-tellurides, alloys etc. (Cawthorn *et al.,* 2002) and are commonly associated with silicates, BMS and chromite (Penberthy *et al.,* 2000; Cawthorn *et al.,* 2002; Godel *et al.,* 2010). These PGM are generally concentrated and recovered using the flotation method of the metallurgical or mineral processing techniques.

Some of the PGM are highly amenable to flotation (e.g., sulphides), meaning they are easy to recover, while others have slow flotation rate during recovery (e.g., bismuth-tellurides) as stated in Vermaak (2005) and Penberthy *et al*. (2000). This varying attributes of PGM may results in significant amounts of valuable PGE being lost to flotation tailings. Such losses are mostly influenced by limited understanding of the different process mineralogical factors such as the PGM phases and

abundance, association, and grain size distributions (Penberthy *et al.,* 2000; Chetty *et al.,* 2009; Pienaar *et al.,* 2017).

Rose *et al.* (2011), Rose (2016) and Rose *et al*. (2018) studied the PGM characteristics, which includes their recoveries at the current TRP operation, however the PGM have varying attributes throughout the strike. Although the varying attributes of PGM are mostly linked to the PGE losses (PGE lost to flotation tailing) by Penberthy (2001), the distribution and characteristics of the various PGM, and how they influence recovery are still not well understood in the UG2 Reef and MR. Understanding the PGM distribution characteristics can provide process mineralogy information that can be used to calibrate the flotation (concentrator) plant to recover most existence of the PGM effectively and efficiently (optimally). Knowledge of the PGE mineralisation plays an important role in understanding the distributions and characteristics of PGE in the PGE-bearing ore deposits.

Various authors including Schouwstra *et al.* (2000) and Penberthy *et al.* (2000) acknowledged the complex variability of the PGM distribution and characteristics in the UG2 Reef, which are also exhibited in the MR as described by Rose (2011). These complex variability of the PGM distribution and characteristics along the strike in the Eastern BC also occurs at TRP. In the Eastern BC (TRP surroundings) there are several platinum mines, the oldest being the Modikwa Platinum Mine which opened its operations in the 1920's (TRP, 2016). The number of platinum mines in the surroundings of the TRP increases competition in the platinum market, and therefore the need for a better understanding the PGM distribution and characteristics for feasibility and optimal recovery of PGE at the potential mine extension area (Buffelshoek prospect) arose.

1.3. Aims and objectives of the study

The aim of this study was to investigate mineralogical characteristics and distribution of the platinum-group elements (PGE) in the Upper Group 2 Chromitite (UG2) Reef and Merensky Reef (MR) intersected in the boreholes drilled on the Buffelshoek 368 KT Farm, Two Rivers Platinum Mine (TRP) in an attempt to provide information that can be useful to optimise beneficiation of the PGE from the ores.

The objectives of the study were to:

- determine the process mineralogical characteristics (platinum group minerals (PGM) phases and their modal abundance, association and grain size distributions, as well as textural relationships between silicates, chromites and base metal sulphides) in the UG2 Reef and MR using reflected light microscopy, mineral liberation analyser and electron microprobe; and
- determine how the process mineralogical characteristics (including distributions and controls of PGE in the PGM) will affect the PGE recoveries in the UG2 Reef compared to the MR using flotation methods at the TRP.

1.4. Structure of the dissertation

In Chapter 1 an overview of the study, aims and objectives, location of the study area and some recent literature are presented.

Chapter 2 provides a detailed description of the study area, generalised geology of the study area, location and stratigraphic column of the boreholes studied and platinum-group elements grades through the stratigraphy.

Chapter 3 provides the relevant literature reviewed to give a detailed background of the geology of the Bushveld Complex in particular, the Critical Zone of the Rustenburg Layered Suite, and some background on the flotation of platinum-group elements.

Chapter 4 provides the methodology followed to achieve the objectives of the study. This includes a brief description of the mineral liberation analyser technique, elaboration on the borehole sampling technique, polished block preparations to reflected light microscopy description and electron microprobe analysis procedure used.

Chapter 5 presents the results of the ore petrographic investigation and backscattered electron images from the electron microprobe, the platinum group minerals chemistry from the electron microprobe, the variation plots of platinum-group elements obtained from the Two Rivers Platinum Mine (assay data), and variation plots of the rock chemistry obtained from the mineral liberation analyser.

Chapter 6 presents a detailed interpretation and visualisation of the characteristics and mineralisation of the platinum-group elements useful for mineral processing. This includes distributions of platinum group elements, modal mineralogy of the rocks, platinum group minerals phases and abundances, associations and grain size distributions, and deportments of palladium-platinum group elements.

Chapter 7 provides a discussion of the various characteristics of the UG 2 Reef and MR based on the results from this study compared to other studies to reach a conclusion.

The end of the dissertation contains the reference list and appendices of additional information including results.

CHAPTER 2 DETAILS OF THE STUDY AREA

2.1. Description of the study area

The TRP started in 2007 with full operation in 2008 (Esterhuizen, 2014). In 2015, the farms Kalkfontein and Tweefontein were incorporated in the TRP, followed by incorporation of the farm Buffelshoek (TRP mine report, 2016) as a prospect. Recently, a decision by TRP management to explore the opportunity of mining the MR led to studies on the MR, which is currently not yet mined (Rose, 2016).

The Buffelshoek prospect (hereafter referred to as Buffelshoek) which is located south-west of the TRP in the Eastern Bushveld Complex sits directly on the outcrops of gabbronorite and norite of the Main Zone of the Rustenburg Layered Suite (Figure 2.1). The Upper Group 2 chromitite (UG2) Reef intersected at depth (> 500 m) at the Buffelshoek prospect is found to be thinner than that observed at the current TRP operation., Buffelshoek prospect is also characterised by a granitic intrusion / outcrop attributed to the Lebowa Granite outcrops on the western side (Figure 2.2).

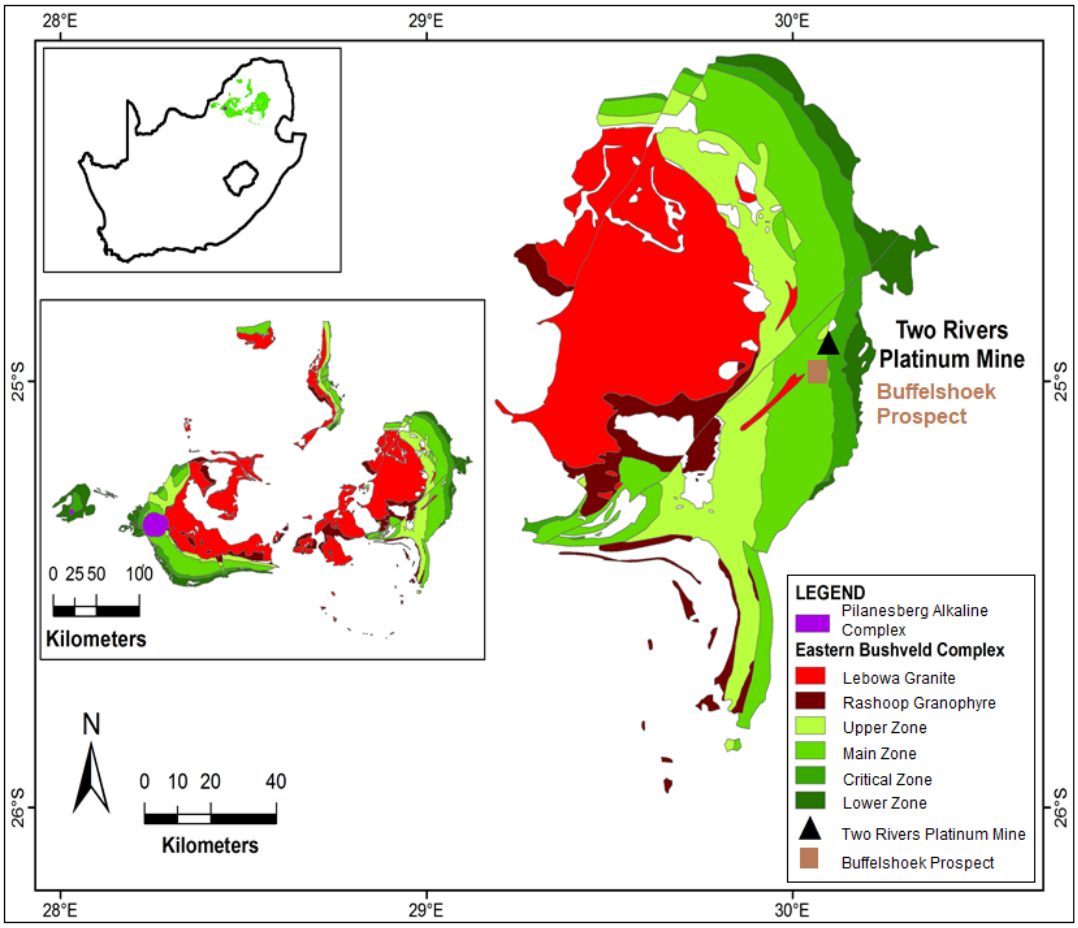

Figure 2.1: Location of the study area in relation to the Eastern Bushveld Complex regional geology, geology data from the Council for Geoscience (2021).

2.2. Locality map and borehole locations

The TRP made available three boreholes BFH003, BFH006 and BFH007 located in the south-eastern portion of Buffelshoek prospect (Figure 2.2). These boreholes had approximate depths of up to 821 m and have several deflections drilled to intersect the reefs at multiple points. The deflections are denoted D0 – vertically downwards, D1, D2, D3, D4, etc. for deflections with varying directions (azimuths) at depth. This study focused on BFH003D1 and BFH003D2 – the first and second deflections,

BFH006D0 and BFH006D1 – original vertical drill-hole and the first deflection and BFH007D0 – the vertical drill-hole.

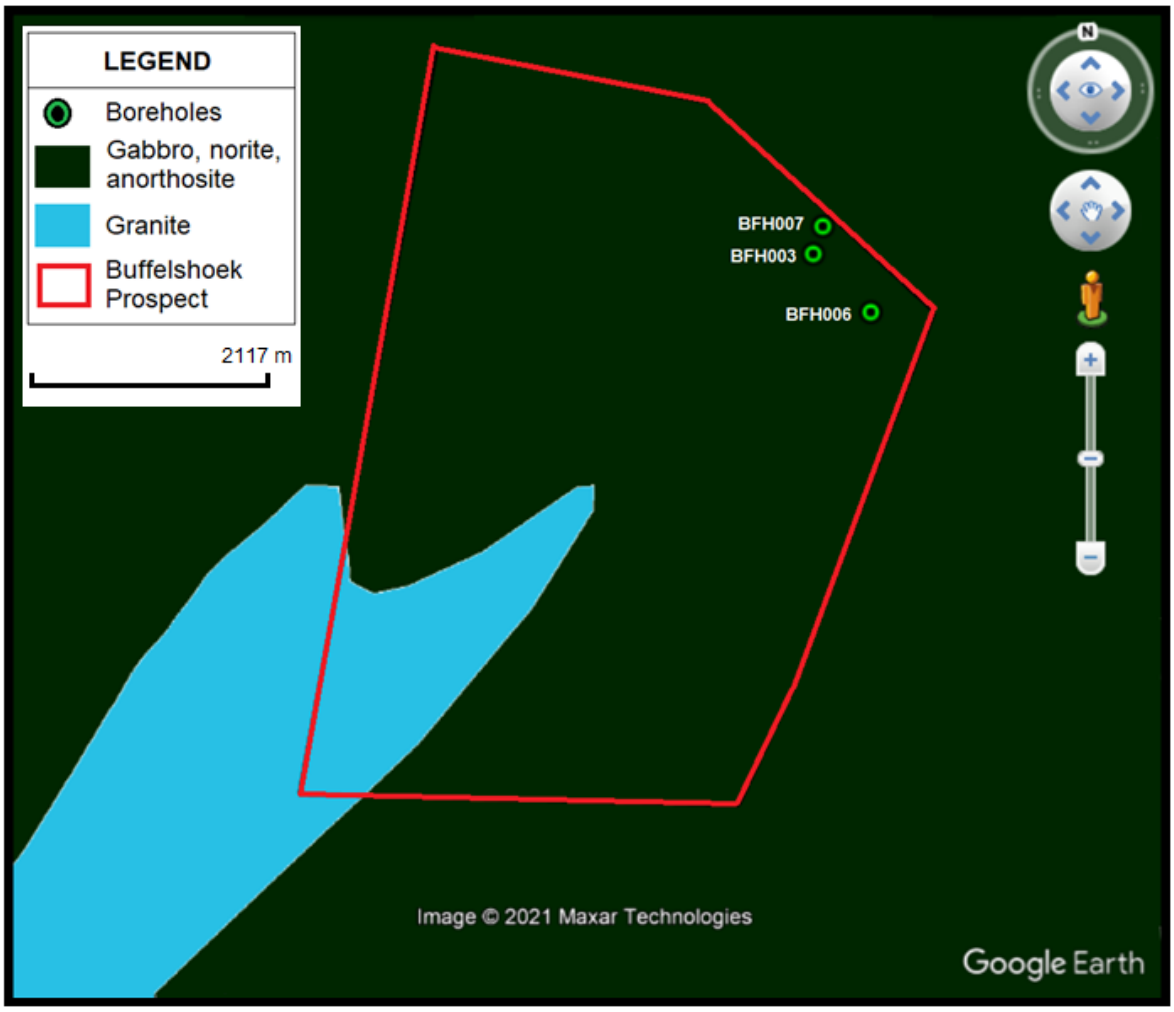

Figure 2.2: Local generalised geology of the Buffelshoek 368 KT (Buffelshoek) Farm showing the boundary of the farm and locations of the boreholes studied, geology from the Council for Geoscience (2021).

2.3. Borehole logs and platinum-group element grades

The UG2 Reef can be classified into three distinct Reef facies based on disruptions by pyroxenites: (1) UG2 Normal Reef; characterised by a thick un-disrupted main

chromitite layer, (2) UG2 Split Reef; characterised by an internal pyroxenite lens (typically > 10 cm) within the main chromitite layer and (3) UG2 Multiple Split Reef; characterised by numerous pyroxenite lenses occurring within the main chromitite layer (Mabuza, 2007). The lithological logs in Figures 2.3 to 2.7 represent the generalised stratigraphic column of the UG2 Reefs (Normal, Split and Multiple Split) and the Merensky Reef (MR) at Buffelshoek. Buffelshoek has a range of platinum-group elements (PGE) grade distributions from low to very high grades also seen in Figures 2.3 to 2.7.

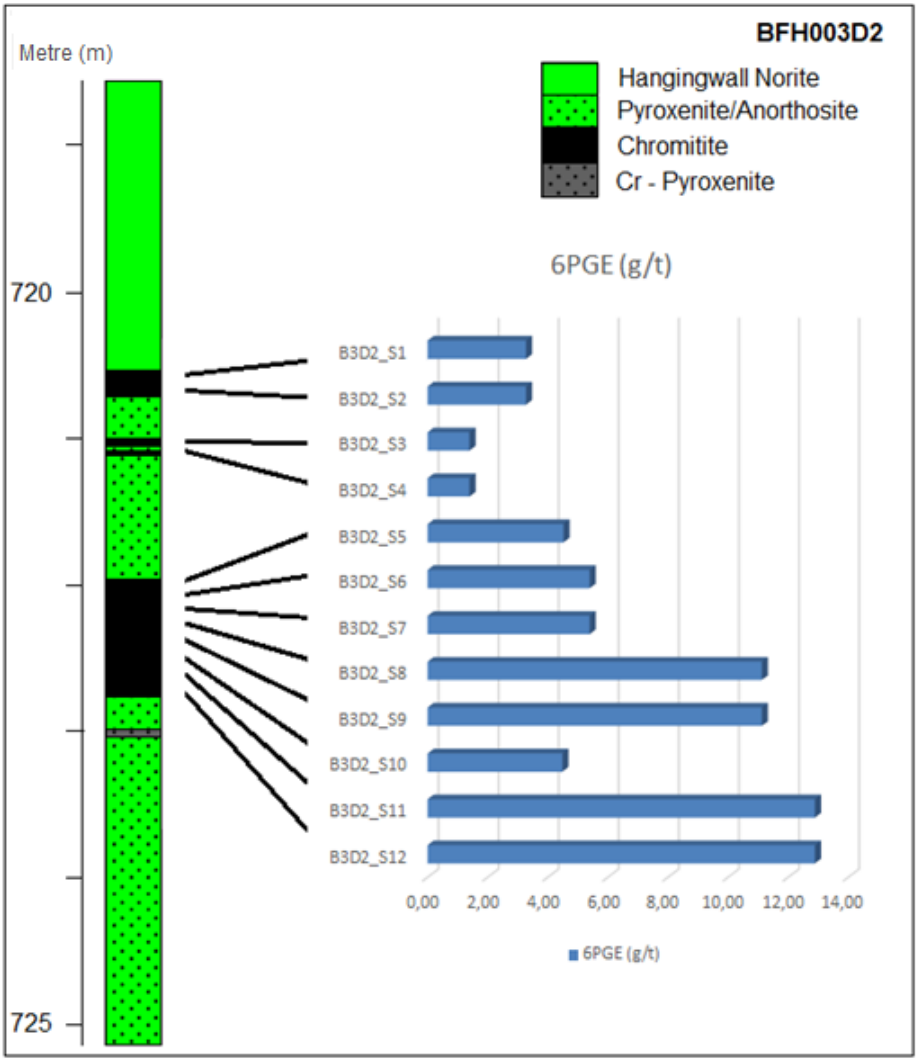

Figure 2.3: Generalised stratigraphic column and PGE grades of the UG2 Normal Reef (BFH003D2).

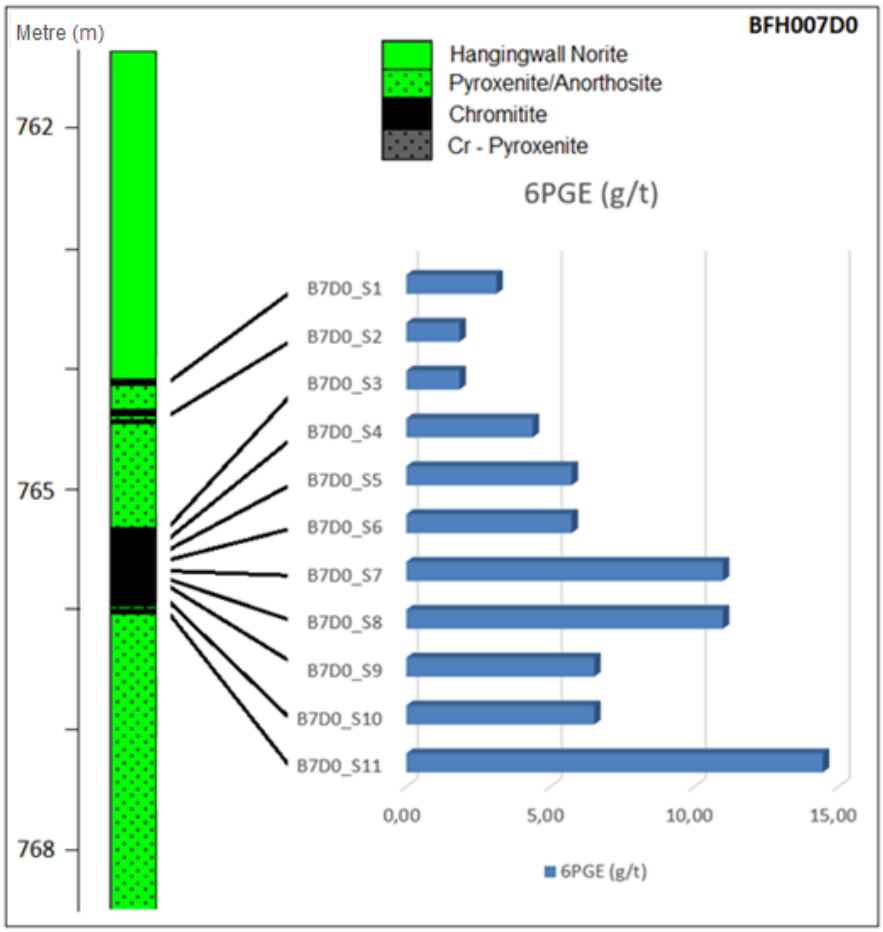

Figure 2.4: Generalised stratigraphic column and PGE grades of the UG2 Normal Reef (BFH007D0) with a small internal pyroxenite (< 0.05 m).

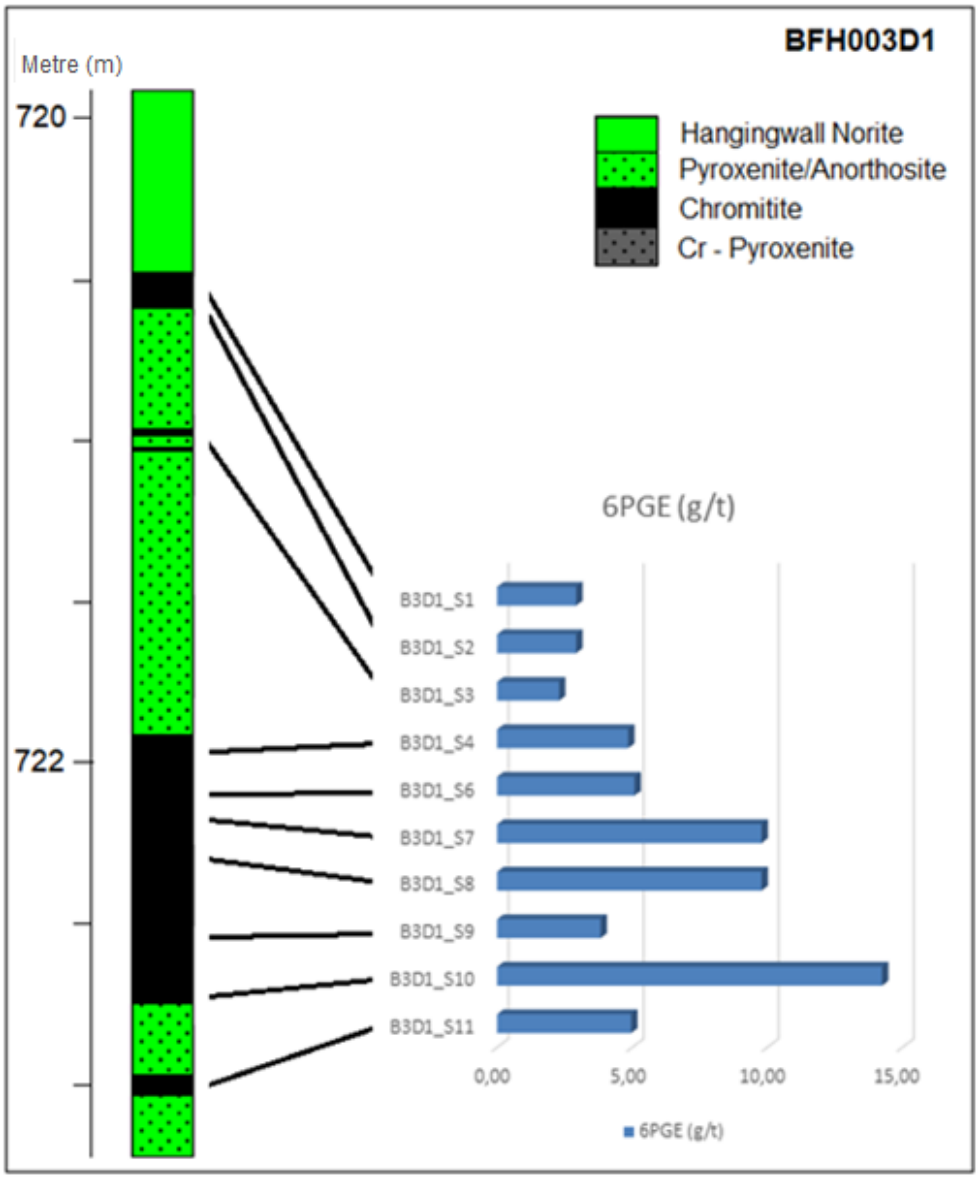

Figure 2.5: Generalised stratigraphic column and PGE grades of the UG2 Split Reef (BFH003D1).

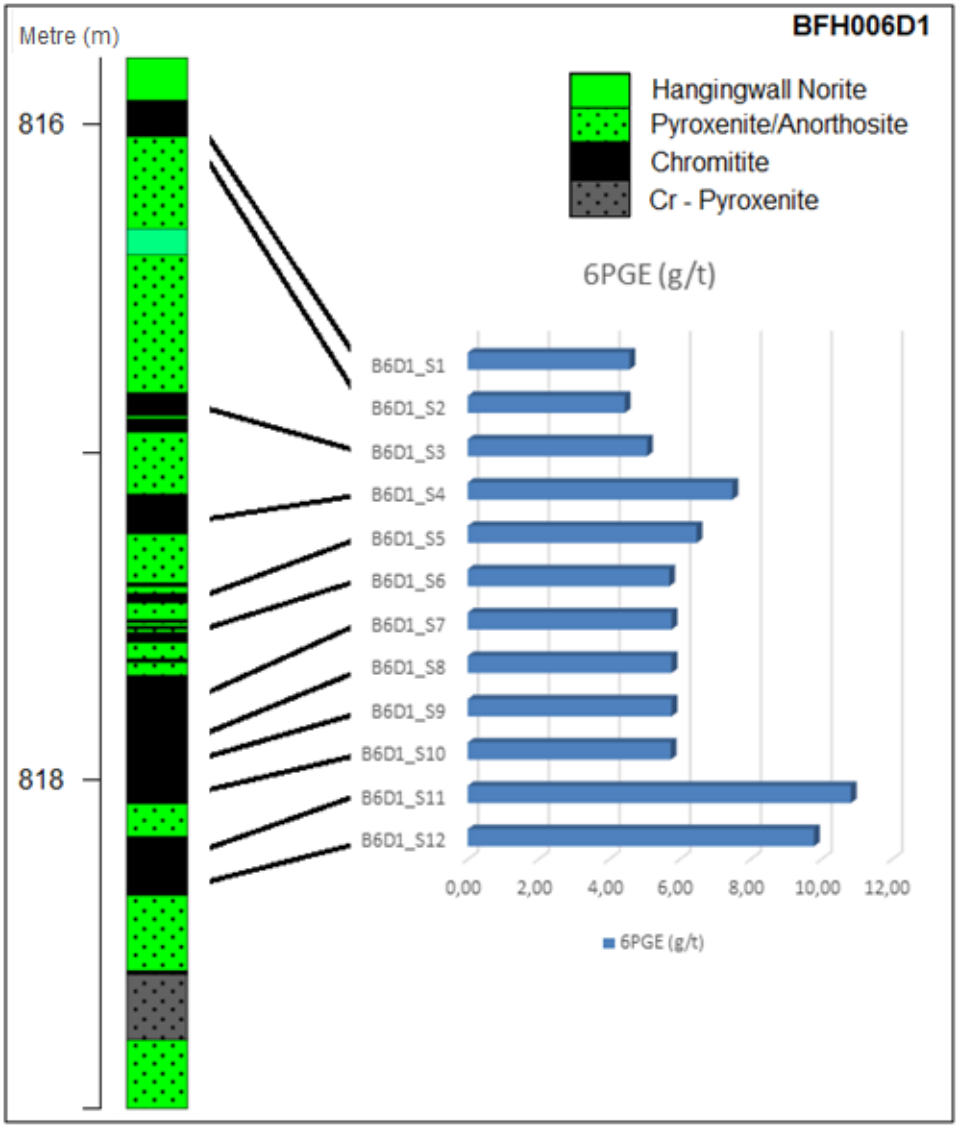

Figure 2.6: Generalised stratigraphic column and PGE grades of the UG2 Multiple Split Reef (BFH006D1).

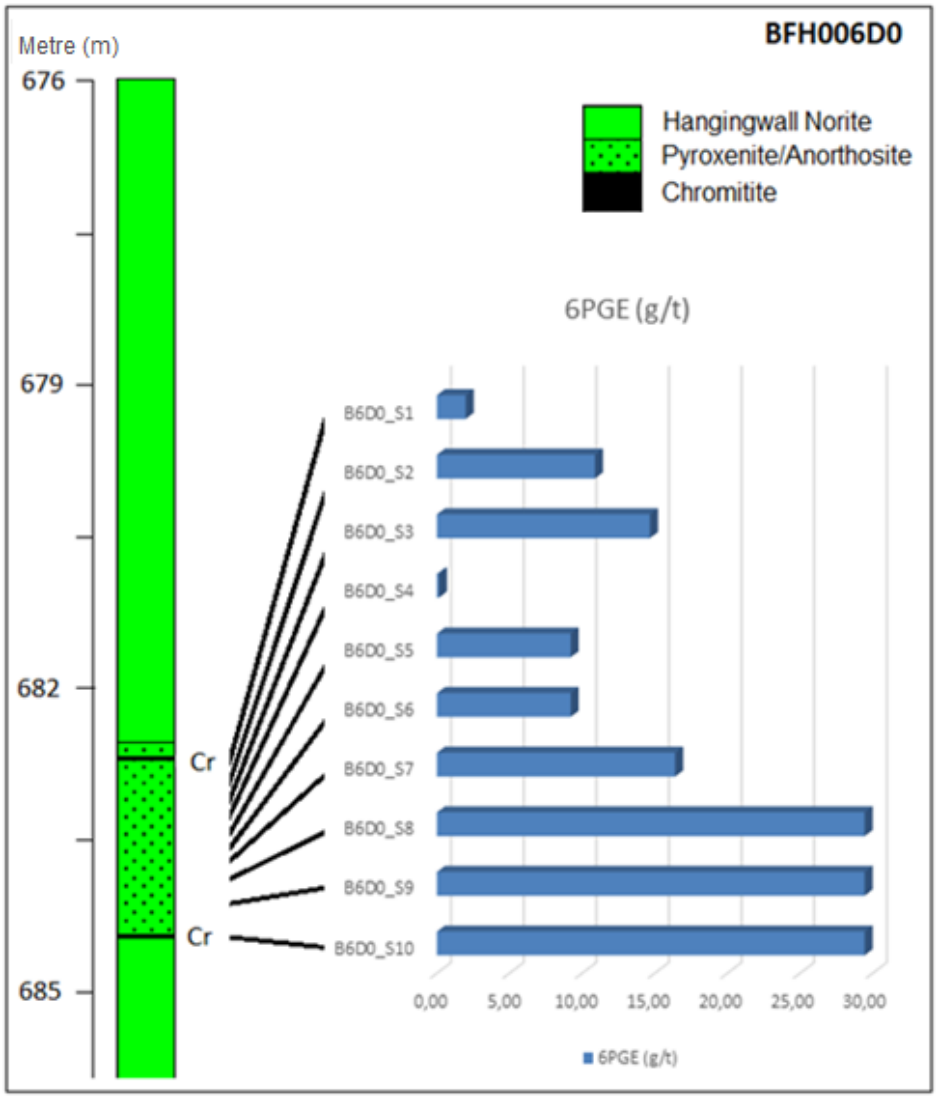

Figure 2.7: Generalised stratigraphic column and PGE grades of the Merensky Reef (BFH006D0).

CHAPTER 3 PREVIOUS WORK

3.1. The Rustenburg Layered Suite of the Bushveld Complex

The Bushveld Complex (BC) hosts one of the world's largest known layered mafic suites, the Rustenburg Layered Suite (RLS). The RLS contains some of the most important platinum-group elements (PGE: Pt, Pd, Rh, Ir, Os, Ru) resources in the world (Willemse, 1969; Hulbert and Von Gruenewaldt, 1982; Cawthorn, 1999; Osbahr *et al.*, 2014). The BC also consists of felsic suites, namely the Rashoop Granophyre Suite and the Lebowa Granite Suite (SACS, 1980; Von Gruenewaldt *et al.*, 1985; Cawthorn, 1999a). The BC was emplaced about 2.06 Ga (Walraven *et al*., 1990; Cawthorn and Walraven, 1998) into an intraplate setting referred to as the Transvaal sequence or sedimentary basin (Eriksson *et al*., 1991; Eriksson *et al*., 1995). Figure 3.1 shows the simplified geology of the BC which covers approximately 65 000 km^2 (Eales and Cawthorn, 1996; Cawthorn and Walraven, 1998).

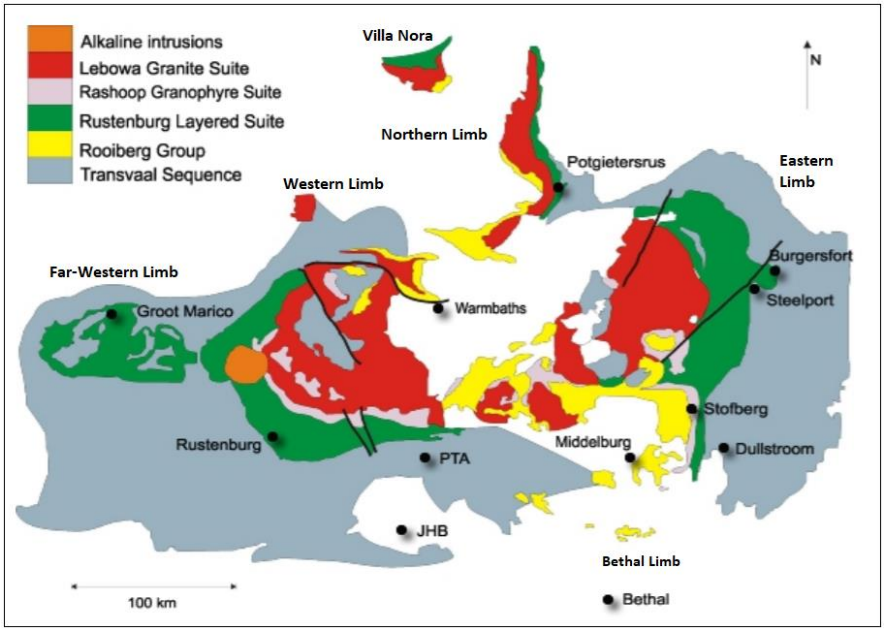

Figure 3.1: General (Simplified) geology of the Bushveld Complex showing the four major Limbs, the Western (including Far-Western), Eastern, Northern / Potgietersrus (including Villa Nora) and satellite Bethal Limbs, modified after Kinnaird (2005).

Some authors (Walraven, 1997; Buchanan *et al*., 1999; Buchanan *et al.,* 2002; Kinnaird, 2005) includes to the BC the Rooiberg Group formations and volcanics (felsites), also seen in Figure 3.1. The various suites, formations and volcanics of the BC are widely studied and can further be divided into detailed lithological groups. The focus of this study is based on the RLS of the BC. The RLS, is a mafic-layered sequence outcropping in the Western, Eastern and Northern Limbs. It was generally accepted that the RLS in the Western and Eastern Limbs are similar but differ to that of the Northern Limb as shown in Figure 3.2, until recently when Grobler *et al.* (2018) and Langa *et al.* (2020) published new developments on the Northern Limb (Figure 3.4).

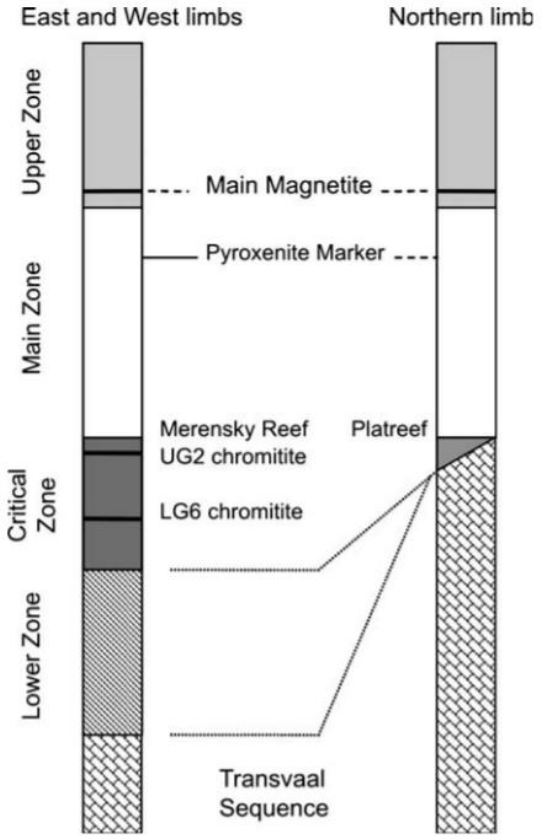

Figure 3.2: Generally accepted stratigraphic column of the relationship between the RLS at the Northern Limb to that of the Western and Eastern Limbs after White (1994).

The RLS comprises a sequence of dunites, harzburgites, pyroxenites, norites and gabbros, anorthosites, diorites, chromitites and magnetitites (ultramafic to mafic lithologies) grouped stratigraphically from the bottom upwards into five units, namely the Marginal Zone, Lower Zone, Critical Zone, Main Zone and Upper Zone (Vermaak 1976; SACS, 1980; Scoon and Teigler, 1995; Buick *et al*., 2001; Cramer, 2001; Eales, 2002; Ashwal *et al*., 2005; Kinnaird *et al*., 2005; Naldrett *et al*., 2008; Voordouw *et al*., 2010; Rose, 2016; Grobler *et al*., 2018). The RLS varies in thickness with an average thickness of about 7.6 km (Seabrook, 2005; Rose, 2016). The generalised stratigraphy of the RLS widely accepted in the BC is shown in Figure 3.3 and the geology of the RLS is summarised as follows:

The **Marginal Zone (MarZ)** at the bottom of RLS consists mainly of fine to medium-grained norites, which vary in thickness by location, reaching a thickness of 800 m in selected areas of the Eastern Limb (Cawthorn and Walraven, 1998; Johnson *et al*., 2006). The MarZ overlays the Transvaal Supergroup (Vermaak, 1976), and is not continuous throughout the BC and the textures of the units indicates evidence of rapid cooling of differentiated magma and some crustal assimilations (Cawthorn and Walraven, 1998).

The **Lower Zone (LZ)** overlaying the MarZ, or the Transvaal Supergroup where the MarZ is not developed, consists mainly of dunites, harzburgites and pyroxenites, which like the MarZ, also vary in a thickness, reaching thickness of about 1600 m (Cameron, 1978; Hulbert and Von Gruenewaldt, 1982; Johnson *et al*., 2006). The LZ can be divided based on the observed cyclic units into subzones, from bottom upwards as Basal Subzone, Lower pyroxenite Subzone, Harzburgite Subzone and Upper pyroxenite Subzone (Cameron, 1978; Rose, 2016).

The **Critical Zone (CZ)** mostly overlies the LZ and can be divided into the Lower Critical Zone (LCZ) and Upper Critical Zone (UCZ). The CZ can either be described as a pyroxenitic unit (Eales and Cawthorn, 1996) or as a noritic to anorthositic unit (Ashwal *et al*., 2005), reaching a thickness of about 1000 m (Ashwal *et al*., 2005; Johnson *et al*., 2006). Essentially the CZ comprises of cyclic units of pyroxenites, chromitites, norites and anorthosites. The cyclic units are attributed to repeated injections of magma into the magma chamber followed by fractionation (Eales *et al*., 1986; Mitchell *et al*., 1998). Most importantly, the CZ hosts mineralisation of PGE, Ni, Cu, minor Au and Cr (Hatton and Von Gruenewaldt, 1987; Schouwstra *et al*., 2000).

The chromite deposits are grouped into the Lower, Middle and Upper Group chromitite layers from the base upwards (Johnson *et al*., 2006). The Lower Group (LG) chromitites have seven chromitite seams, namely LG1 to LG7. The Middle Group (MG) chromitites have four seams, namely the MG1 to MG4. The Upper Group (UG) chromitites have three seams, namely UG1, UpUG2 and the UG3 in the Eastern Limb (Johnson *et al*., 2006). The MG chromitites mark the transition between the UCZ and the LCZ, characterised by an anorthosite layer (with cumulus plagioclase) at the base of the UCZ (Penberthy, 2001; Barnes and Maier, 2002; Johnson *et al*., 2006).

PGE deposits within the UCZ are hosted in the UG2 chromitite (UG2) Reef, Merensky Reef (MR), Platreef (Barnes and Maier, 2002; Schouwstra, *et al*., 2000) and Flatreef (Grobler *et al*., 2018; Langa *et al*., 2020). The UG2 Reef and MR are found in the Western and Eastern Limbs, and the Platreef and Flatreef in the Northern Limb (Grobler *et al*., 2018; Langa *et al*., 2020). The Platreef is correlated to the CZ and overlies the Transvaal Supergroup or Archean granites in some places (Maier and Eales, 1997).

The **Main Zone (MZ)** overlies the CZ and mostly comprises of norites and gabbronorites, with minor anorthosites and pyroxenites (Von Gruenewaldt, 1973). The MZ reaches a thickness of about 3400 m (Barnes and Maier, 2002). In some areas of the Northern Limb where the Platreef is not developed, mostly in the north, the MZ overlies Archean granitic rocks (Maier and Eales, 1997).

The **Upper Zone (UZ)** overlies the MZ and comprises of gabbros and anorthosite (with magnetite, Fe-rich pyroxene and / or apatite in some places). And the UZ reaches a thickness of about 2700 m (Reynolds, 1985) and hosts up to 24 magnetitite layers in the Eastern Limb (Molyneux, 1974; Reynolds, 1985; Cawthorn and Walraven, 1998; Johnson *et al*., 2006).

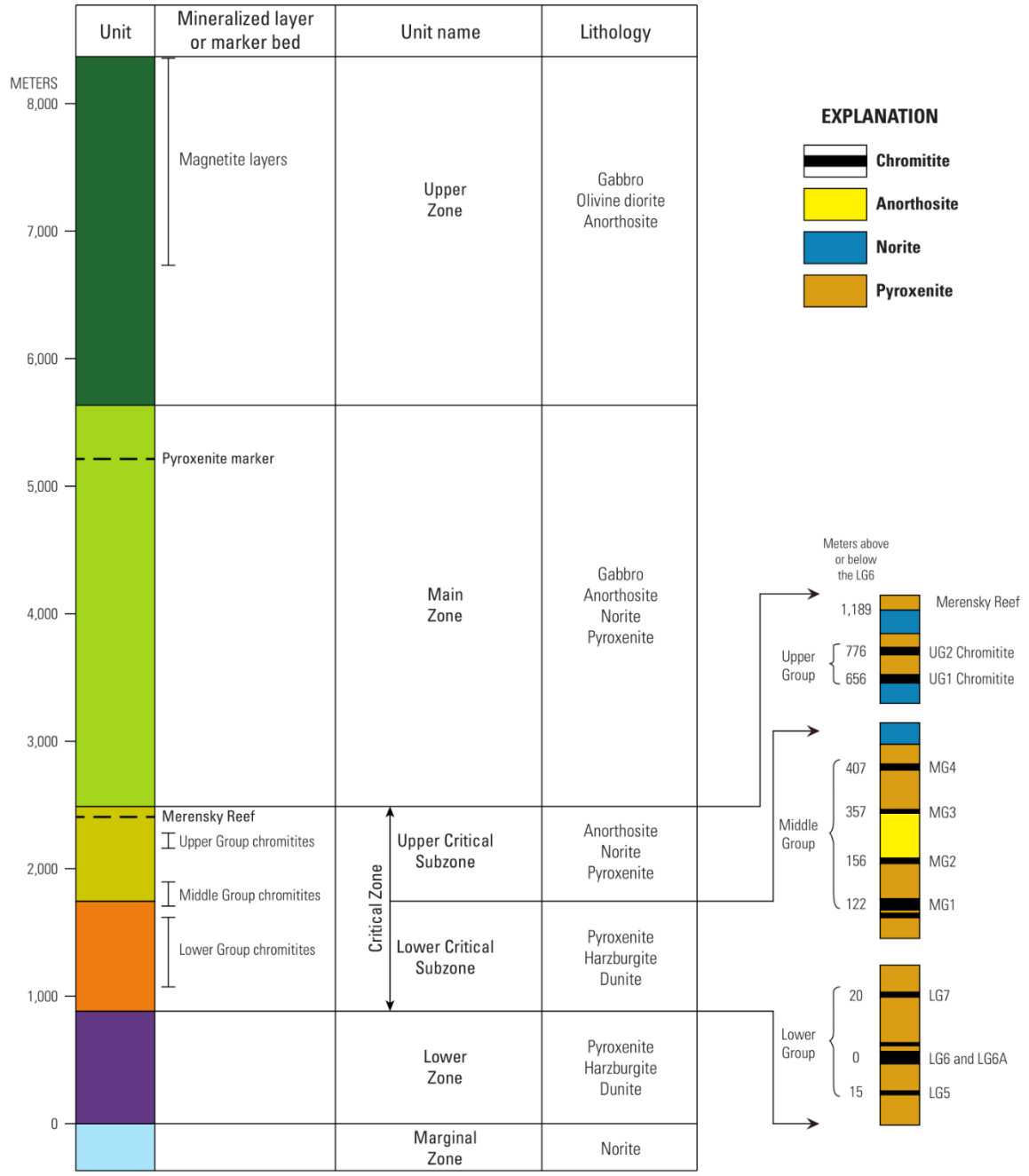

Figure 3.3: Illustration of the most accepted generalised stratigraphy of the RLS (Zientek, 2014).

New developments from Grobler et al. (2018) and Langa et al. (2020):

The Northern Limb was previously only thought to only exhibit contact-style PGE mineralisation (Buchanan *et al*., 1981; Gain and Mostert, 1982; Buchanan and Rouse, 1984; Cawthorn *et al*., 1985; Vermaak, 1995; Maier and Eales, 1997; Harris and Chaumba, 2001; Holwell *et al*., 2005; Hutchison and Kinnaird, 2005; Maier *et al*., 2008). Grobler *et al*. (2018) and Langa *et al*. (2020) have recently described the platiniferous Flatreef also hosted in the Northern Limb. Unlike the Platreef, the stratigraphy of the Flatreef within the RLS can almost entirely be correlated with the stratigraphy of the RLS in the Western and Eastern Limbs (Figure 3.4).

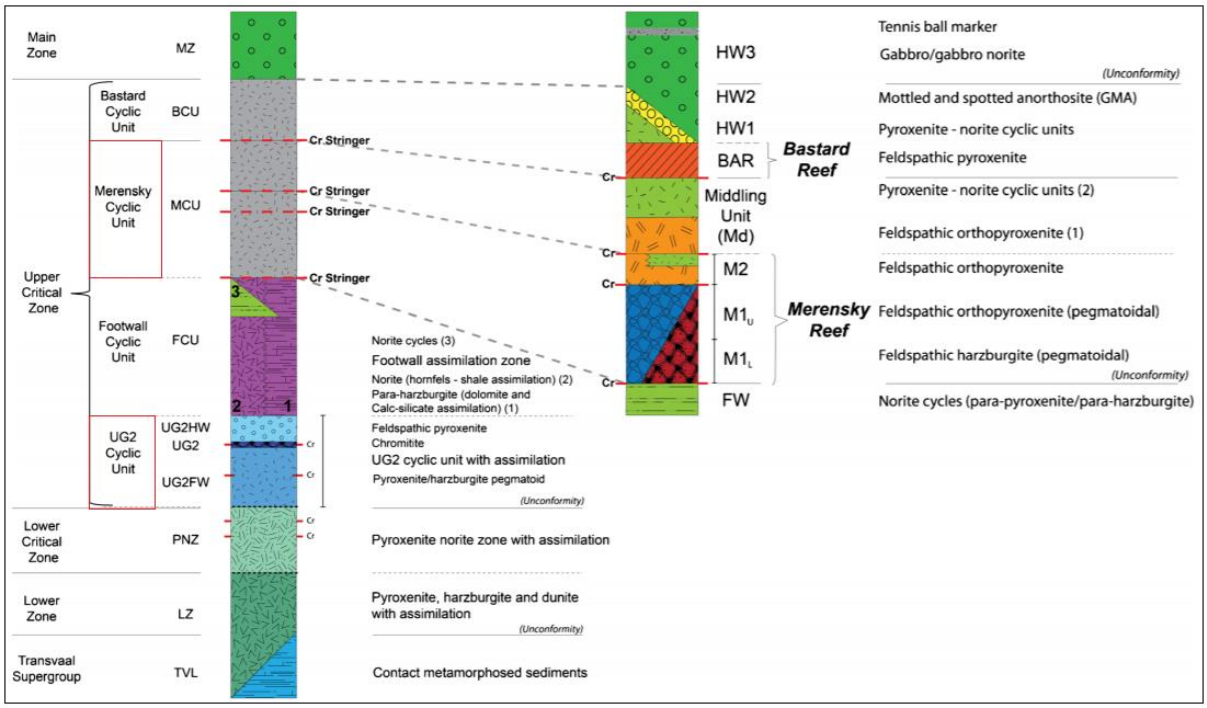

Figure 3.4: Stratigraphic corelation of the UG2 and Merensky Reefs to the Flatreef and the new general stratigraphy of the RLS in the Northern Limb of the Bushveld Complex where the Flatreef is located (Grobler *et al*., 2018).

3.2. The Upper Group 2 Chromitite and Merensky Reefs

The UG2 Reef and MR as previously mentioned are found in the UCZ of the RLS. The TRP is currently mining the UG2 Reef for PGE and PGE associated metals (Ni, Cu, Au, Co) with chromium as by product (Mabuza, 2007; Rose *et al*., 2018). Hans Merensky first discovered the PGE in this area in the 1920's on the farm Maandagshoek (now Modikwa Platinum Mine) (TRP, 2016).

The UG2 Reef is approximately 1 m thick but can vary from 0.4 to 2.5 m as a lithological unit and consists of about 60-90% chromite, 5-25% interstitial orthopyroxenes, and other silicate minerals (McLaren and De Villiers, 1982; Schouwstra *et al*., 2000; Penberthy *et al*., 2000; Barnes and Maier, 2002). Above the UG2 Reef is a hanging wall pyroxenite characterised by three thin (< 20 cm thick) chromitite seams, commonly referred to as Leader seams (Leader 1, 2 and 3 from top downwards towards the UG2 Reef) (Hahn and Ovendale, 1994; Schouwstra *et al*., 2000; Penberthy, 2001; Mabuza, 2007). Figure 3.5 shows an illustration of the three UG2 Reef facies; (1) UG2 Normal Reef, (2) UG2 Split Reef and (3) UG2 Multiple Split Reef as described after Mabuza (2007) in section 2.3 above (also supported by Rose *et al*., 2018).

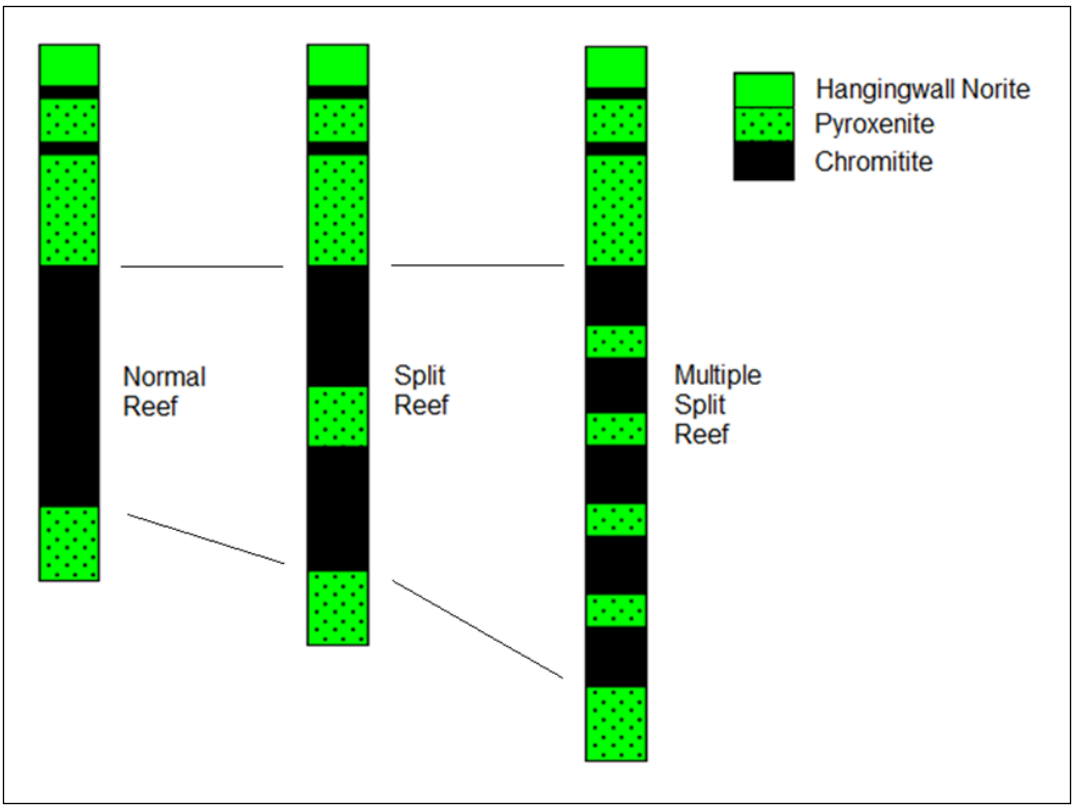

Figure 3.5: Illustration of the generalised UG2 Reef facies (Normal, Split and Multiple Split Reefs) at the TRP, based on Mabuza (2007).

The Merensky Reef is lithologically about 4 cm to 4 m thick and consists predominantly of orthopyroxene, plagioclase, and other silicate minerals (Cawthorn, 1999; Osbahr *et al*., 2013; Rose, 2016). The Merensky Reef is mostly bound by 2 mm to > 40 mm chromitite stringers at the top and the bottom and is generally characterised by a fine to pegmatoidal feldspathic-pyroxenite (Cawthorn, 1999; Rose, 2016). The MR is sometimes disrupted by iron-rich ultramafic pegmatites (IRUP) (Viljoen and Scoon, 1985; Scoon and Mitchel, 2004). The UG2 Reef and MR at TRP are also disrupted by potholes, dykes, and faults (Mabuza, 2007). The UG2 Reef generally occurs about 20 to 400 m below the MR (Hahn and Ovendale, 1994; Schouwstra *et al*., 2000; Barnes and Maier, 2002). At the TRP the UG2 Reef occurs about 140 m below the MR separated by a sequence of non-mineralised norites and

anorthosites (Mabuza, 2007). Various authors (including von Gruenewaldt (1989), Cawthorn (2002), and Kinnaird (2005)) discussed the genesis of the UG2 Reef and MR, which is not presented here, and the authors acknowledge the controversial nature of the theories.

3.3. The platinum group element mineralisation

In the Bushveld Complex (BC), PGE mineralisation is known to be mostly in the UG2 Reef, MR, Platreef and Flatreef. The UG2 Reef, MR and Flatreef can be classified as reef-type PGE mineralisation (Naldrett, 2004; Kinnaird, 2005; Grobler *et al*., 2018; Langa *et al.,* 2020) and the Platreef as contact-style PGE mineralisation (Naldrett, 2004; Kinnaird, 2005). The genesis of the PGE mineralisation is widely discussed and varies between different authors. Generally accepted is the theory of immiscible sulphide melt acting as collectors of PGE and fractionating (or segregating) from silicate or oxide melt to concentrate the PGE in a different environment, be it reef-type or contact-type deposition (Robb, 2005).

The PGE mineralisation in the UG2 Reef and MR has common association with Cu, Ni and Au (Maier, 2005; Rose, 2016). The PGE in the UG2 Reef and MR mostly occur as platinum group minerals (PGM) and to some extent as solid solutions in base-metal sulphides (BMS) (Penberthy *et al*., 2000; Cawthorn *et al*., 2002; Godel *et al*., 2008; Godel *et al*., 2010; Rose *et al*., 2018). The PGM can be broadly grouped into sulphides (e.g., braggite, cooperite, malanite, laurite and vysotskite), arsenides, bismuth-tellurides, antimonides, alloys etc. (Von Gruenewaldt *et al*., 1990; Penberthy *et al*., 2000; Schouwstra *et al*., 2000, Cawthorn *et al*., 2002; Cawthorn, 2011; Vermaak, 2005; Voordouw *et al*., 2010). The PGM grain boundaries are commonly associated with BMS (pentlandite, chalcopyrite, pyrrhotite) and silicates, and in the UG2 Reef also with chromite (Penberthy *et al*., 2000; Cawthorn *et al*.,

2002; Godel *et al*., 2010). The PGM grain sizes in the UG2 Reef are generally smaller than those of the MR (Penberthy *et al*., 2000). The PGM barely exceed 30 microns in diameter (Schouwstra *et al*., 2000).

Penberthy and Merkle (1999) attribute the formation of discrete PGM to the expulsion of PGE from BMS during crystallisation, which were subsequently aligned along the outer boundary of the host BMS. In the chromitite, which are sulphur poor compared to the pyroxenite, some authors proposed that the sulphides which concentrated the PGE were later lost (Naldrett and Lehmann, 1988; Maier and Barnes, 2008; Naldrett *et al*., 2012). In their work, Page *et al.* (2011) indicated a positive correlation between chromium and Iridium-PGE (IPGE: Ir, Ru and Os) when chromite plays an important role in controlling PGE mineralisation.

Other studies such as Hiemstra (1979) and Boudreau and McCallum (1992) respectively suggested that settling chromite grains and ascending fluids which were rich in Fe-PGE alloys phases concentrated the PGE. MacCall (2016) have suggested that the BMS acted as collectors of PGE as PGM during the crystallisation of layered intrusions. Whilst Naldrett (2009) suggested that IPGE were concentrated separately by chromite grains which encapsulated laurite and alloys present in the magma, and the PPGE were concentrated separately by segregation of small amounts of sulphide liquid.

3.4. The froth flotation of platinum group minerals

Platinum-group elements are generally recovered from PGM using the flotation method in most operations including the TRP. The flotation method is a mineral processing (metallurgical) technique used to separate valuable minerals (PGM) from

gangue minerals (silicate, etc.) in ores. This method uses the hydrophobic (water repellent) nature of some PGM and BMS to separate from each other and from gangue. During the flotation process a frother is used to form bubbles, where the PGM are separated by attaching themselves to the bubbles due to their hydrophobic nature. The reagents such as sodium isobutyl xanthate, sodium ethylcellulose and dithiophosphate are used as collectors to encourage PGM attachment to the bubbles (Newell *et al.*, 2000; Kawatra, 2011; Rose *et al*., 2018).

The bubbles with PGM attached are referred to as froth. The froth floats (hence froth flotation) and gets separated by being concentrated as one product (hence concentrator), thus the processing plant can be referred to as concentrator, froth flotation or flotation plant. Material that are hydrophilic remains in the system and is flushed away as tailings (Newell *et al.*, 2000; Kawatra, 2011) (see Figure 3.6).

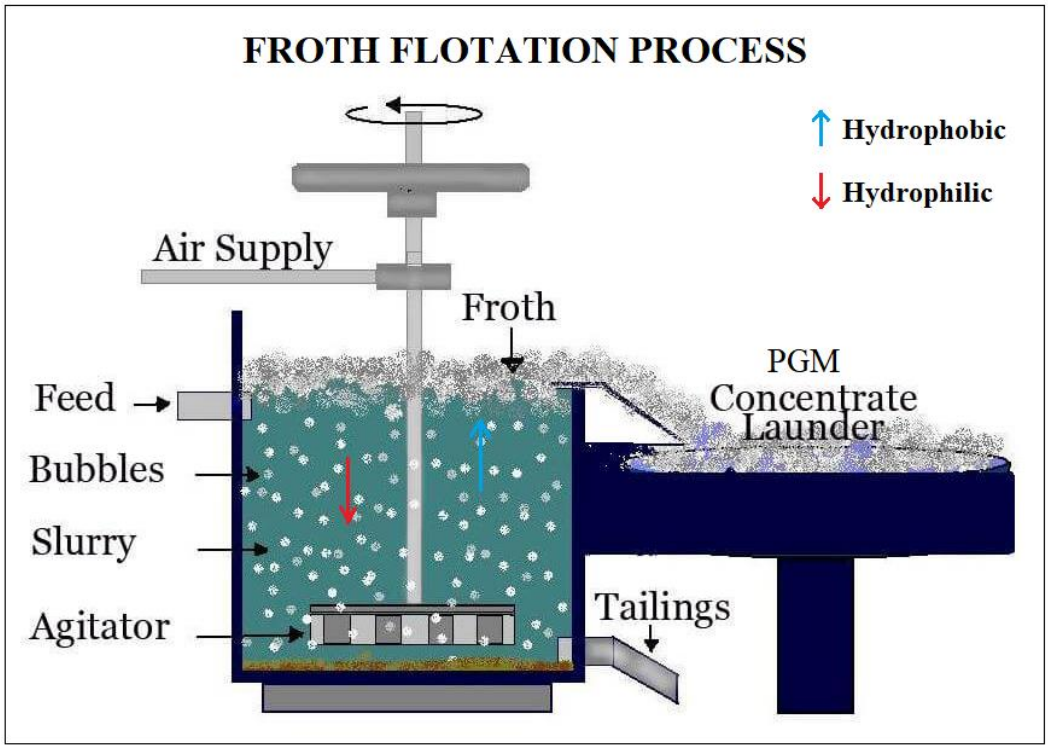

Figure 3.6: Illustration of the froth flotation process for the recovery of PGM (Michaud, 2021).

The recovery rates of PGM using froth flotation are influenced by process mineralogical factors such as textural relationships of PGM to other minerals (locked, liberated, etc.), PGM phases (type of mineral or composition) and abundance (amount of a PGM phase in relation to others), PGM association (shared grain boundary) and PGM grain size distributions (Penberthy *et al*., 2000; Penberthy 2001; Vermaak, 2005). Some PGM respond better to flotation than others. Table 3.1 summarises the flotation recovery rates of some of the most common PGM groups. For example, the PGE sulphides and arsenides floats better and faster than PGE tellurides and oxides (oxides respond very poorly to flotation), whilst the alloys have variable flotation rates (Vermaak, 2005).

Table 3.1: Simplified list of physical characteristics and recovery behaviour of some grouped PGM, adapted after Vermaak (2005).

PGM Group	Sizes	Density	Flotation Recovery
Sulphides	Often coarse	High	Good
Tellurides	Variable	Low	Poor
Arsenides	Variable	Medium	Good
Alloys	Often coarse	Very high	Variable
Oxides	Fine	Low	Very poor

The flotation rates of PGM have been widely studied (e.g., Penberthy *et al.* (2000), Vermaak (2005) and Shackleton (2007)). The PGM associated with BMS respond well to flotation compared to non-liberated PGM associated with silicates (Penberthy *et al*., 2000). The BMS also have varying rates of flotation (e.g., chalcopyrite floats better and faster than pyrrhotite). The flotation rates are also influenced by alteration effects, in that a fresh pyrrhotite will typically float better and faster than an oxidised pyrrhotite (Miller *et al*., 2005). Shackleton (2007) also indicated that flotation is more efficient if the BMS are moderately oxidised or not oxidised. The palladium-platinum group elements (PPGE) sulphides typically float better and faster that Iridium-PGE

(IPGE) sulphides (e.g., Laurite) and the flotation rates of very fine floatable particles are generally lower than that of coarser particles (Penberthy *et al.,* 2000).

In-house TRP information, TRP (2016) indicates that historically the understanding of PGE mineralisation was limited to BMS in silicate-rich rock and therefore the flotation plants were mainly designed to process PGE sulphides in silicates rich rocks, which substantiate the ease of flotation of PGE sulphide and PGM associated with BMS in the Merensky Reef (silicate-rich rock) compared to an oxide-rich rock (UG2 Reef). Now, with better understanding of the PGE mineralisation, and in particular, the characteristics of the PGM, the flotation plants are adjusted (calibrated) to accommodate non-sulphides PGMs (including in oxide-rich rocks). These adjustments amongst others are mostly done through developing reagents that will collect non-sulphide PGM during flotation. However, due to the complex chemistry and properties of PGM, there is variability in the effectiveness of reagents used in flotation plants. Thus, for example, reagents that effectively favour bismuth-tellurides may suppress sulphides. In this regard, the knowledge of PGM phases and modal abundance in the ores can assist effectively in determining the type and proportion of reagent to be used to collect the most abundant phases. Additionally, general industry knowledge indicates that the grain size distributions of the PGM provide information in determining the power used in the crusher to pulverise the rocks to a level of grain size suitable to liberate most of the PGM, noting however that very finely grounded rock may have adverse effects resulting in PGM remaining in the slurry and subsequently reporting to tailings.

CHAPTER 4 RESEARCH METHODS

4.1. Introduction

The purpose of this chapter is to elaborate on the procedures and techniques (analytical, interpretation and others) used to successfully reach the aims and objectives of the study.

4.2 Fieldwork and Sampling

4.2.1 Fieldwork

A mine visit was conducted in April 2019 to log and sample the drill cores made available by the TRP. The samples collected were analysed using three analytical techniques (1) reflected light microscopy, (2) mineral liberation analyser (MLA) and electron microprobe (EMPA). During the visit the resident geologists verbally shared some valuable published and unpublished information that assisted in better understanding the UG2 Reef and MR at the TRP.

Following the mine visit, the TRP Geology Team provided the Buffelshoek prospect assay data which included concentrations of the PGE, Cu, Ni, Co and Au in the UG2 Reef and MR at Buffelshoek. The assay data were obtained from analysing samples collected as half-core at an average interval of about 10 cm. The half-core samples were pulverised and analysed using X-ray Fluorescence (XRF) and Inductively coupled plasma mass spectrometry (ICP-MS) by the TRP. The assay data was reported as parts per million (ppm) for PGE and Au, and as percentages for Co, Ni and Cu.

4.2.2 Sampling

The boreholes BFH003D1, BFH003D2, BFH006D0, BFH006D0 and BFH007D0 were lithologically logged from where the deflections of the boreholes started. In the reefs, logging was completed on half-core remaining from initial sampling done by TRP. A list of samples and the analysis techniques used is provided in Appendix A. Figure 4.1 is a photo (not to scale) of the deflection D0 of BFH006 to show the borehole logged, and the half-core within the Reef.

Figure 4.1: A photo of borehole BFH006D0 to show the half-core logged and sampled (not to scale).

Quarter-core samples of about 10 cm each of the UG2 Reef and MR were collected from the boreholes. Cutting and sampling was completed at the TRP. The 10 cm samples were further cut at the University of Limpopo to about 2 - 3 cm systematically along the stratigraphy to prepare polished blocks (as seen in Figure 4.2). A total of 56 polished blocks were prepared. Using the TRP assay data, higher grade polished blocks were selected for further analysis to increase the chance of targeting the platinum group mineral (PGM) present.

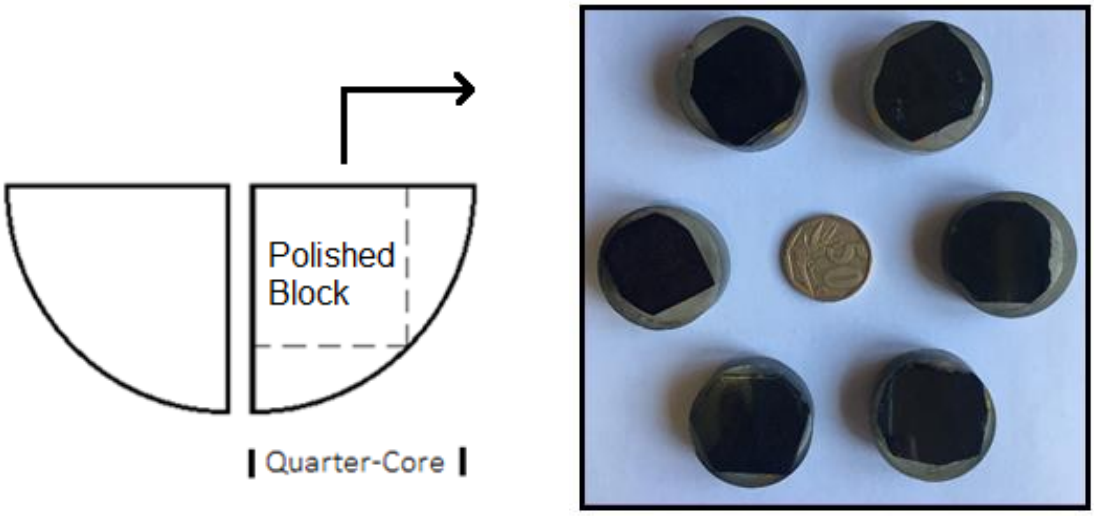

Figure 4.2: Illustration of the quarter core sampled, and a photo of the polished blocks prepared from the quarter core.

4.3. Reflected Light Microscopy

The polished blocks were initially studied using the Nikon Reflected Light Microscope (RLM) at the North-West University and University of Limpopo. The RLM (Figure 4.3) illuminates bright light on the polished stub through the objective (5x, 10x, 20x or 50x magnifier) and because the light cannot be transmitted through the stub it is reflected into the objective. Various ore minerals exhibit different properties that can be observed under plane and crossed polarised reflected light. These known properties were used to identify the visible ore minerals. Under the reflected light textural relationships of identified ore minerals in the stub (lithology) were identified. Nadeau and Davidson (2012) describe the RLM as the most sensitive and widely used microscopy to assess opaque specimens. In the field of geology and metallurgy the RLM is widely used to determine the textures of ores for genesis and mineral processing dating back to Short (1931), hence this technique was chosen.

Figure 4.3: Photo of the Nikon Microscope used for reflected light analysis.

4.4. Mineral Liberation Analyser

A FEI 600F field emission Mineral Liberation Analyser (MLA) coupled with Energy-dispersive spectrometers (EDS) and Back-scattered electron (BSE) grey scale setup was used to analyse high-grade samples, at the University of Johannesburg. The MLA is essentially an automated Scanning Electron Microscopy (SEM) which has proved its use in obtaining detailed process mineralogical information quickly and effectively (Gu, 2003; Fandrich *et al.,* 2007; Viljoen *et al.,* 2012; Pszonka and Sala, 2018; Schulz *et al.,* 2019). Quantitative mineralogy studies (for BMS and PGM samples) using the MLA initially employs extended backscattered image (XBSE), then a full EDS termed grain X-ray mapping (GXMAP) and a sparse phase liberation lite (SPL_Lt) routines, which operates on BSE grey level of 20 to 255. GXMAP is set-up for 3000 particles per run, 150x magnification and image size of 500 pixels at 15 microseconds per spot. SPL_Lt is set-up for 150x magnification and image size

of 500 pixels at 4 microseconds per pixel. The GXMAP and SPL_Lt are followed by the TouchUp option in the Image processing to eliminate the unknown from the initial analysis (Rose, 2016). A total of 44 high grade polished block samples were selected for the MLA analysis.

The following process mineralogical and geochemical data were derived:

- the modal mineralogy of the samples,
- the calculated assay data used to present sample's geochemistry, which should match the ICP / XRF assay data,
- the PGM phases and corresponding formula used, however in cases where the mineral chemistry of the PGM does not match any known minerals in webmineral.com, the formula was put as a PGM name for example (PdBiTe).
- The mass% of PGM minerals found (normalised to 100%) and number of PGM grains.
- The PGE deportment showing minerals that hosts (control) the Pd, Pt and Rh.
- The total PGM and the PGM subgroup grain size distribution data and the PGM association data.

4.5. Electron Microprobe Analyser

The Electron Microprobe Analyser (EMPA) was selected based on the ability to measure concentrations of elements in microscopic volumes of solid specimens and in geology, spot analysis of quantitative chemistry of minerals (Chatterjee, 2012; Rinaldi and Llovet, 2015; Osbahr *et al*., 2015; Cameca, 2018). For this study, the EMPA was used for spot analysis of the PGM.

Based on the results of the MLA, 17 samples were selected for analysis using the CAMECA SX-100 EMPA which is coupled with four vertical wavelength dispersive spectrometers (WDS) at the University of Johannesburg (photo of the EMPA can be seen in Figure 4.5). The EMPA set-up used, ran at 20 kV accelerating voltage and 40 nA electron beam current measuring S, Fe, Co, Ni and Cu on Kα lines, Os, Pb and Bi on Mα lines and the Pt, Pd, Rh, Ir, Ru, Au, Te, Hg, Sb, Ag, Zn, As, Sn and Se on Lα lines. All elements were calibrated on elemental reference materials except for S (pyrite), Sb (stibnite), Hg (cinnabar) and Pb (galena).

Figure 4.4: Photo of the EMPA facility at the University of Johannesburg taken during the analysis of the samples.

The analysis was completed by targeting grains mostly larger than 3 microns using colour contrast in BSE images, where brighter areas indicated heavier mean atomic numbers (i.e., PGM). These grains were spotted and analysed one at a time for all the elements setup in the WDS. The brighter phases were searched manually to

perform the spot analysis and some PGM were specifically searched for by plotting coordinates obtained from the MLA on the BSE images of samples on the Excel spreadsheet. Then the sample in the EMPA was orientated in the same direction to obtain the location of the PGM targeted. These specifically targeted grains (known PGM) were used to confirm the chemistry and existence of the PGM (e.g., mineral kharaelakhite was confirmed).

A total of 112 PGM grains were analysed. Grains larger than 3 microns gave total PGM chemistry compositions between 98 and 102 wt% which were used in this study. Grains less than 3 microns gave total PGM chemistry compositions of less than 98 wt% due to the size of the beam of the EMPA (3 micrometre diameter), which analyses the surroundings of the PGM if less than 3 micron resulting in a limitation of the EMPA to effectively analyse smaller grains, and therefore these results were not used.

4.6. Data Analysis

The open-source program Google Earth Pro was used to create geological maps using the geology obtained from the Council for Geoscience and to overlay the locations of the boreholes (data obtained from TRP) and the boundary of the study area (Buffelshoek 368 KT Farm boundary obtained from the Chief Survey General of South Africa). The open-source program R coupled with geochemical analysis add-on GCDKit were used to plot the binary and ternary diagrams of the chemistry data obtained from the TRP assay data, MLA data and EMPA data. Excel was extensively used to interpret the TRP assay data and MLA data.

CHAPTER 5 ORE PETROGRAPHY AND GEOCHEMISTRY

The purpose of this chapter is to present the textural relationships between BMS, PGM, silicates and / or chromite obtained from reflected light microscopy and BSE imaged from EMPA. The chapter will also present the PGM chemistry obtained from the EMPA, and samples geochemistry based on calculated assay data obtained from the MLA.

5.1. Textural relationships of base metal sulphides, platinum group minerals, silicates and chromite

The three UG2 Reef facies (Normal, Split and Multiple Split Reefs) have similar minerals and textural relationships, therefore the petrographic analysis of the UG2 Reef is not differentiated by Reef facies type and within the stratigraphy. The chromites (Figure 5.1 to 5.4 and Appendix B.1.1) in the UG2 Reef exhibit various textures. The medium to very coarse grained chromites are attributed to coalescence and recrystallisation of small grains. The chromite grains range from subhedral to anhedral and some of the grains shows annealing textures (including triple junctions).

Various silicate minerals were observed in the UG2 Reef, but not differentiated due to limitation to identification in the reflective light microscopy technique. The silicate minerals are mostly interstitial to chromites and some to BMS. The silicate minerals occur as inclusions in BMS and chromite in places, with some of these inclusions appearing very similar to replacement grains. In rare cases, the silicates exhibit intergrowth textures with chromites (e.g., Figure 5.2 E) and BMS (e.g., Figure 5.4

C). Some of the silicates observed are interstitial to BMS, whereas other silicates are enclosing the BMS. The silicates also exhibit subrounded to irregular textures.

The UG2 Reef is comprised dominantly of chromites with pentlandite and chalcopyrite occurring interstitial to chromite and silicate minerals. The pentlandite and chalcopyrite also exhibit intergrowth or replacement textures. Pyrrhotite is rarely found in the UG2 Reef samples (Figure 5.3 A) and often show intergrowth with pentlandite (Figure 5.3 D). Pentlandite, chalcopyrite and pyrrhotite also occur enclosed within silicates or chromite grains. The two most dominant BMS, pentlandite and chalcopyrite observed in the UG2 Reef, show variable grain shapes (Figure 5.4) from subhedral, anhedral to irregular.

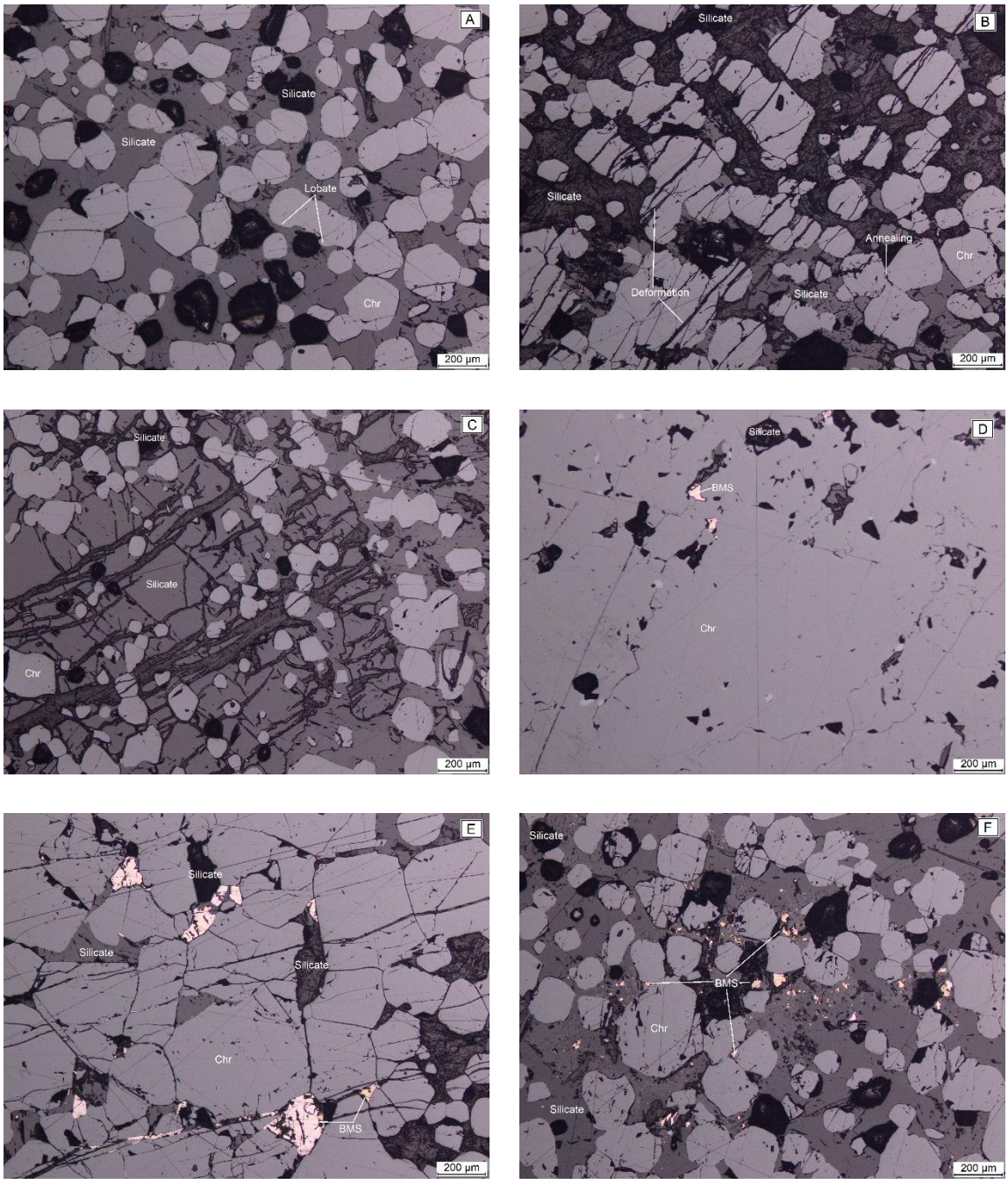

Figure 5.1: Photomicrographs (Plane Polarised Light - PPL) of the UG2 Reef showing some textures of chromite/s (Chr) to BMS and silicates. (A) Disseminated chromites with lobate texture and interstitial silicates, (B) Deformed chromites, (C) Chromites (fine to medium grains) associated with deformed silicate, (D) Completely recrystallised chromites, (E) Clustered chromites (very coarse) associated with BMS and (F) Disseminated BMS associated with chromites (fine to coarse grained).

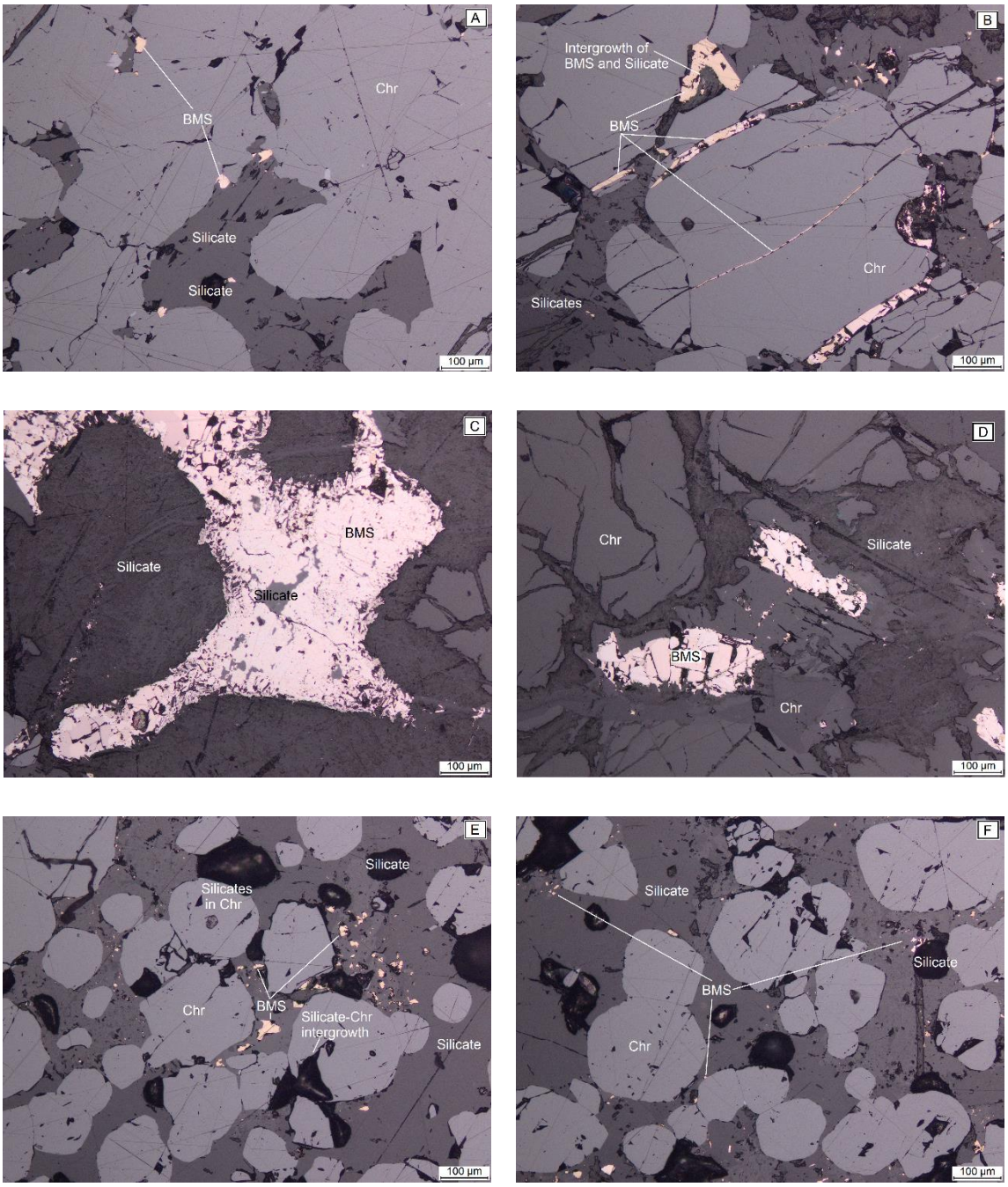

Figure 5.2: Photomicrographs (PPL) of the UG2 Reef showing some textures of BMS to chromites and silicates. (A) BMS occurring at grains boundaries of silicates and chromites, (B) BMS formed post deformation, (C) Massive BMS formed late enclosing silicates (inclusions), (D) Intergrowth of BMS formed before deformation and Disseminated (E) and Scattered (F) BMS within silicates and associated with chromites.

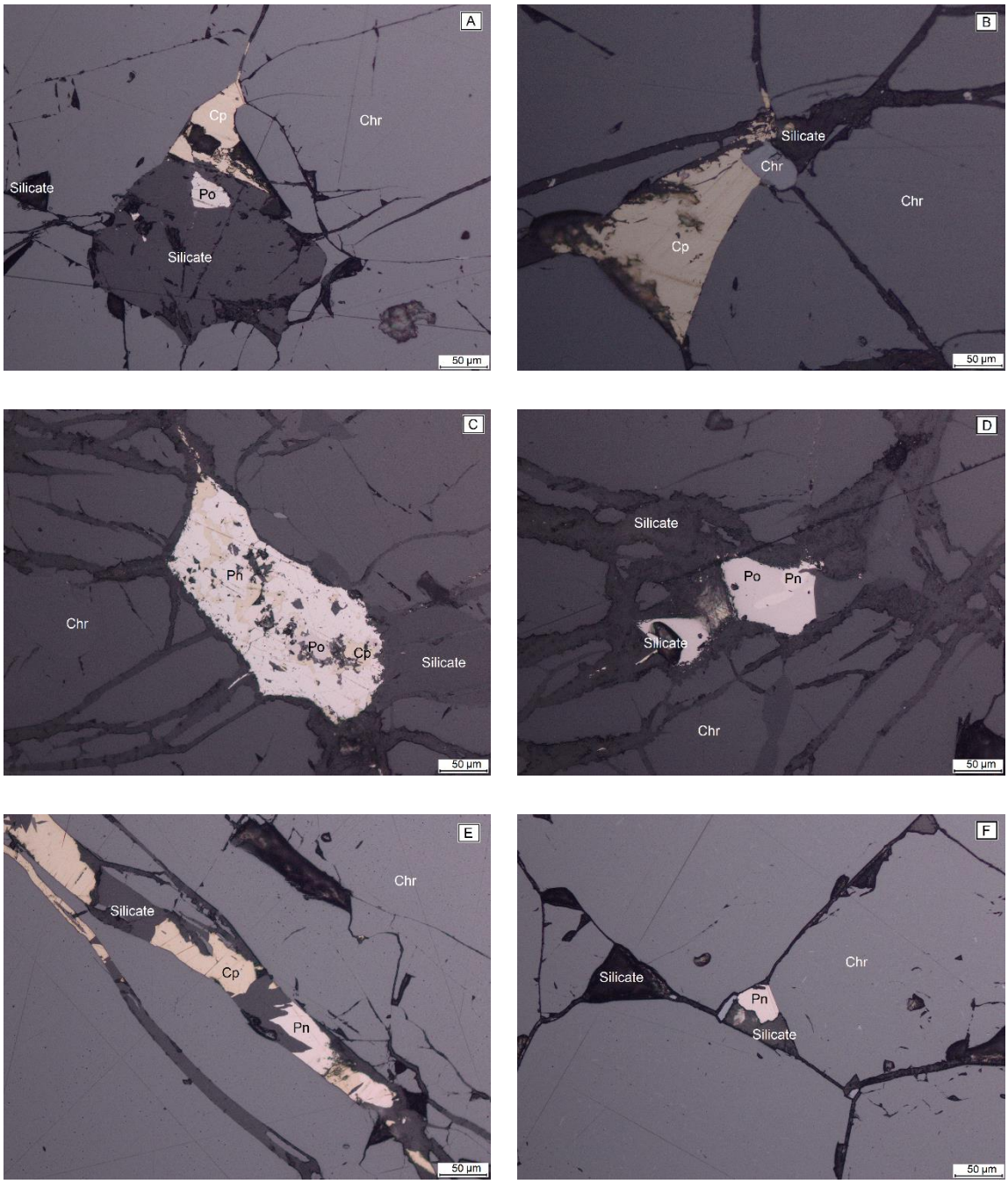

Figure 5.3: Photomicrographs (PPL) of the UG2 Reef showing identified BMS and their association. (A) Chalcopyrite [Cp] associated with silicate [Si] and chromite [Chr], then pyrrhotite [Po] associated with Si, (B) Cp associated with Si and Chr, (C) Pentlandite [Pn] enclosing Cp and Po, grain associated with Si and Chr, (D) Po associated with Si and Chr, Pn replacing Po, (E) Cp replacing Pn and (F) Pn associated with Si and Chr.

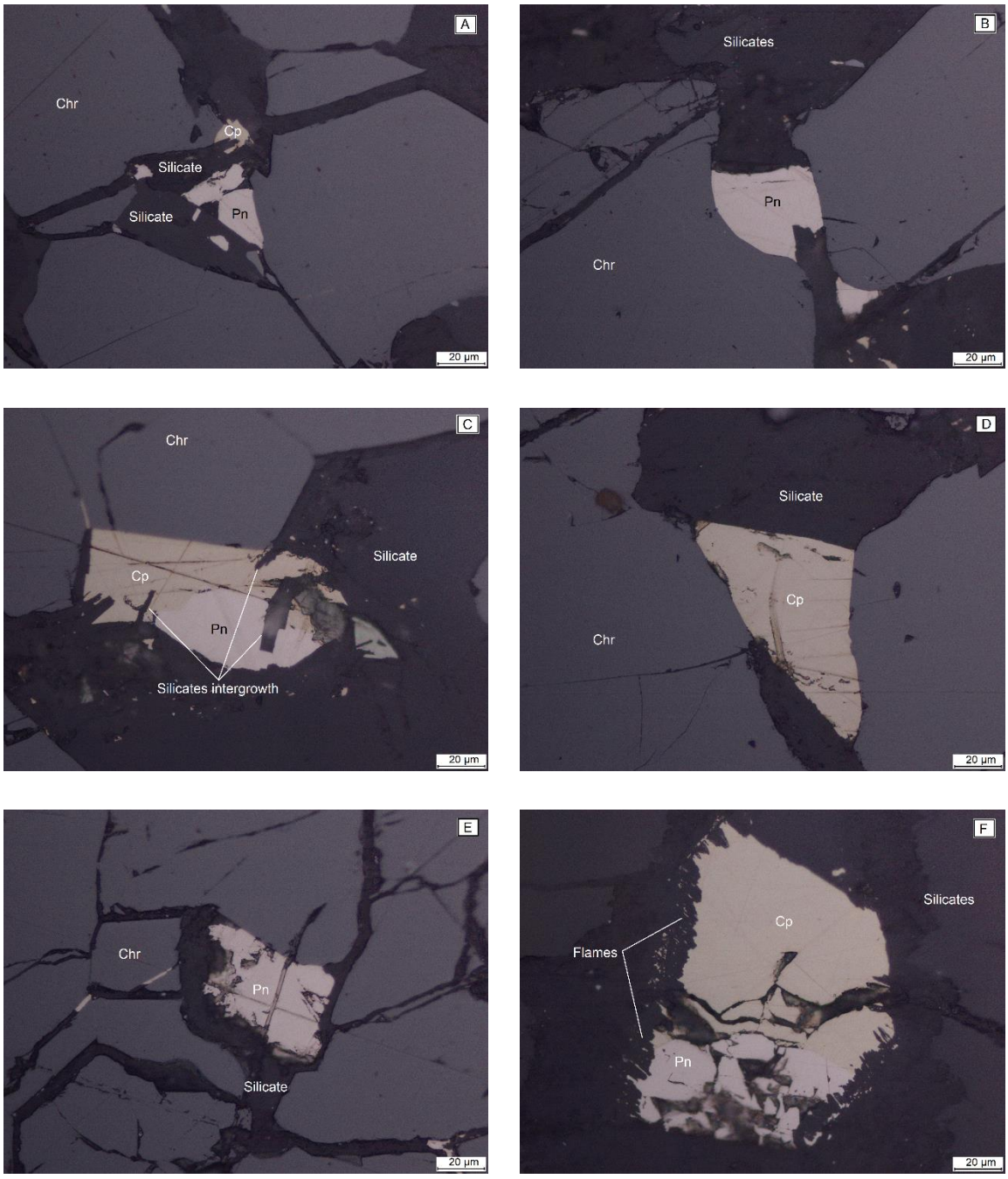

Figure 5.4: Photomicrographs (PPL) of the UG2 Reef showing subhedral to irregular grains of Pn and Cp identified. (A) Cp and Pn subhedral to irregular, (B) Subhedral Pn, (C) Irregular Cp and Pn, (D) Subhedral Cp, (E) Irregular Pn and (F) Irregular Cp and Pn.

The fine grained chromites are mostly disseminated cumulus probably formed by crystal settling during fractional crystallisation. The annealing texture can be attributed to slow cooling during crystallisation or slow heating during recrystallisation. The chromites also show post crystallisation deformation characteristics shown by the occurrence of fractures.

The MR samples exhibit very similar mineralogy and textures. The MR (Figure 5.5 to 5.7 and Appendix B1.2) is mostly comprised of silicate minerals which are interstitial to the BMS and chromites. Similar to the UG2 Reef, the silicate minerals are also not differentiated. Based on the dominant abundance of the BMS in the MR, most of the characterisation are for the BMS.

The BMS are found throughout the MR samples, from very fine (scattered) to very coarse (massive). Like the UG2 Reef the MR is also comprised mainly of three BMS (pentlandite, chalcopyrite and pyrrhotite) as observed and dominated by pentlandite and pyrrhotite followed by chalcopyrite. Unlike the UG2 Reef, the BMS in the MR mostly occur replacing one another (replacement textures) (Figure 5.5 D) or as intergrowths (Figure 5.6 E). The replacement textures are characterised by chalcopyrite replacing pentlandite and / or pyrrhotite and silicates replacing some BMS. The BMS generally exhibit sharp contacts between each other in the MR.

Pentlandite is commonly associated or occur as euhedral (blocky texture) grains along the boundary of pyrrhotite. Pyrrhotite occur mostly as large grains that are euhedral, subhedral to irregular, and associated / intergrown mostly with silicates. Chalcopyrite occurs mostly replacing other BMS and in places (Figure 5.7 B) occur as individual subhedral grains.

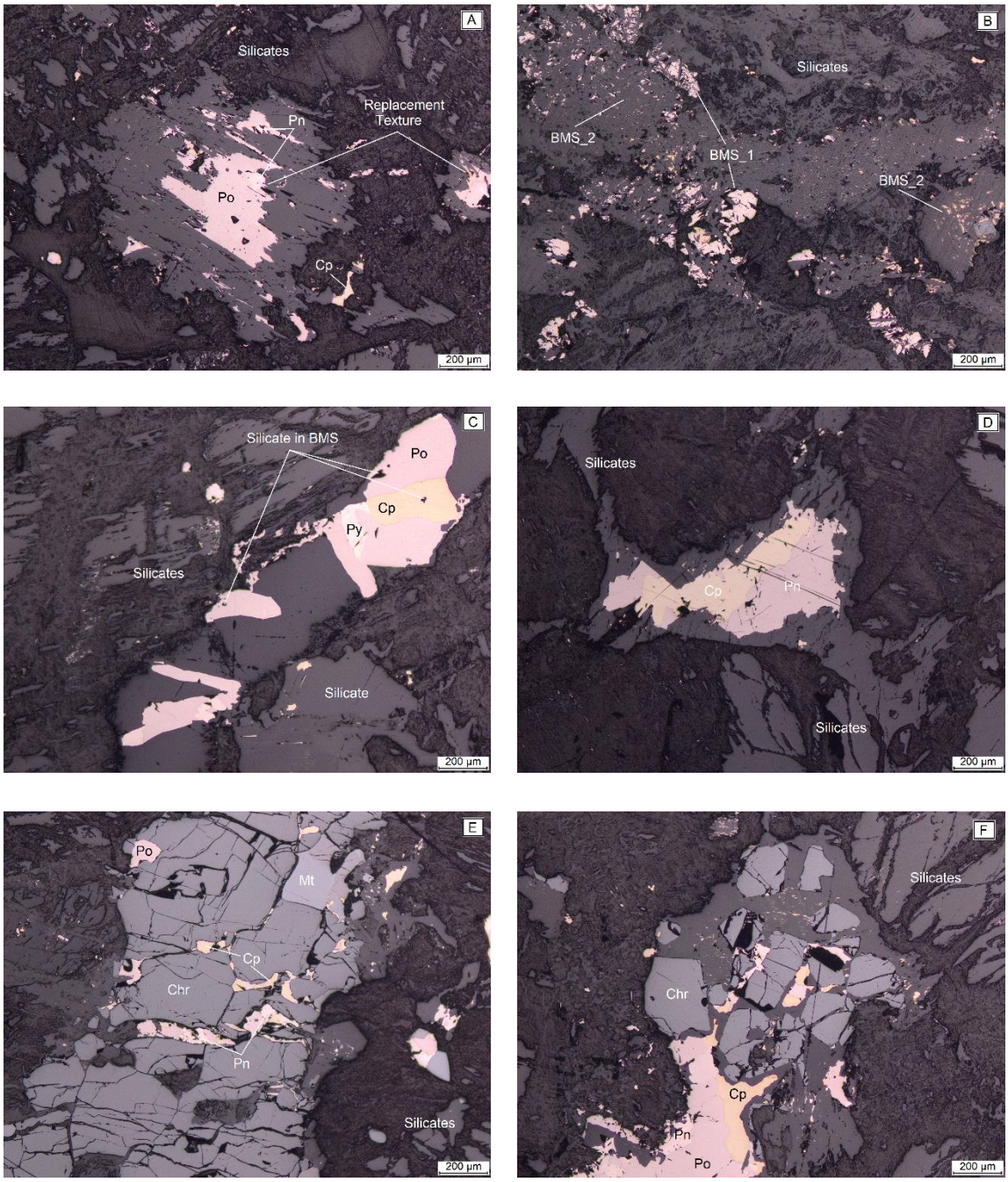

Figure 5.5: Photomicrographs (PPL) of the MR showing textures of silicates, chromites, BMS (including pyrite [Py]) and magnetite [Mt]. (A) Replacement of silicates by BMS, (B) BMS_1 formed post crystallisation, BMS_2 formed before recrystallisation – mottled with silicates, (C) Irregular shaped Py in Po, (D) Cp replacing Pn from within, grain replacing silicate, (E) Chromites in chromitite stringer associated with interstitial BMS and Mt and (F) Pockets of chromites in a silicate.

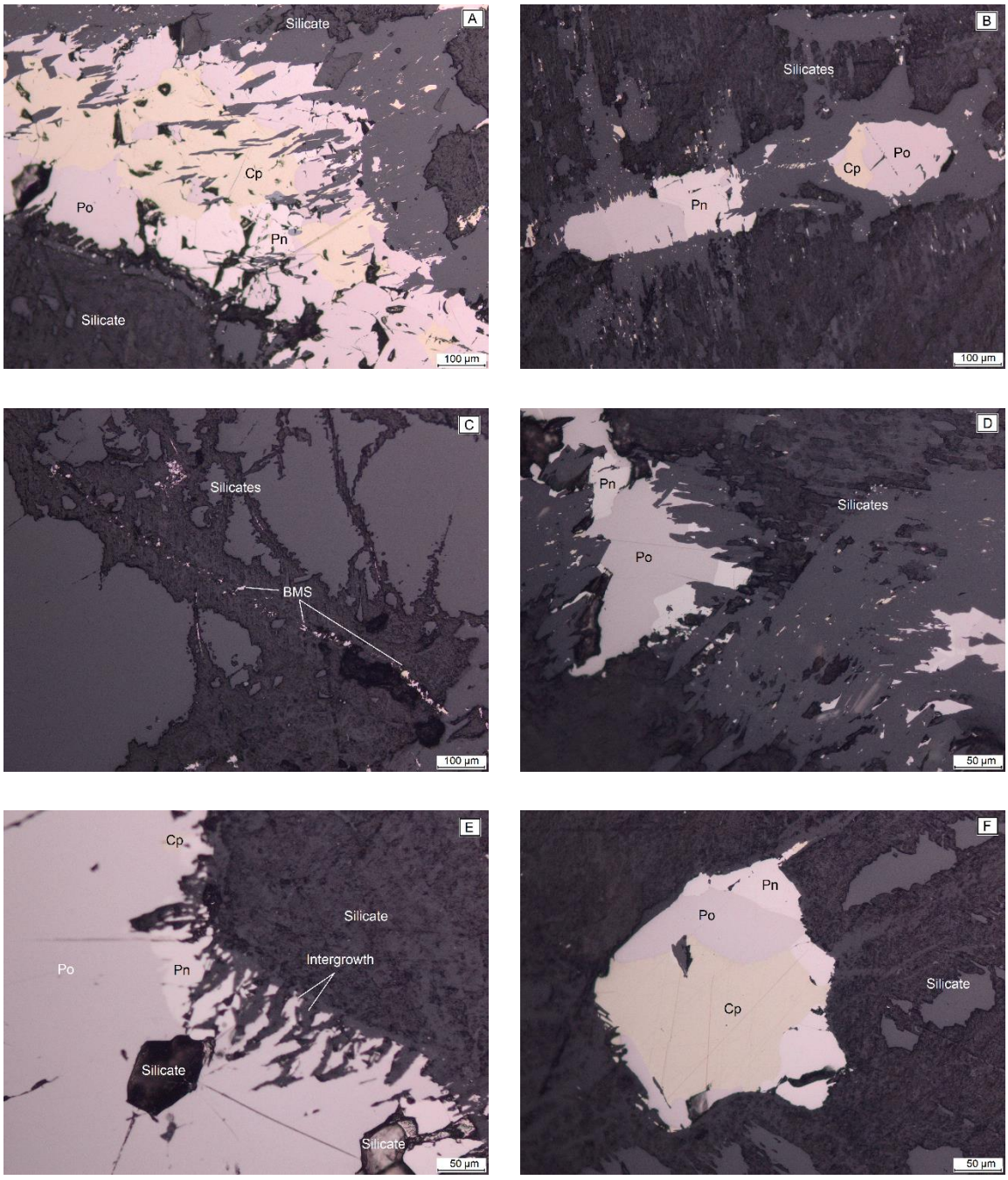

Figure 5.6: Photomicrographs (PPL) of the MR showing textures of BMS to silicates. (A) Replacement texture of silicates, Cp, Pn and Po, (B) Cp replacing Po from within, grain enclosed by silicates, (C) Disseminated BMS along veins, (D) Euhedral Pn along Po boundary, grain intergrowing with silicate, (E) Massive Po intergrowth with silicate and (F) Cp replacing Po and Pn.

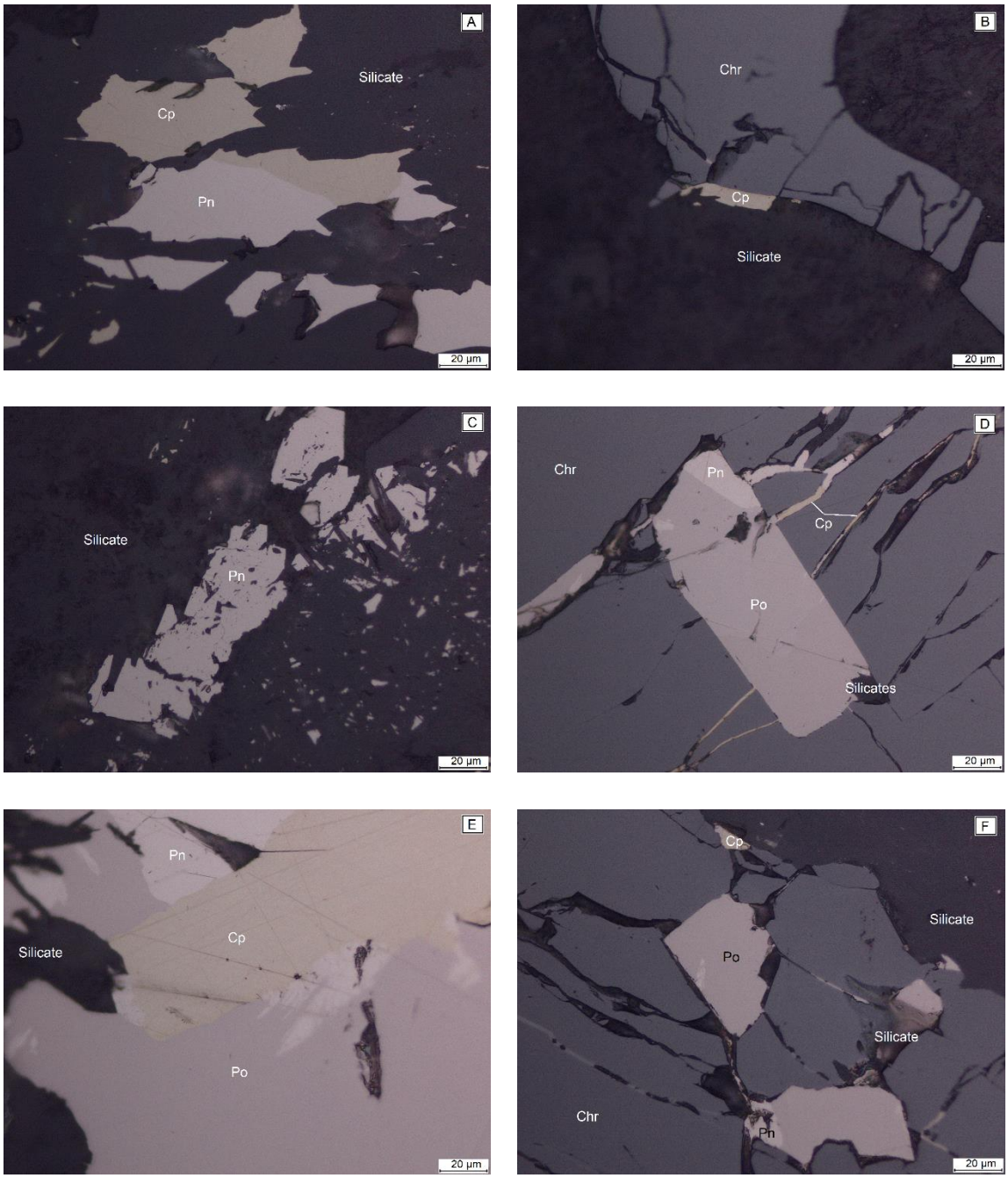

Figure 5.7: Photomicrographs (PPL) of the MR showing identified BMS and their association. (A) Cp and Pn associated with silicate, (B) Subhedral Cp associated with chromite and silicate, (C) Pn associated with silicate, (C) Cp, Pn and Po, and (D), (E) and (F) Cp, Pn and Po associated with chromites and silicates.

The textures observed in Figures 5.5 to 5.7 and Appendix B.1.2 are attributed to various stages of BMS mineralisation, in that some silicates occur within BMS and some BMS occur within silicates, where the minerals occurring within indicates earlier formation. The chromites in the MR occur as minor pockets (Figure 5.5 F) and as chromitite stringers (Figure 5.5 E). In rare instances, minor amounts of pyrite (Figure 5.5 C) and magnetite (Figure 5.5 E) grains were observed.

The PGM in the UG2 Reef and MR are generally sub-microscopic and therefore were only observed using more advanced analytical techniques such as EMPA and MLA. Figure 5.8 shows some of the PGM observed using the EMPA. The PGM are not differentiated by phases or groups (e.g., PGE sulphides or arsenides, etc) and their grains are generally subrounded to irregular in shape. As shown in Figures 5.8 to 5.11, the PGM are mostly associated with BMS, silicate and chromite.

The larger PGM grains (greater than 10 microns) may be observed under a reflected light microscopy and these minerals exhibit the following properties: grey colour, no bireflectance / pleochroism under plane polarised reflected light and are isotropic under crossed polarised reflected light. Detailed ore petrographic investigation of the PGM under reflected light microscopy was beyond the scope of this study. Below (Figure 5.11) is an example of a PGM under reflected light.

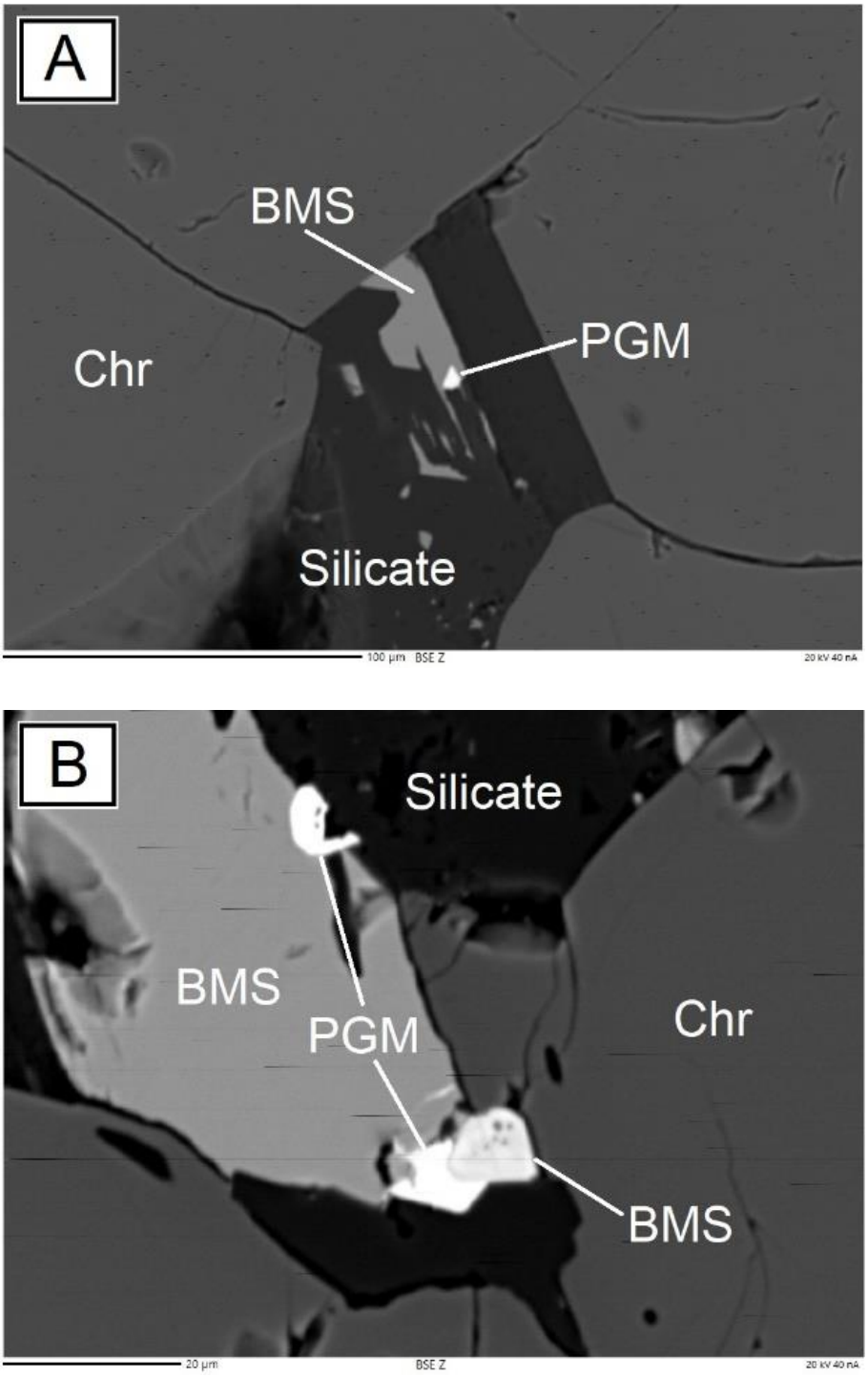

Figure 5.8: Backscattered electron (BSE) images showing textures and association of PGM in the UG2 Reef. (A) PGM associated with BMS and Chromite and (B) PGM associated with BMS.

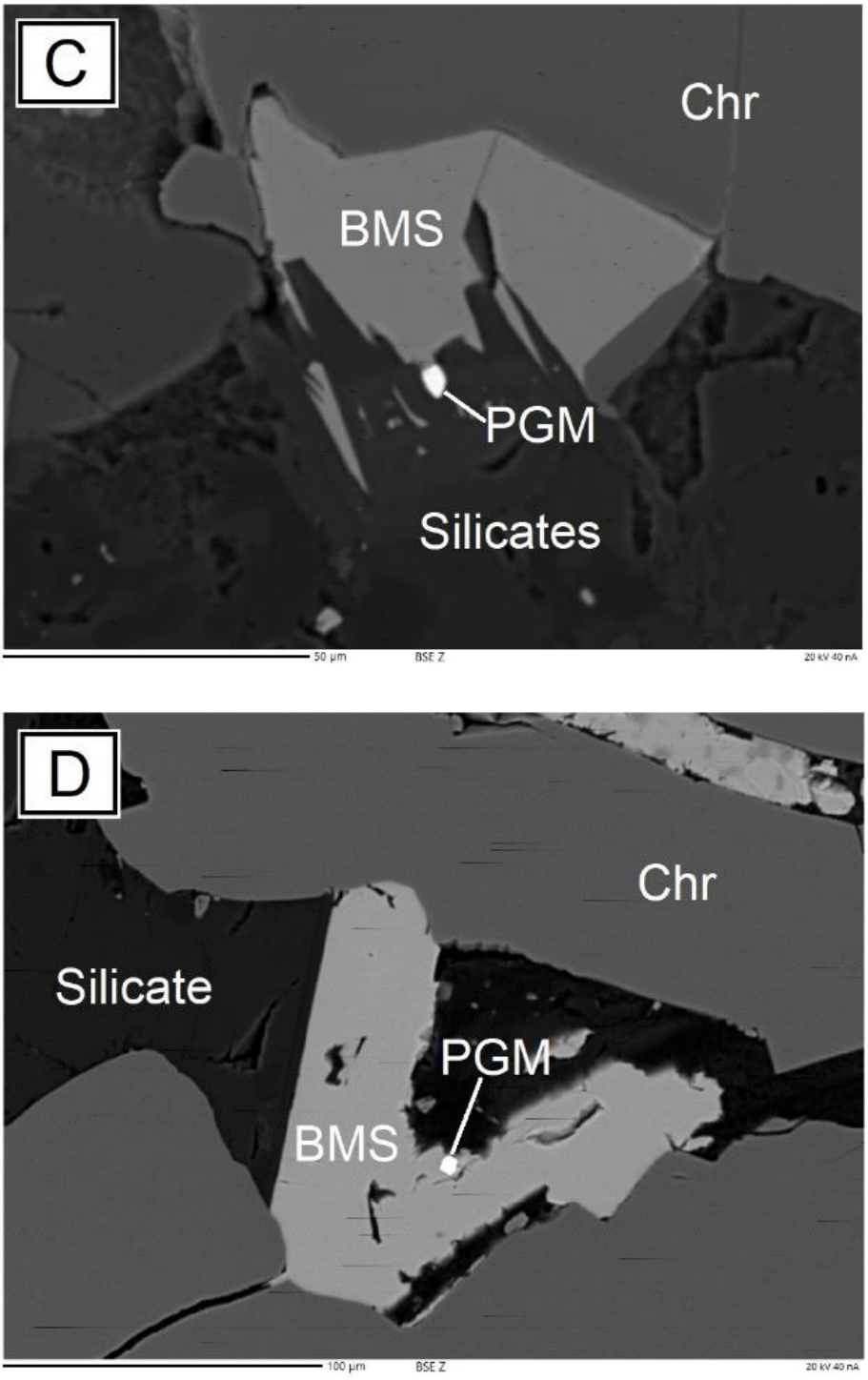

Figure 5.9: Backscattered electron (BSE) images showing textures and association of PGM in the UG2 Reef. (C) and (D) PGM associated with BMS and silicates.

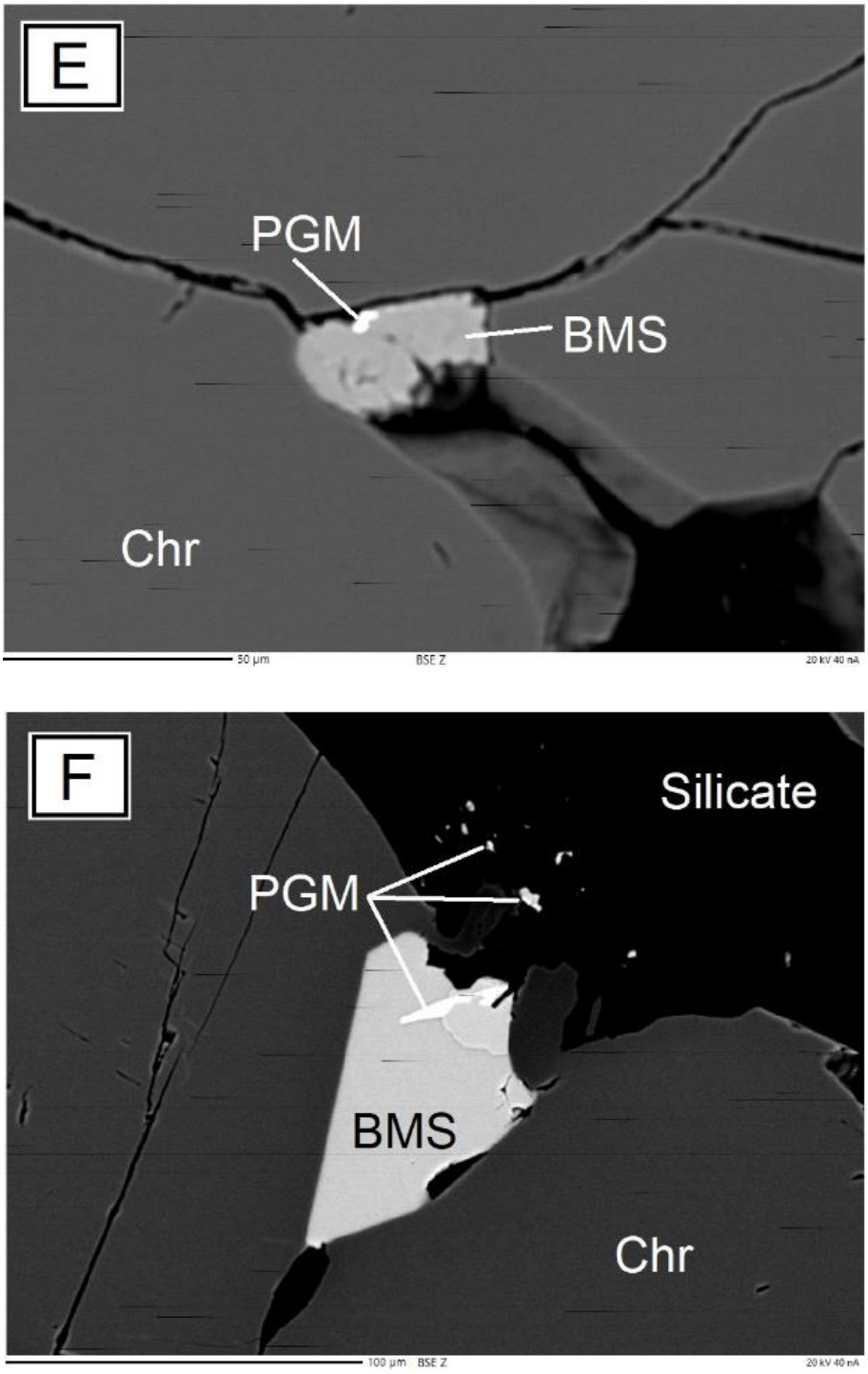

Figure 5.10: Backscattered electron (BSE) images showing textures and association of PGM in the UG2 Reef. (E) PGM associated with BMS and Chromite and (F) PGM in BMS and PGM enclosed in silicates.

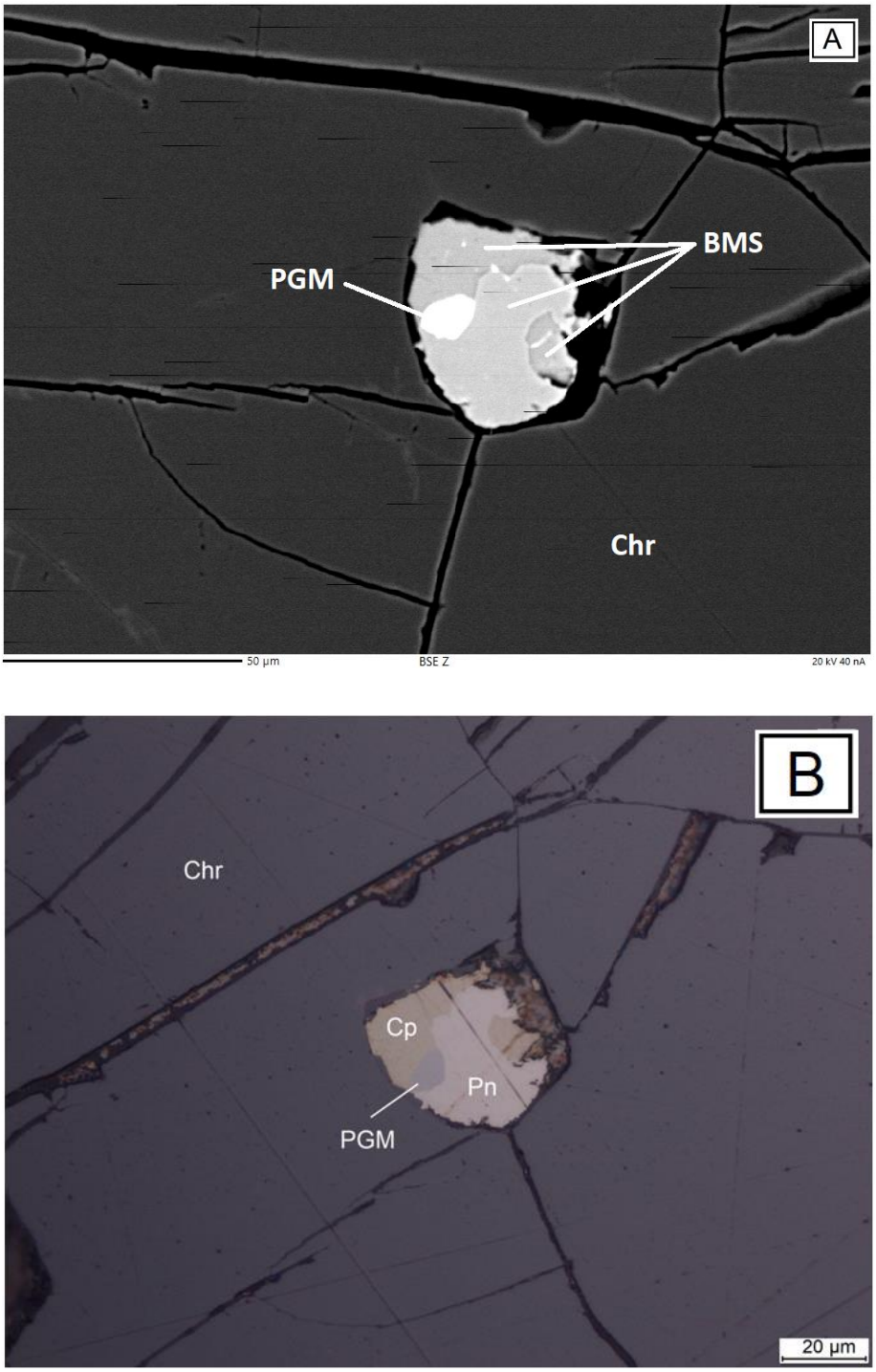

Figure 5.11: A PGM mapped with EMPA – BSE image (A) and an example of the same PGM observed under reflected light microscope – photomicrograph (B).

5.2. Platinum group mineral chemistry

The PGM analysed are classified into eleven groups, namely, (1) PGE-Fe-S-Cu-Ni-Pb (2) PGE-S-As, (3) PGE-As, (4) PGE-Bi-Te, (5) PGE-Cu-S, (6) PGE-Cu-Fe-S, (7) PGE-Ni-Fe-S, (8) PGE-Ni-S, (9) PGE-Fe-S, (10) PGE-S and (11) PGE-Alloys / Complex. The groups are based on the dominant elemental compositions and relatable PGM. A summary of the grouping is shown in Table 5.1 and the whole set of the mineral analysis results obtained from EMPA are detailed in Appendix C. The minerals kharaelakhite, cooperate, laurite, sperrylite, PtIrRuOsSAs (unknown), PdBiTe (unknown), and Pt-Fe (alloy) were specifically targeted.

The grouped PGM exhibit considerable compositional variation of PGE content up to 83 wt%. The individual PGM are presented in each group and Appendix D1.1. shows the PGM mapped by MLA and their general formulas which can be referred to for this section. The most seen PGM are in Groups PGE-S, PGE-Ni-S (including PGE-Ni-Fe-S and the PGE-Fe-S-Cu-Ni-Pb respectively), and this can be associated with abundance and larger grain sizes of these PGM.

Table 5.1: Selected PGM chemistry to illustrate the grouping of the PGM composition from EMPA results.

Group	As	Bi	Te	Cu	Ni	Fe	Sb	Pb	S	Pd	Pt	Rh	Ru	Ir	Os	Others	Total
Group 1: PGE-Fe-S-Cu-Ni-Pb	0,00	0,04	0,00	**8,11**	**7,12**	**7,92**	0,00	**24,02**	**19,74**	0,02	32,18	0,10	0,00	0,00	0,00	0,06	99,31
	0,00	0,00	0,00	**8,57**	**7,02**	**7,48**	0,00	**23,83**	**19,86**	0,01	32,47	0,06	0,02	0,06	0,03	0,35	99,76
	0,00	0,03	0,00	**7,51**	**9,09**	**8,96**	0,01	**22,29**	**21,28**	0,00	30,48	0,07	0,00	0,00	0,00	0,33	100,06
Group 2: PGE-S-As	**2,76**	0,00	0,00	0,00	0,43	2,36	0,01	0,00	**36,03**	0,54	0,34	0,21	**43,91**	8,20	5,69	0,08	100,56
Group 3: PGE (Pt)-As	**41,98**	0,00	0,01	0,21	0,01	1,12	0,87	0,10	0,34	0,00	**53,47**	0,03	0,03	0,79	0,05	0,21	99,22
Group 4: PGE-Bi-Te	0,05	**13,25**	**53,36**	0,00	3,17	0,64	0,02	0,00	0,01	7,32	21,61	0,02	0,01	0,00	0,04	0,16	99,66
	0,00	**11,08**	**54,26**	0,04	2,44	1,15	0,04	0,05	0,04	6,87	23,59	0,00	0,00	0,00	0,04	0,10	99,70
	0,00	**30,69**	**27,69**	0,02	0,79	0,94	0,01	0,84	0,03	39,27	0,00	0,00	0,00	0,00	0,00	0,10	100,39
Group 5: PGE-Cu-S	0,00	0,00	0,00	**12,51**	0,92	1,00	0,03	0,05	**28,24**	0,00	37,58	6,56	0,21	7,57	0,34	4,71	99,72
	0,00	0,00	0,01	**12,51**	3,72	2,23	0,03	0,07	**29,40**	0,00	39,29	6,38	0,01	0,79	0,03	5,61	100,08
Group 6: PGE-Cu-Fe-S	0,00	0,00	0,00	**6,78**	8,40	**6,01**	0,04	0,11	**26,01**	0,91	35,93	9,20	0,04	4,07	0,02	1,05	98,57
	0,01	0,03	0,00	**11,24**	0,11	**17,20**	0,00	0,04	**12,91**	0,00	59,05	0,00	0,00	0,00	0,03	0,01	100,63
Group 7: PGE-Ni-Fe-S	0,00	0,00	0,00	0,00	**40,75**	**23,90**	0,02	0,00	**33,47**	0,03	0,01	0,00	0,00	0,00	0,01	1,67	99,86
	0,00	0,00	0,00	0,01	**31,93**	**33,88**	0,00	0,01	**33,45**	0,40	0,00	0,05	0,06	0,03	0,01	0,62	100,45
Group 8: PGE-Ni-S	0,01	0,00	0,00	0,04	**7,55**	0,66	0,02	0,03	**19,75**	23,56	48,22	0,00	0,02	0,00	0,01	0,19	100,06
	0,00	0,02	0,03	0,00	**62,09**	0,60	0,00	0,00	**35,58**	0,00	0,02	0,01	0,01	0,00	0,04	1,97	100,37
	0,01	0,00	0,00	0,00	**61,91**	0,79	0,00	0,01	**35,73**	0,00	0,00	0,00	0,03	0,01	0,02	1,98	100,49
Group 9: PGE-Fe-S	0,01	0,00	0,00	0,46	4,80	**14,74**	0,00	0,06	**5,89**	0,06	72,01	0,10	0,19	0,00	0,05	0,20	98,57
	0,00	0,00	0,00	0,05	2,08	**6,14**	0,00	0,03	**20,56**	0,15	69,76	0,00	0,00	0,00	0,05	0,06	98,88
	0,00	0,00	0,00	0,00	39,50	**24,10**	0,00	0,03	**33,26**	0,04	0,02	0,14	0,00	0,02	0,01	1,57	98,69
	0,31	0,00	0,00	0,00	0,43	**12,11**	0,05	0,00	**40,66**	0,53	0,02	1,64	37,65	4,15	2,10	0,21	99,86
Group 10: PGE-S	0,00	0,01	0,02	0,08	1,75	1,11	0,01	0,28	**17,23**	0,88	**77,01**	0,11	0,04	0,00	0,00	0,17	98,70
	0,00	0,00	0,00	1,33	0,80	1,62	0,00	0,01	**15,91**	1,07	**79,30**	0,01	0,01	0,00	0,02	0,10	100,18
	0,09	0,00	0,00	0,24	0,13	1,21	0,03	0,00	**37,63**	0,57	0,03	0,86	**51,57**	2,93	5,23	0,08	100,60
	0,26	0,00	0,00	0,01	0,33	2,75	0,00	0,01	**36,06**	0,55	0,01	0,82	**48,03**	4,60	7,14	0,09	100,66
Group 11: PGE-Alloys / Complex																	
PGE-Bi-Te-As	**16,07**	**9,41**	**36,12**	0,01	1,74	1,54	0,02	0,00	0,11	4,86	29,26	0,12	0,00	0,03	0,01	0,69	97,26
PGE-Sb (-Cu-Fe-As)	**2,49**	0,00	0,00	**2,02**	0,02	**2,72**	**24,13**	0,02	2,20	**65,43**	0,04	0,00	0,00	0,00	0,00	0,36	99,43

The **PGE-Fe-S-Cu-Ni-Pb** group contains Pt (about 30 wt%) as the main PGE, with Ir as the second most abundant PGE. The mineral kharaelakhite is the main Pt carrier in the group 1 minerals. Kharaelakhite is one of the most dominant PGM at the Buffelshoek and it is very rare in literature, therefore this mineral has been confirmed with EMPA as shown in the BSE image (Figure 5.12).

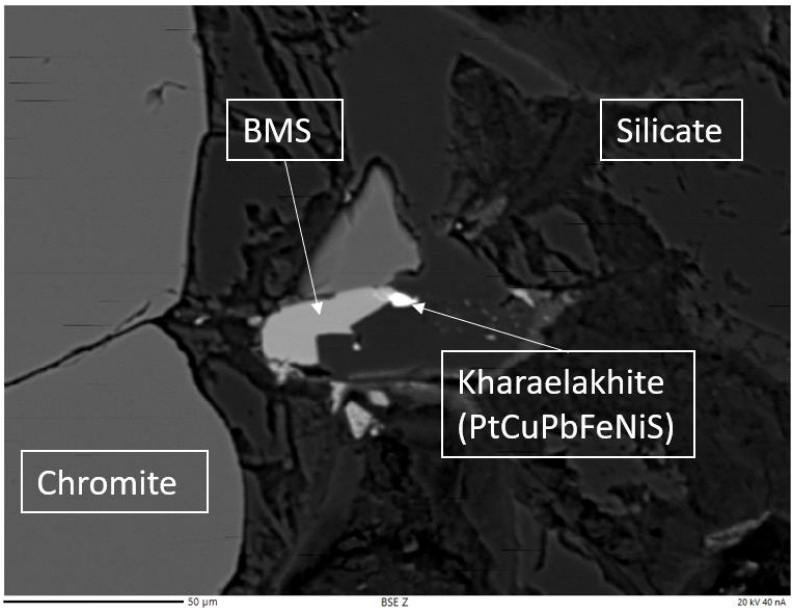

Figure 5.12: BSE image from EMPA showing kharaelakhite in the UG2 Reef confirmed by quantitative mineral chemistry.

The **PGE-S-As** and **PGE-As** groups contain Pt as the dominant PGE with varying compositions. Ruthenium shows dominance in some of the mineral phases and there is variable occurrence of Ir, Os, Rh, Pd in other mineral phases. The mineral phases in the Groups 2 and 3 include hollingworthite, platarsite, sperrylite, atheneite, palladoarsenide, and unnamed phases (PtPdSAs), (PtAsRhS), (PtIrRuOsSAs), (PdAsNi), (PtSbAs), and (PtPdAsSb). Figure 5.13 shows a plot of the PGM composition of the Groups 2, 3 and 11. Some minerals grouped as PGE-Complex (complex PGM) in Group 11 contains Pt-As-S and are presented later.

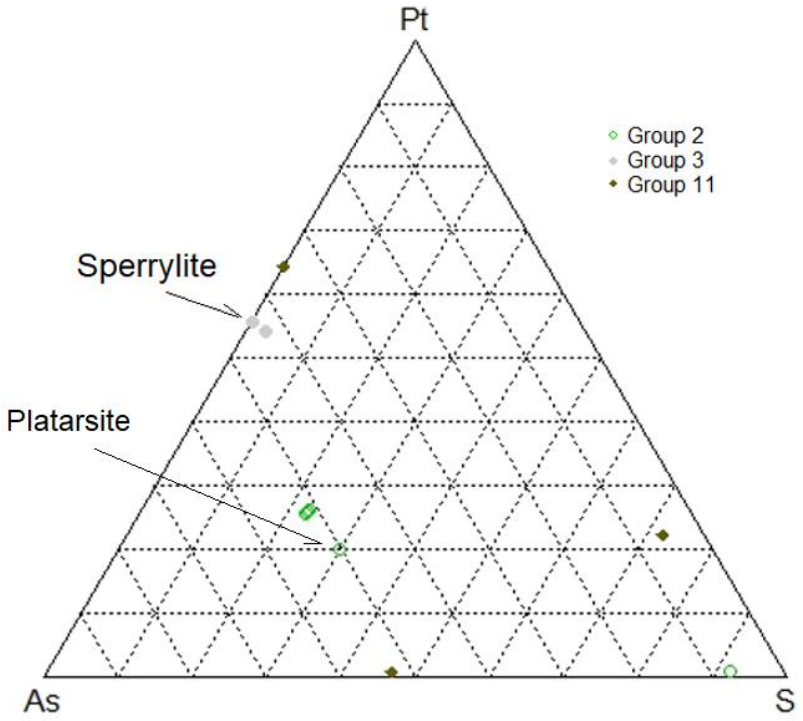

Figure 5.13: Ternary diagram of the composition in wt% of the PGE-S-As and PGE-As minerals at Buffelshoek. Vertices of the ternary plot adopted from Vermaak (2005).

The **PGE-Bi-Te** contain Pt in varying contents (20 - 40 wt%) as the dominant PGE. Pd is dominant in some minerals and generally the remaining PGE content consisting of Rh, Ir, Ru and Os are less than 1 wt%. The PGM in Group 4 includes moncheite, maslovite, merenskyite, kotulskite, michenerite, temagamite, pasavaite, keithconnite, sobolevskite, potarite, polarite, froodite, insizwaite, (PdTeBi), (PtBiTe) and (PdPtBi). Figure 5.14 shows plots of the PGM composition of the Groups 4 and 11. Some minerals grouped as PGE-alloys in Group 11 contains Bi-Te and are presented later.

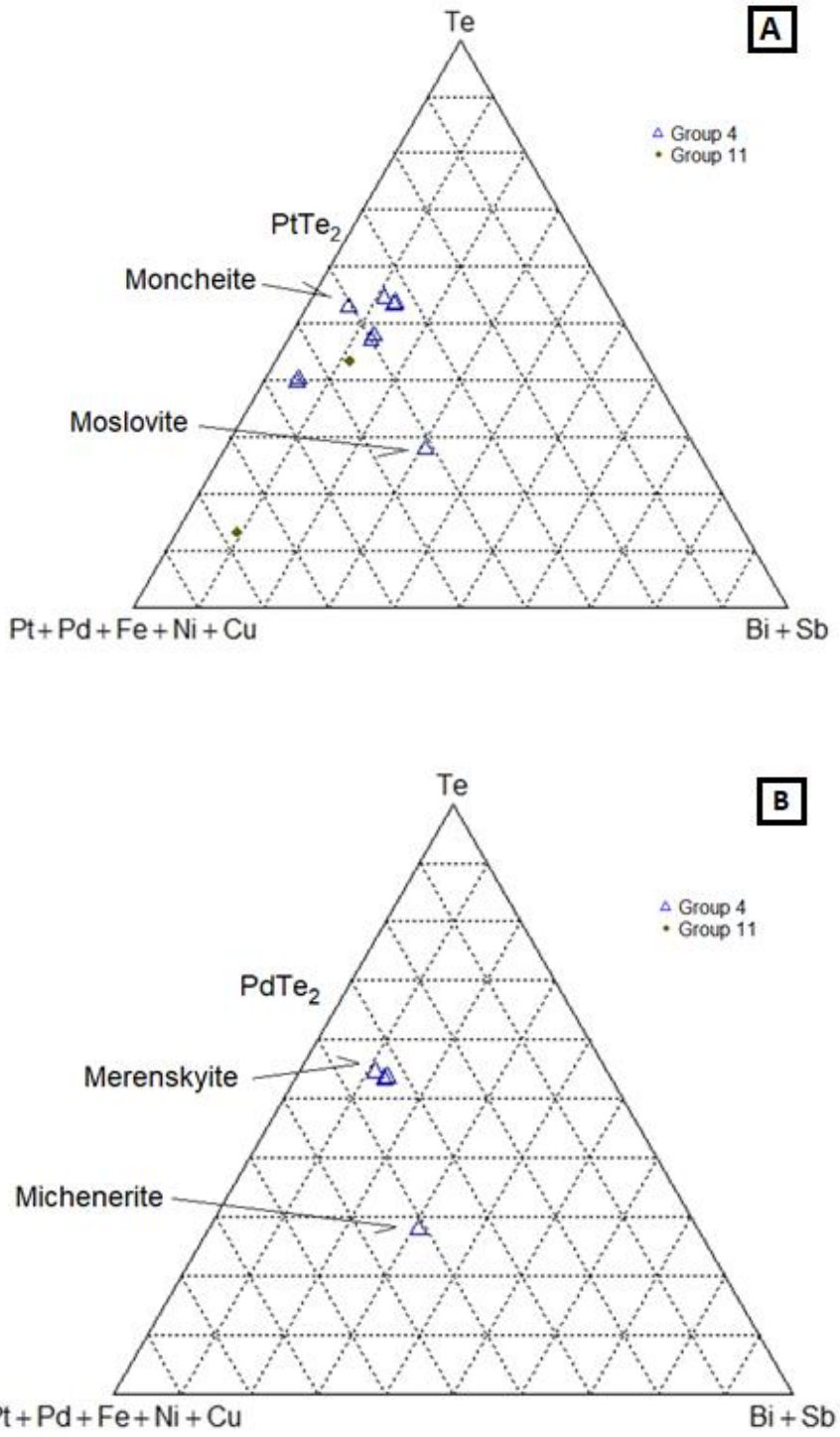

Figure 5.14: Ternary diagrams of the composition in wt% of the Pt-Bi-Te at the Buffelshoek. (A) Pt dominated and (B) Pd dominated. Vertices of the ternary plots are adopted from Vermaak (2005).

The **PGE-Cu-S** and **PGE-Cu-Fe-S** groups contain Pt with variable contents up to 78 wt%, followed by Rh and Ir in their abundance. Other PGE (Pd, Ru Os) contents are generally less than 1 wt%. The main PGM in these two groups (Groups 5 and 6) is (PtRhCuS). The BMS chalcopyrite can be attributed to be the (CuFeS) containing PGE, however it is not reported as PGM in the MLA results.

The **PGE-Ni-S** and **PGE-Ni-Fe-S** groups commonly contain Pd or Pt in variable proportion as the dominant PGE, followed by Ru (< 3 wt%) and generally < 1 wt% of other PGE (Rh, Ir and Os). The Groups 7 and 8 PGM include braggite, vysotskite and Group 11 PGE-alloys typically ferronickelplatinum.

The **PGE-Fe-S** and **PGE-S** groups mostly contain Pt and Ru as the dominant PGE. The remaining PGE are less dominant but present in abundance of > 1 wt%. The PGM in Groups 9 and 10 includes mainly laurite, erlichmanite and cooperite. Figure 5.15 is a plot of Ru, Ir and Os where S is assumed to be fixed as S_2 to represent the composition of these three PGE.

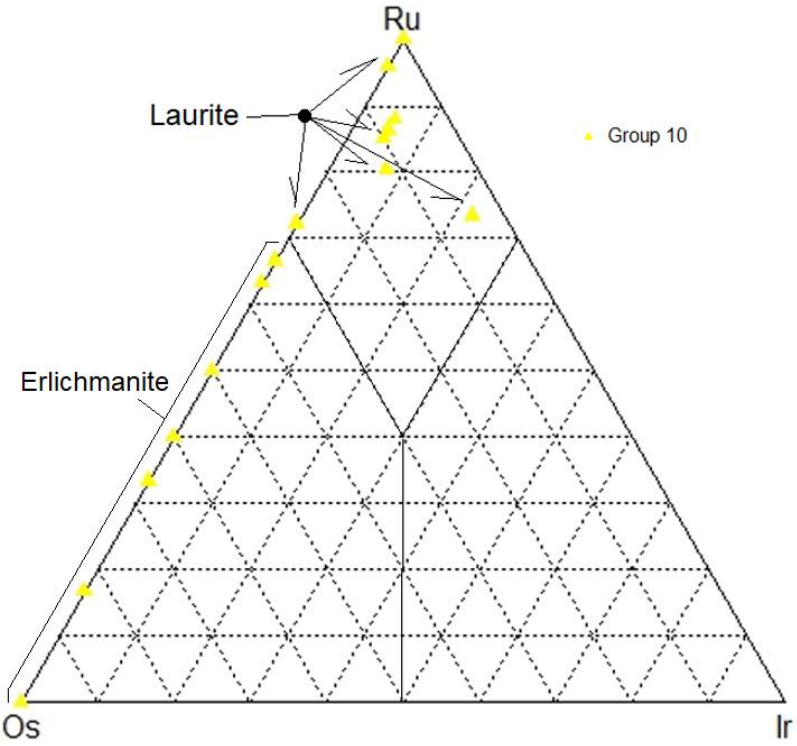

Figure 5.15: Ternary diagram of the composition in wt% of Ru-Os-Ir for the PGE-S minerals at Buffelshoek.

The PGM (Group 11), **PGE-alloys / complex** contains variable abundances of the PGE, which includes PGE-Bi-Te-As-Ni-S, PGE-Bi-Te-As, PGE-Cu-Fe-Ni-S, PGE-Sb-Cu-Fe-As and PGE-Fe. The complex PGM within Group 11 containing Bi-Te were compared to the PGE-Bi-Te group (Group 4) and there was no correlation observed.

5.3. Geochemistry based on Mineral Liberation Analysis

This section presents variations of minor and major elements of the UG2 Reef and MR at Buffelshoek based on the sample's geochemistry from the calculated assay data obtained from the MLA. The distribution of various elements in the different UG2

Reef facies (Figures 5.16 to 5.19), generally overlaps, however the overall geochemistry can be distinguished to that of the MR.

The MR is characterised by higher Mg# (where Mg# = Mg / (Mg + Fe)) and Mg, Si, Mn, Cu and S contents with lower Cr# (where Cr = Cr / (Cr +Al)) and Fe, Al, Cr and Ti contents. The UG2 Reef is characterised by higher Cr# and Fe, Al, Cr and Ti contents with lower Mg# and Mg, Si, Mn, Cu and S. In both the UG2 and MR the content of Ca is lower compared to Al, and the Ni and (Fe + Mg) contents overlaps. The cryptic variations of these elements differentiate the UG2 Reef from the MR at the Buffelshoek, generally forming two populations (Figures 5.16 to 5.19).

The UG2 Reef is generally characterised by; Cr increasing with Fe, (Cr + Al) increasing with Fe and (Si + Mg) increasing as (Ni + Cr) decreases. In both the UG2 Reef and MR, generally Mg increasing as Al decrease, Si increase as Fe decrease, Si increase with Mg and V increase with Cr, and two distinct populations of the Reefs chemistry is observed.

In the MR, generally Mg# > 0.35, Mg > 10, Si > 15, S > or = 1, Cu > 0.15 and in the UG2 Reef Cr# > 0.5, Cr > 15, Fe > 12.5, Al > 6.5, Ti > 0.2, V > 0.06 and Ni + Cr > 15 and Co > 0.012 (Figures 5.16 to 5.18), all these values are in percentage. The (Na + K + Al) contents in the UG2 Reef is generally more than that of the MR, yielding to distinct populations when compared to the (Fe + Mg + Ca) and Si in a ternary plot (Figure 5.19).

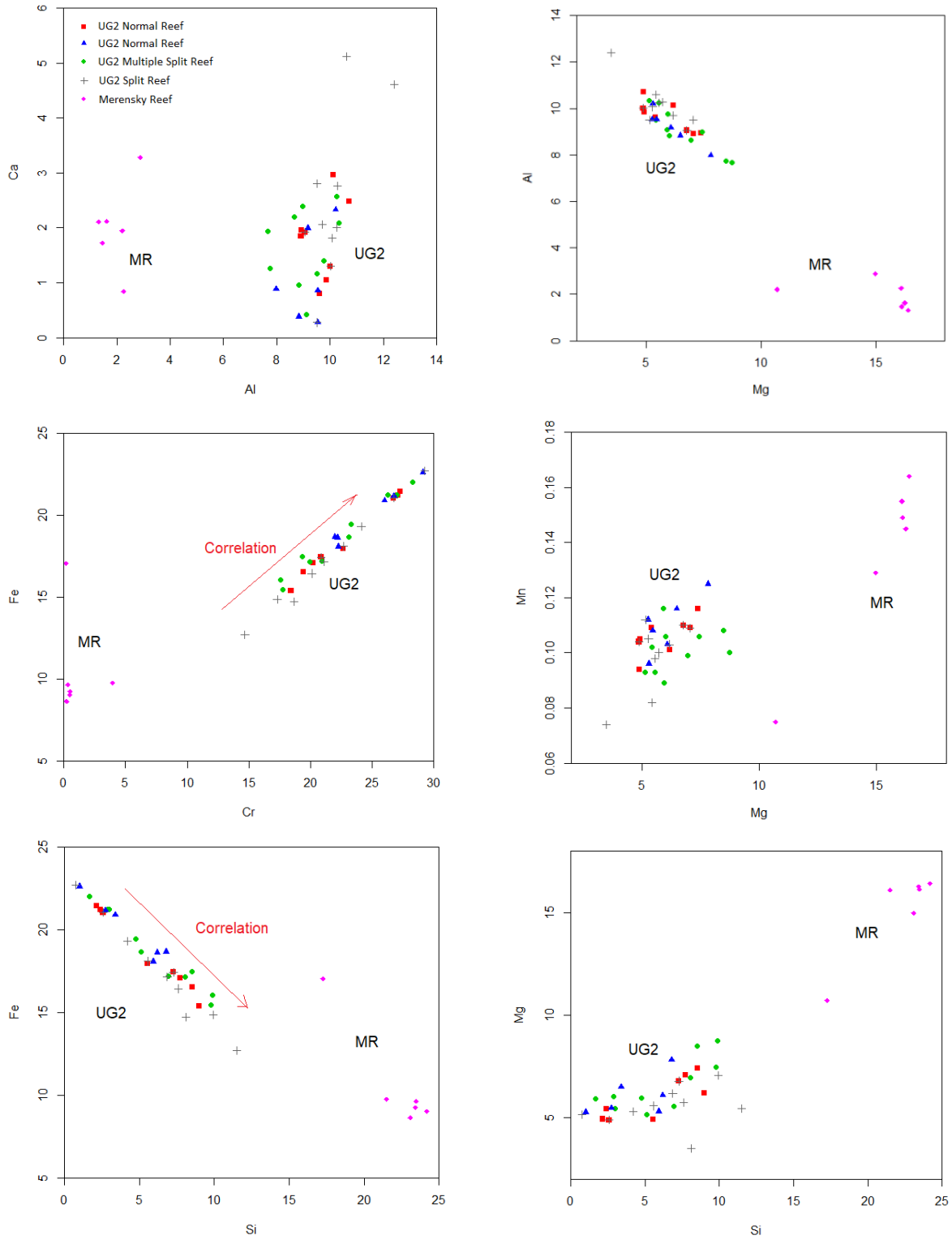

Figure 5.16: Binary plots of the chemistry (%) of the UG2 Reef and MR obtained from the MLA. Ca vs Al, Al vs Mg, Fe vs Cr, Mn vs Mg, Fe vs Si and Mg vs Si.

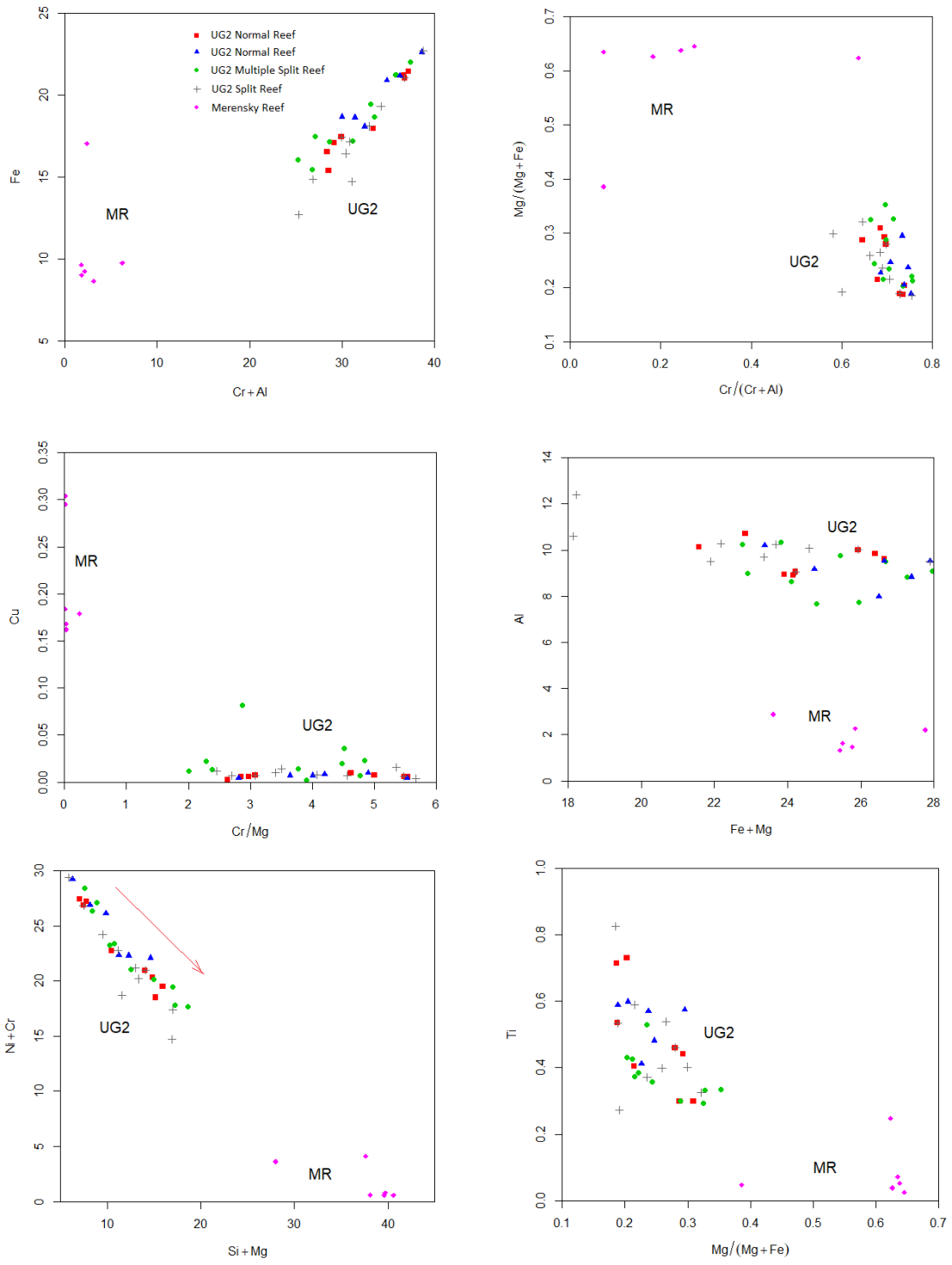

Figure 5.17: Binary plots of the chemistry (%) of the UG2 Reef and MR obtained from the MLA. Fe vs Cr + Al, Mg# vs Cr#, Cu vs Cr/Mg, Al vs Fe + Mg, Ni + Cr vs Si + Mg and Ti vs Mg#.

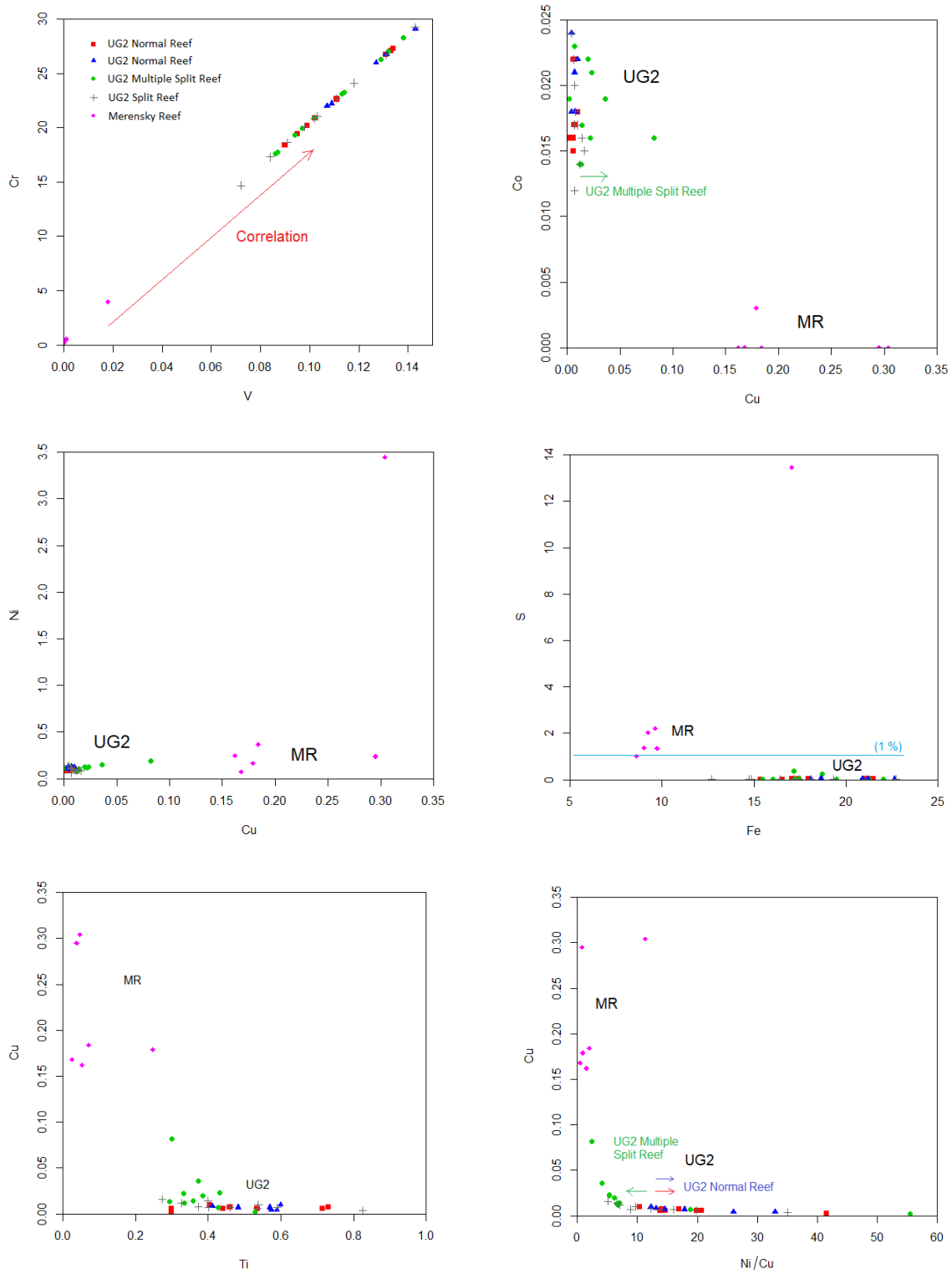

Figure 5.18: Binary plots of the chemistry (%) of the UG2 Reef and MR obtained from the MLA. Cr vs V, Co vs Cu, Ni vs Cu, S vs Fe, Cu vs Ti, Cu vs Ni/Cu.

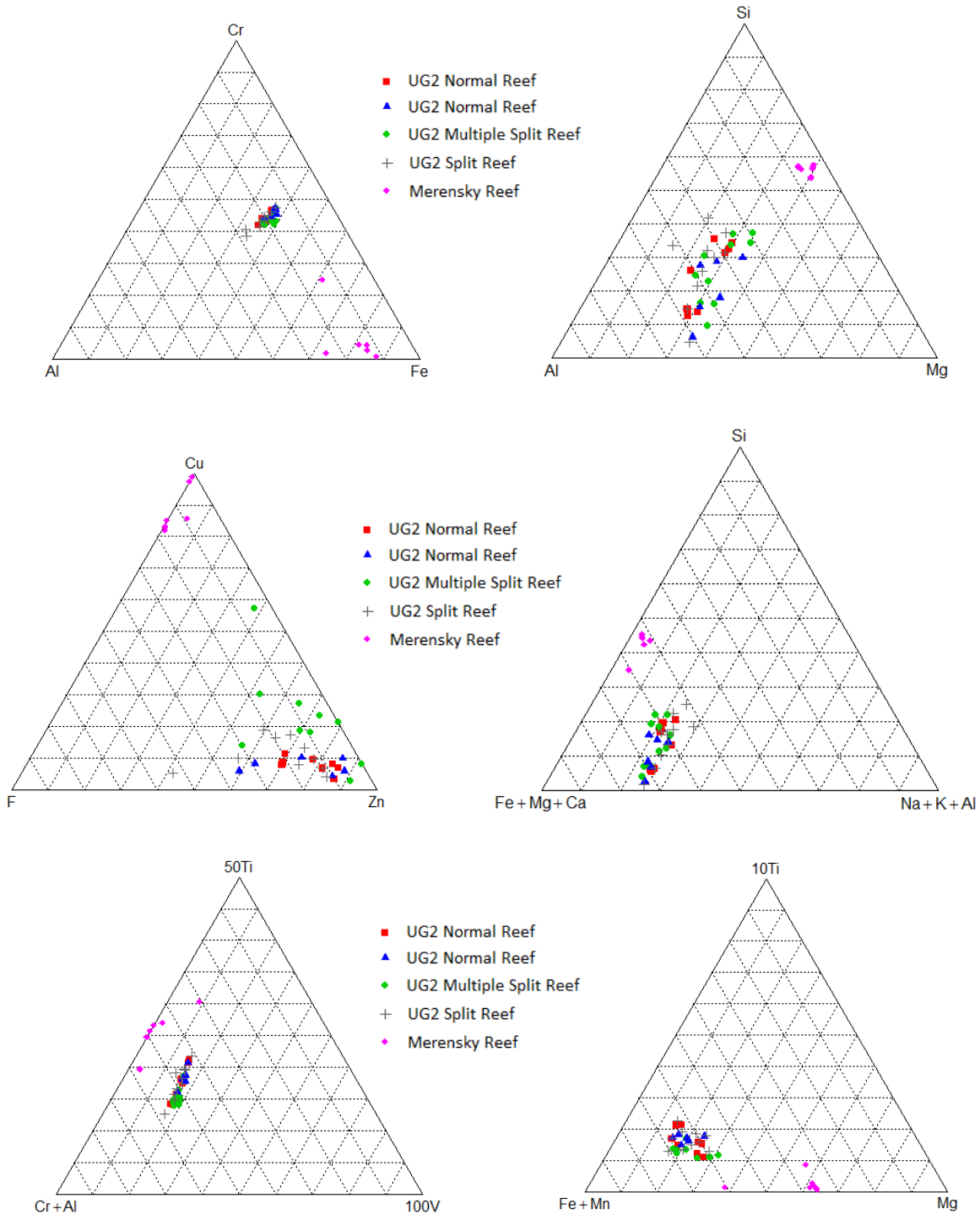

Figure 5.19: Ternary plots of the chemistry (%) of the UG2 Reef and MR obtained from the MLA.

CHAPTER 6 CHARACTERISTICS AND MINERALISATION OF PLATINUM GROUP ELEMENTS

6.1. Platinum group elemental distributions

The PGE distributions in the samples based on XRF / ICP-MS data obtained from the TRP are presented in Figures 6.1 to 6.5 to provide insight of the individual elemental contribution in the UG2 Reef facies (Normal, Split and Multiple Split Reefs) and MR.

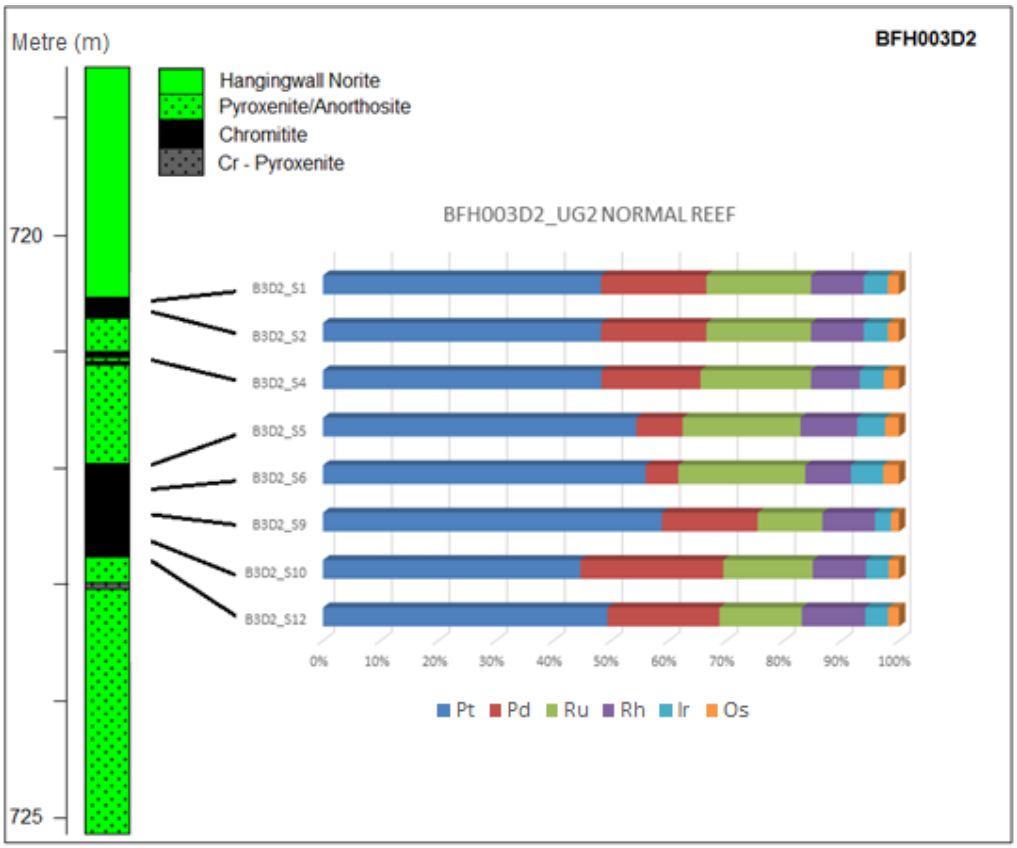

Figure 6.1: Distributions of PGE in the UG2 Normal Reef, borehole BFH003D2.

The borehole BFH003D2 is dominated by Pt, followed by varying concentrations of Pd and Ru. Rhodium, Ir and Os are the least with decreasing abundance respectively.

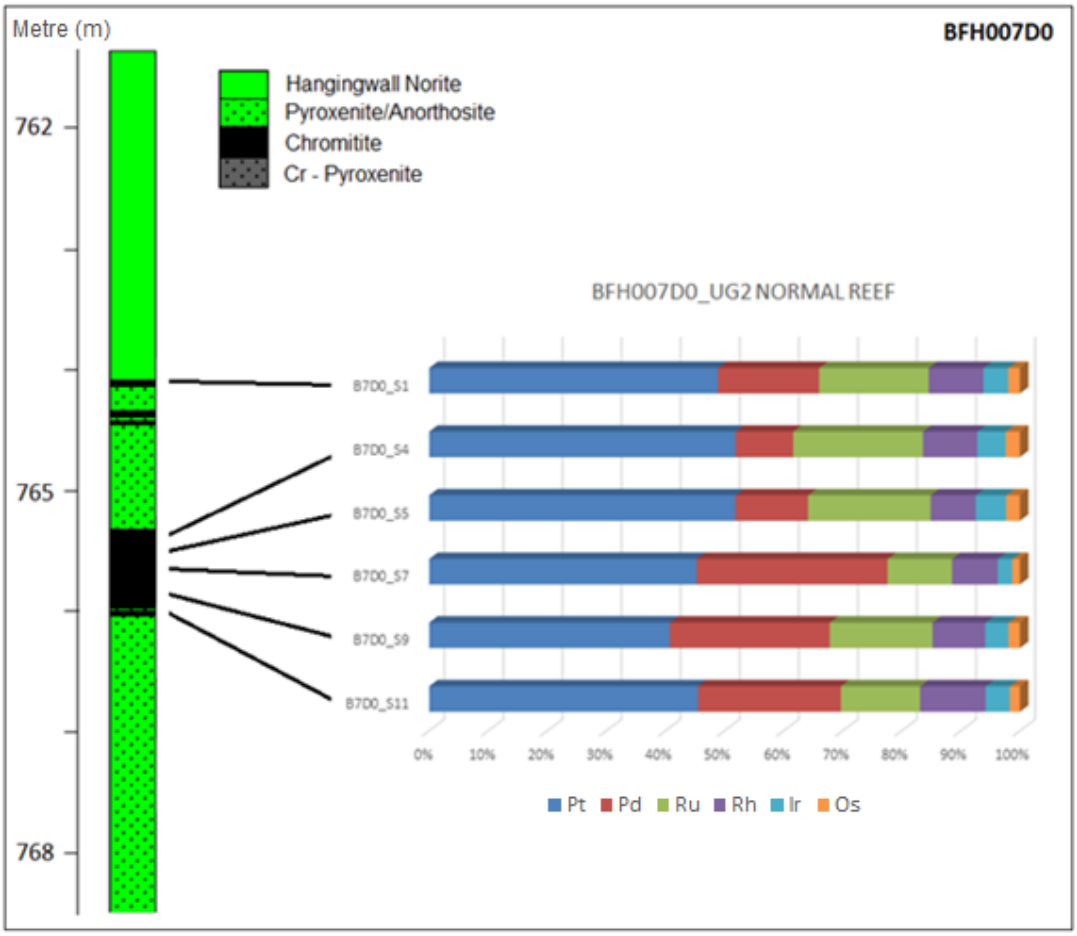

Figure 6.2: Distributions of PGE in the UG2 Normal Reef, borehole BFH007D0.

The PGE distributions of the Normal Reef with internal pyroxenite (< 10 cm), borehole BFH007D0, exhibit similar characteristics to that of the undisrupted Normal Reef (BFH003D2), with Pt most abundant than the varying Pd and Ru concentrations, and Rh, Ir and Os being the least abundant in a decreasing order.

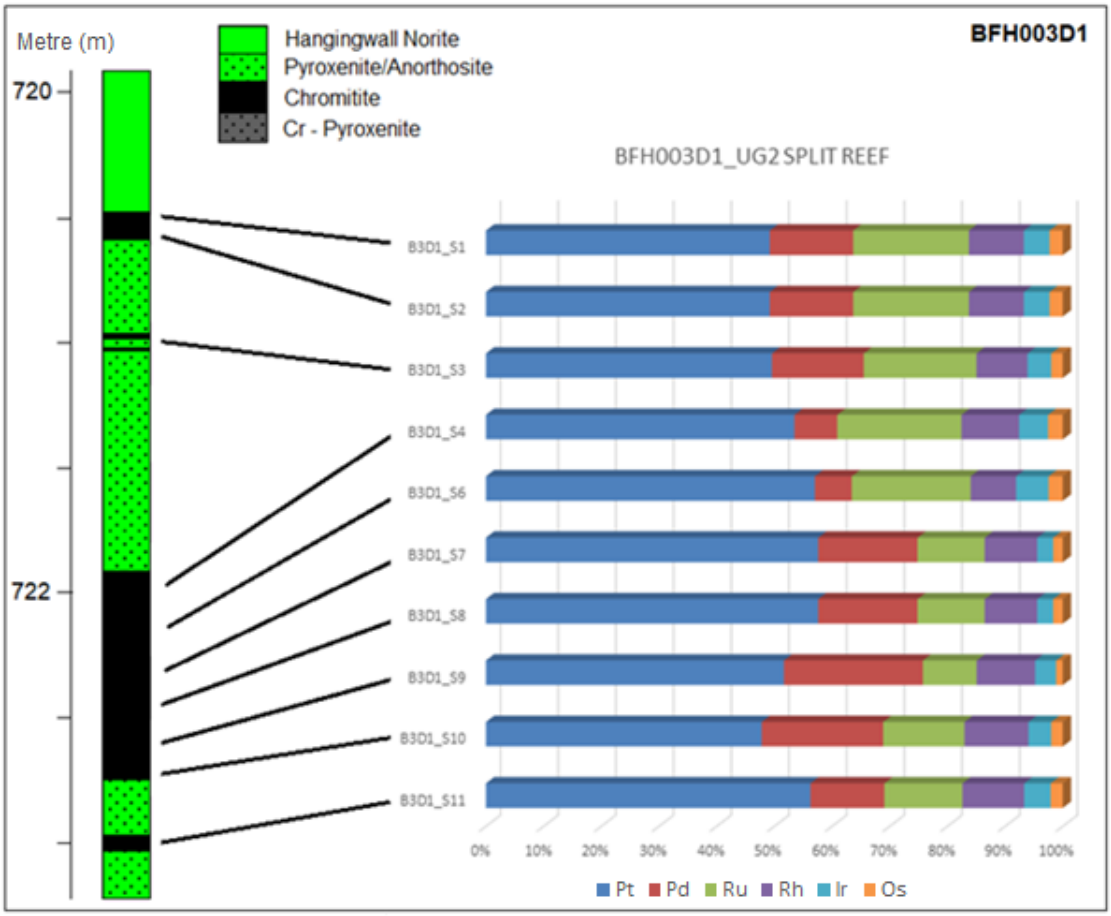

Figure 6.3: Distributions of PGE in the UG2 Split Reef, borehole BFH003D1.

The borehole BFH003D1 hosts the UG2 Split Reef and is also dominated by Pt in all the samples, followed by the variations of Pd and Ru as the second most dominant elements. Rhodium, Ir and Os are also the least dominant in decreasing abundance respectively.

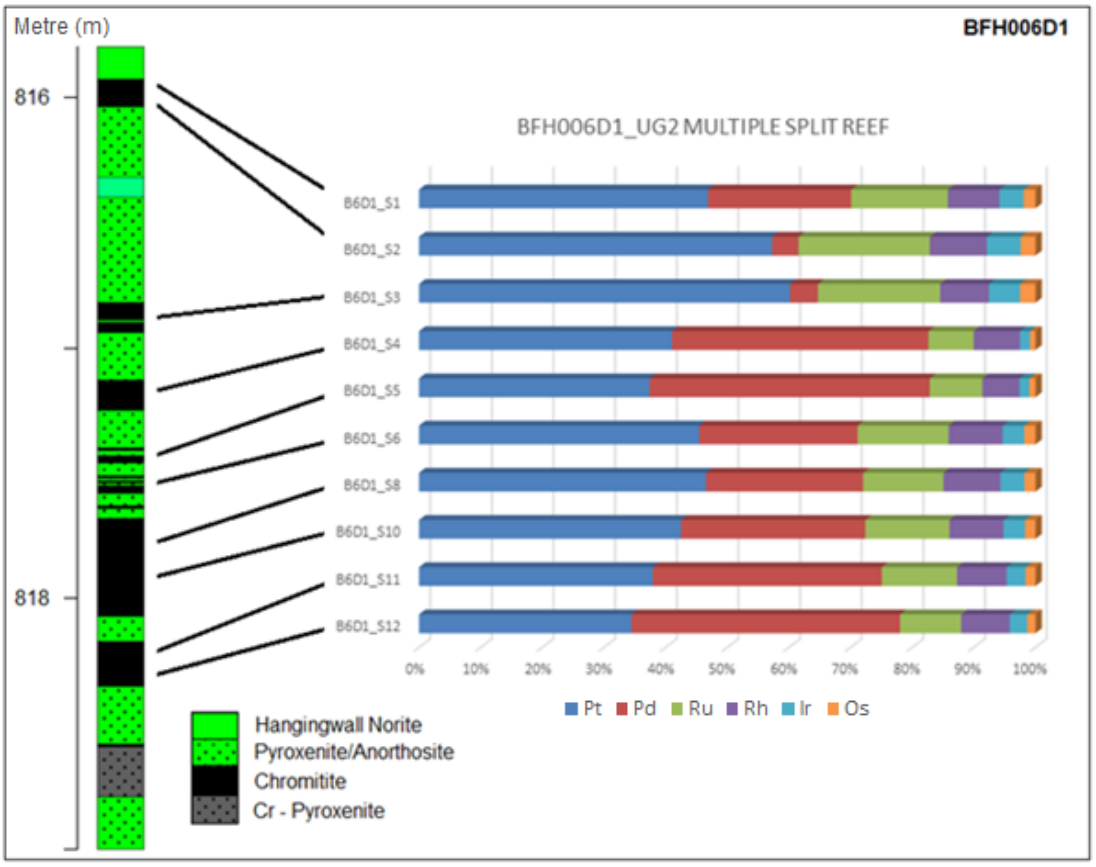

Figure 6.4: Distributions of PGE in the UG2 Multiple Split Reef, borehole BFH006D1.

The Multiple Split Reef, borehole BFH003D1 shows variation in the Pt and Pd concentrations both as the most dominant PGE within the stratigraphy, which is followed by Ru, Rh, Ir and Os in decreasing order of abundance respectively.

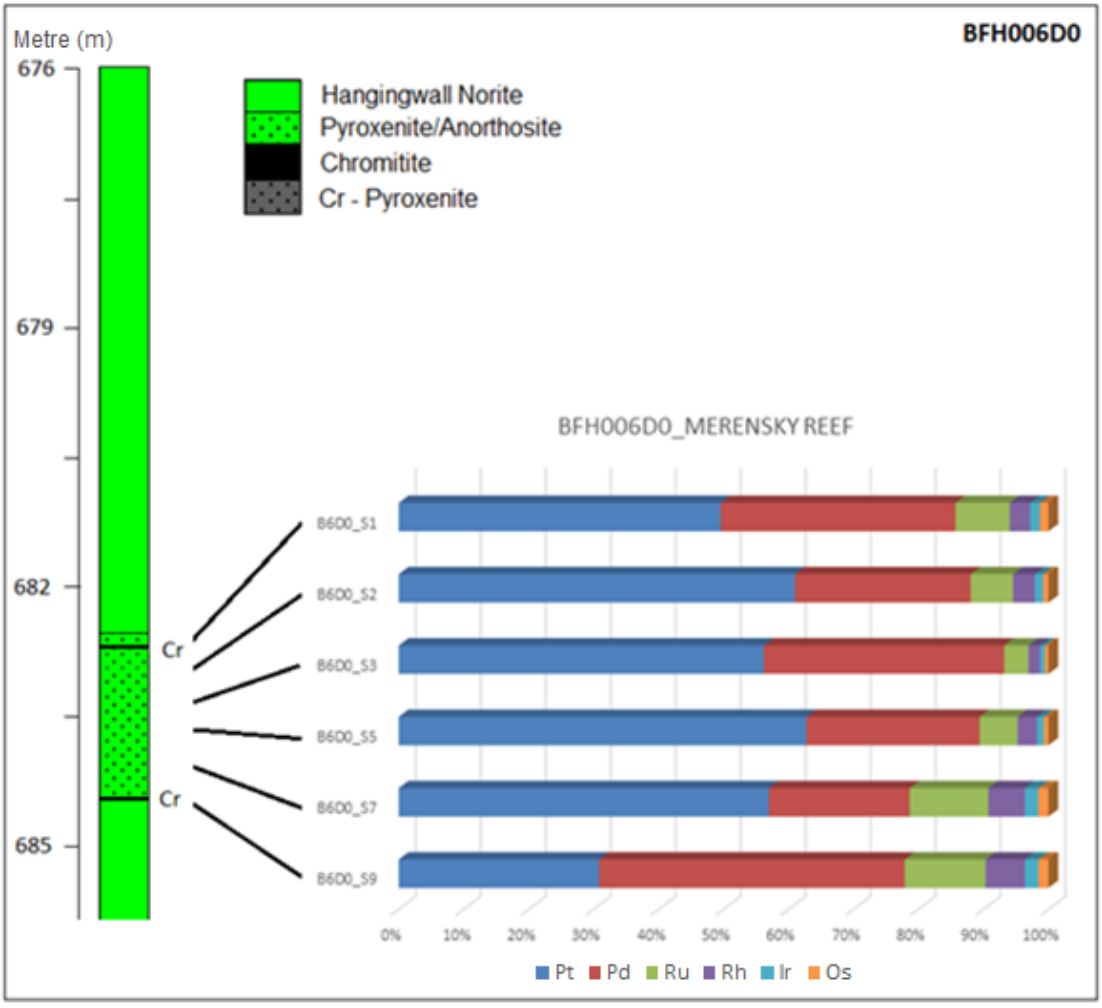

Figure 6.5: Distributions of PGE in the MR, borehole BFH006D0.

The MR is hosted by the borehole BFH006D0 which is mostly dominated by Pt followed by Pd, except for the sample B6D0_S9 which is dominated by Pd followed by Pt. The two most abundant elements (Pt and Pd) are followed by Ru, Rh, Ir and Os in decreasing order of abundance respectively.

6.2. Modal mineralogy

The UG2 Reef comprises chromite (70-80%), plagioclase (5-15%), orthopyroxene (6-8%) and other minerals such as clinopyroxene, talc, mica, chlorite, carbonates, and sulphides. The sulphides are generally < 0.1% and mostly dominated by pentlandite and chalcopyrite. Figure 6.6 is a graphical representation of the modal mineralogy of the various UG2 Reef facies showing very low content of sulphides. Figure 6.7 is a representation of only the sulphides to show the different proportions. The UG2 Reef is generally dominated by pentlandite followed by chalcopyrite and very rarely pyrrhotite and other sulphides (general total sulphides < 0.1 %), however the UG2 Multiple Split Reef shows a significant amount of pyrite which is comparable in abundance with pentlandite and chalcopyrite (total sulphides > 0.1 %).

The MR comprises about 55% orthopyroxene, 15% amphibole, 8% sulphides, 6% talc, 6% chlorite and other minerals such as clinopyroxene, plagioclase and chromite. The modal mineralogy of the MR with visible sulphides' proportion are shown in Figure 6.8 The sulphides abundances are summarised in Figure 6.9. The sulphides phases are pyrite, pentlandite, pyrrhotite and chalcopyrite with decreasing abundances respectively (each of these sulphide > 0.1% and total sulphides significantly > 1%).

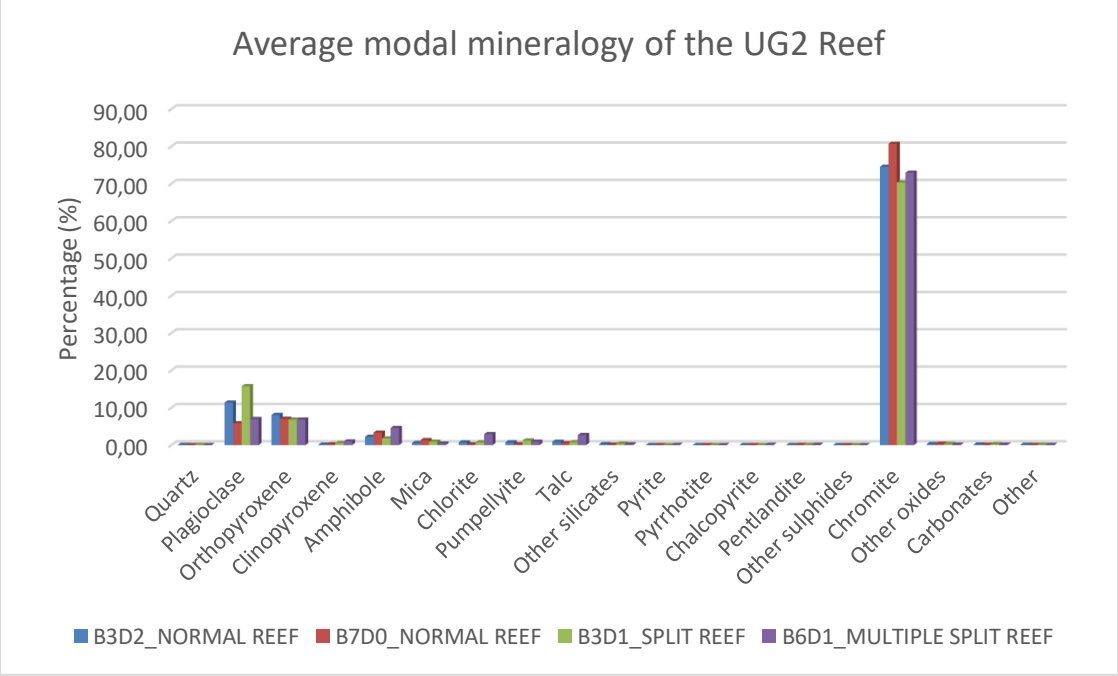

Figure 6.6: Modal mineralogy (%) of the UG2 Reef facies obtained from MLA.

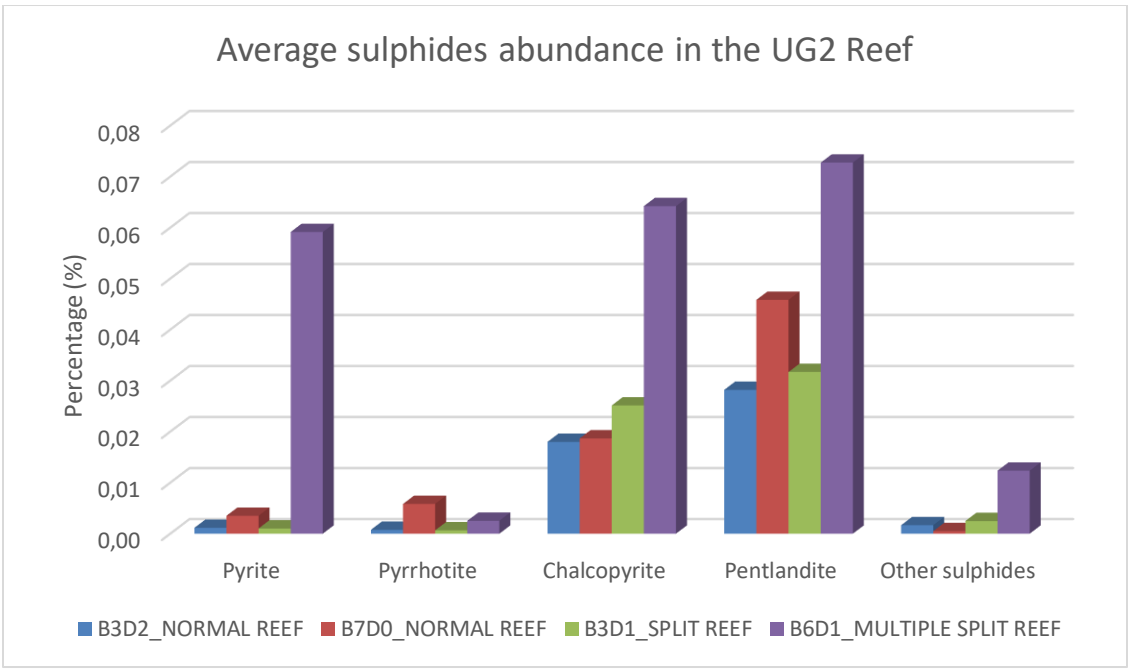

Figure 6.7: Modal mineralogy of sulphide (%) in the UG2 Reef facies obtained from MLA.

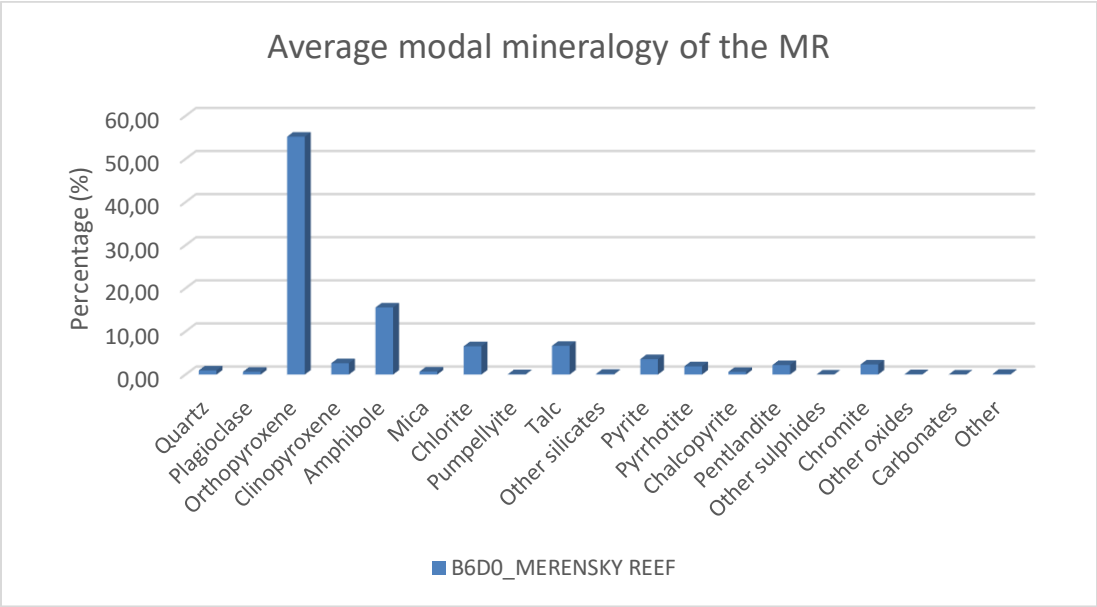

Figure 6.8: Modal mineralogy (%) of the MR obtained from MLA.

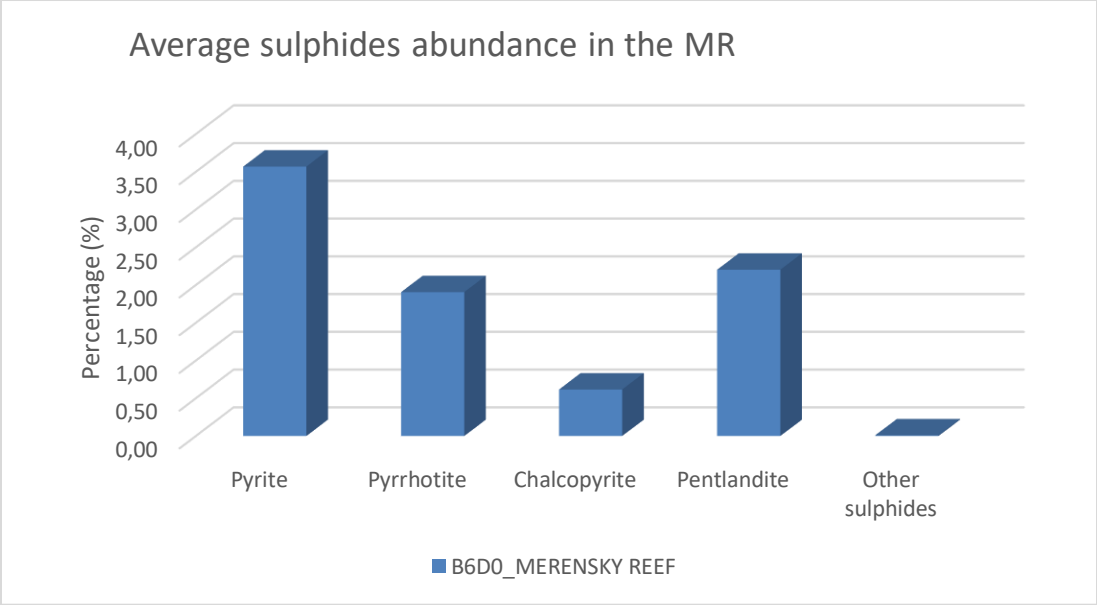

Figure 6.9: Modal mineralogy of sulphide (%) in the MR obtained from MLA.

6.3. Platinum group mineral phases and their abundances

The PGM phases occurring at Buffelshoek are listed in Table 6.1. The PGM phases are broadly grouped as PGE sulphides, PGE arsenides, PGE bismuth-tellurides (Bi-Te), PGE antimonides and PGE alloys. The stratigraphical distributions and abundances of these PGM groups are presented in Figures 6.10 to 6.14. These stratigraphical presentations are plotted using PGM mass% (or area%) normalised to 100% from table 6.1 to represent the relative abundances of the PGM. Also presented in Table 6.1 are the number of grains counted for the various PGM, which are illustrated in Figure 6.15 to show the grain count abundances.

In the UG2 Reef, the PGM are generally dominated by PGE sulphides such as cooperite (PtPdNiFeS), kharaelakhite (PtCuPbFeNiS), braggite (PtPdNiS) and (PtAgRhS), followed by PGE alloys such as isoferroplatinum, plumbopalladinite and ferronickelplatinum, PGE arsenides including sperrylite, atheneite and (PtPdSbAs), PGE Bismuth-tellurides (such as moncheite, kotulskite and sobolevskite), and PGE antimonides (such as mertieite), in decreasing abundances respectively. In the MR the PGM are generally dominated by PGE arsenides such as speryllite, atheneite and (PtPdAsSb), followed by PGE bismuth-tellurides including moncheite, kotulskite, PdTeBi, merenskyite, temagamite, followed by PGE sulphides (cooperite, platarsite, (PtPdSAs), (PdSSe)), PGE antimonides (mertieite, stibiopalladinite) and PGE alloys (isoferroplatinum, plumbopalladinite, zvyagintsevite), in decreasing abundance respectively.

Table 6.1: The PGM phases, mass% and grains count of the boreholes studied.

Grouping	Sub-Grouping	Phases	BFH003D2		BFH006D0		BFH006D1	
			PGM MASS %	GRAIN COUNT	PGM MASS %	GRAIN COUNT	PGM MASS %	GRAIN COUNT
PGE Sulphides	PGE-BMS	Cooperite	55,49	822	19,98	701	45,98	726
		Braggite	6,80	170	0,13	7	8,18	282
		Kharaelakhite	16,61	122	0,09	22	6,98	88
		Vysotskite	0,14	7	0,00	0	1,69	19
		PtRhCuS (unnamed)	4,56	117	0,02	1	3,18	93
	PGE-S	PtSnS	1,29	35	0,02	3	0,26	14
		PdSSe	0,03	2	0,33	3	0,08	7
		PtSAgRh	1,29	51	0,01	1	1,40	50
	PGE-S-As	Hollingworthite	0,00	0	0,00	0	0,00	0
		Platarsite	0,30	13	0,56	29	2,44	61
		PtPdSAs	0,00	0	0,52	9	1,05	33
		PtAsRhS	0,00	0	0,07	10	1,24	32
		PtAsRhS2	0,00	0	0,00	0	0,26	9
PGE Arsenides	PGE-As	Sperrylite	2,77	37	37,29	1114	14,45	345
		Atheneite	0,13	4	2,06	37	1,38	59
		Palladoarsenide	0,06	2	0,00	0	0,20	10
		PdAsNi	0,00	0	0,00	0	0,00	0
		PtSbAs	0,00	0	0,01	2	0,08	4
		PtPdAsSb	0,22	6	0,22	22	0,90	30
PGE Bismuth Tellurides	PGE-Bi-Te	Moncheite	0,68	16	10,93	78	0,66	28
		Maslovite	0,00	0	0,02	2	0,17	2
		Merenskyite	0,00	0	0,25	12	0,00	0
		Kotulskite	0,31	13	8,07	175	0,33	17
		Michenerite	0,02	1	0,17	3	0,03	3
		PdTeBi	0,03	1	2,15	3	0,00	0
		PtBiTe	0,00	0	0,07	4	0,07	2
	PGE-Te	Temagamite	0,02	2	0,27	24	0,13	8
		Pasavaite	0,12	4	0,18	2	0,01	1
		Keithconnite	0,00	0	0,00	0	0,00	0
	PGE-Bi	Sobolevskite	0,25	2	0,16	1	0,02	1
		Potarite	0,00	0	0,00	0	0,10	1
		Polarite	0,00	0	0,00	0	0,02	1
		Froodite	0,00	0	0,00	0	0,00	0
		Insizwaite	0,00	0	0,00	0	0,00	0
		PdPtBi	0,13	3	0,00	0	0,02	1
PGE-Antimonides	PGE-Sb	Stibiopalladinite	0,00	0	4,80	40	0,70	19
		Mertieite	0,84	13	7,00	90	2,73	91
		Geversite	0,00	0	0,00	1	0,41	6
		PdPtSb	0,01	1	0,05	3	0,06	4
PGE-Alloys	Pt and Pd Alloys	Isoferroplatinum	5,86	34	0,12	8	1,23	27
		Atokite	0,01	1	0,00	0	0,00	0
		Ferronickelplatinum	0,50	6	0,00	0	0,11	3
		Rustenburgite	0,14	1	0,03	1	0,15	5
		PtPdSn	0,00	0	0,00	0	0,00	0
		PtPd	0,11	1	0,00	0	0,09	3
	Pd-Pb	Zvyagintsevite	0,07	2	0,23	6	0,26	9
		Plumbopalladinite	0,89	22	1,55	36	2,51	82
		PdPbAu	0,00	0	0,00	0	0,00	0
	Native	Native Au	0,31	4	2,64	16	0,43	7
		Native Pt	0,00	0	0,01	1	0,00	0
		Native Pd	0,00	0	0,00	0	0,00	0
	Other Alloy	Skaergaardite	0,03	1	0,00	0	0,02	1

Table 6.1 (continued): The PGM phases, mass% and grains count of the boreholes studied.

Grouping	Sub-Grouping	Phases	BFH007D0		BFH003D1	
			PGM MASS %	GRAIN COUNT	PGM MASS %	GRAIN COUNT
PGE Sulphides	PGE-BMS	Cooperite	49,72	672	44,78	677
		Braggite	5,16	176	6,72	219
		Kharaelakhite	1,18	42	24,14	116
		Vysotskite	0,03	2	0,23	16
		PtRhCuS (unnamed)	2,73	69	6,80	107
	PGE-S	PtSnS	0,70	13	0,03	2
		PdSSe	0,00	0	0,16	7
		PtSAgRh	0,22	5	0,89	44
	PGE-S-As	Hollingworthite	0,00	0	0,03	2
		Platarsite	0,55	10	0,97	22
		PtPdSAs	0,00	0	0,01	2
		PtAsRhS	0,10	3	0,76	13
		PtAsRhS2	0,00	0	0,09	3
PGE Arsenides	PGE-As	Sperrylite	15,91	264	1,07	12
		Atheneite	0,07	3	0,09	3
		Palladoarsenide	0,00	0	0,10	1
		PdAsNi	0,00	0	0,00	0
		PtSbAs	0,00	0	0,06	2
		PtPdAsSb	0,00	0	0,04	3
PGE Bismuth Tellurides	PGE-Bi-Te	Moncheite	1,16	14	1,89	40
		Maslovite	0,02	1	0,00	0
		Merenskyite	0,00	0	0,00	0
		Kotulskite	0,18	6	0,06	4
		Michenerite	0,05	1	0,02	1
		PdTeBi	0,00	0	0,00	0
		PtBiTe	0,08	1	0,02	1
	PGE-Te	Temagamite	0,00	0	0,01	2
		Pasavaite	0,00	0	0,09	2
		Keithconnite	0,00	0	0,01	1
	PGE-Bi	Sobolevskite	0,00	0	0,00	0
		Potarite	0,00	0	0,00	0
		Polarite	0,00	0	0,00	0
		Froodite	0,00	0	0,00	0
		Insizwaite	0,00	0	0,00	0
		PdPtBi	0,01	1	0,00	0
PGE-Antimonides	PGE-Sb	Stibiopalladinite	0,00	0	0,00	0
		Mertieite	0,02	1	0,38	5
		Geversite	0,00	0	0,00	0
		PdPtSb	0,00	0	0,08	3
PGE-Alloys	Pt and Pd Alloys	Isoferroplatinum	11,23	143	6,76	45
		Atokite	0,00	0	0,00	0
		Ferronickelplatinum	0,24	3	0,54	14
		Rustenburgite	0,02	1	0,02	2
		PtPdSn	0,00	0	0,00	0
		PtPd	0,15	5	0,12	4
	Pd-Pb	Zvyagintsevite	0,69	17	0,39	6
		Plumbopalladinite	9,55	185	2,06	41
		PdPbAu	0,05	2	0,04	2
	Native	Native Au	0,16	1	0,57	7
		Native Pt	0,00	0	0,00	0
		Native Pd	0,00	0	0,00	0
	Other Alloy	Skaergaardite	0,00	0	0,00	0

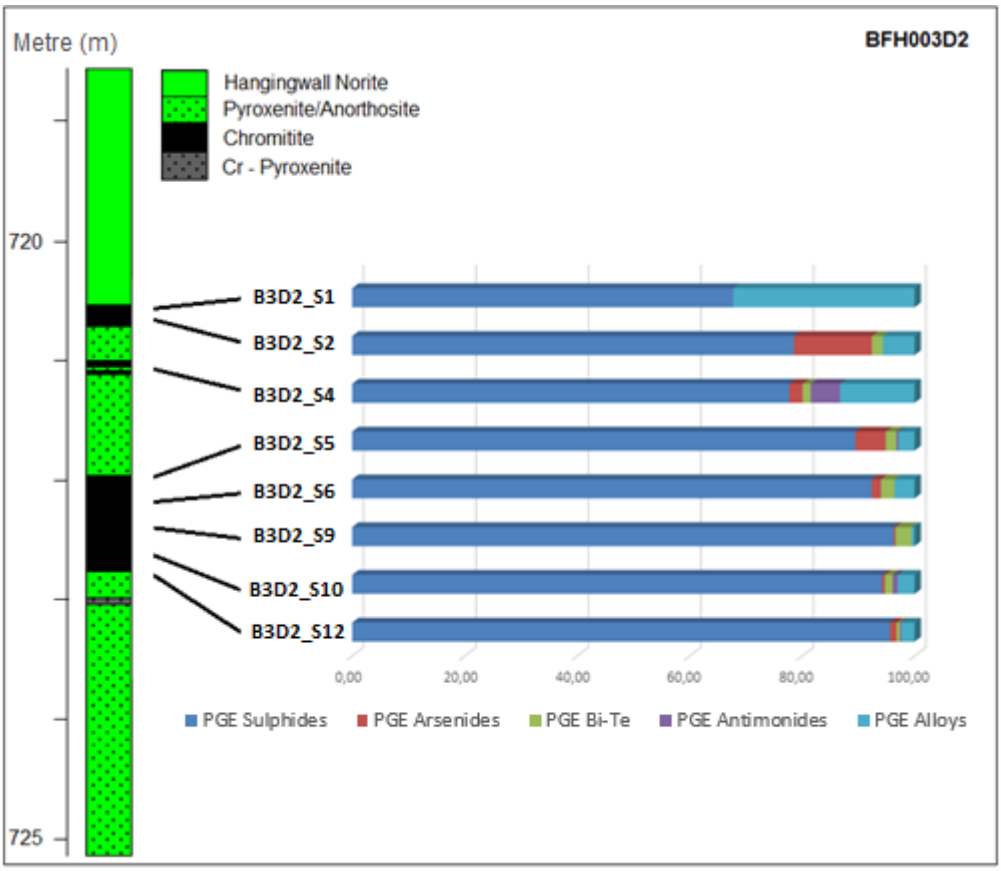

Figure 6.10: Stratigraphical distributions of the grouped PGM in the UG2 Normal Reef, Borehole BFH003D2.

Borehole **BFH003D2** is generally dominated by PGE sulphides throughout the stratigraphy. The PGE sulphides and PGE arsenides relative abundances increases up the stratigraphy. On specific samples from up the stratigraphy downward, the sample ***B3D2_S1*** comprises PGE sulphides (67.8%) and PGE alloys (32.2%) only, which is distinct to the other samples having at least four of the five PGM groups. ***B3D2_S2:*** PGE sulphides (78.5%), PGE arsenides (13.9%) – which is the highest in all the samples, PGE alloys (5.6%) and PGE bismuth-tellurides (1.2%), ***B3D2_S4:*** PGE sulphides (77.7%), PGE alloys (13.3%), PGE antimonides (5.2%) – which is the highest in all the samples, PGE arsenides (2.4%), and PGE bismuth-tellurides (1.4%). ***B3D2_S5:*** PGE sulphide (89.5%), PGE arsenides (5.41%), PGE alloys

(2.9%), PGE bismuth-tellurides (1.9%) and PGE antimonides (0.36%). ***B3D2_S6:*** PGE sulphides (92.4%), PGE alloys (3.6%), PGE bismuth-tellurides (2.4%) and PGE arsenides (1.6%). ***B3D2_S9:*** PGE sulphides (96.3%), PGE bismuth-tellurides (2.8%), PGE antimonides (0.5%) and PGE arsenides (0.36%). ***B3D2_10:*** PGE Sulphides (94.2%), PGE alloys (3.00%), PGE bismuth-tellurides (1.4%), PGE antimonides (0.9%) and PGE arsenides (0.5%). ***B3D2_S12:*** PGE sulphides (95.5%), PGE alloys (2.4%), PGE arsenides (1.2%), PGE bismuth-tellurides (0.57%) and PGE antimonides (0.27%).

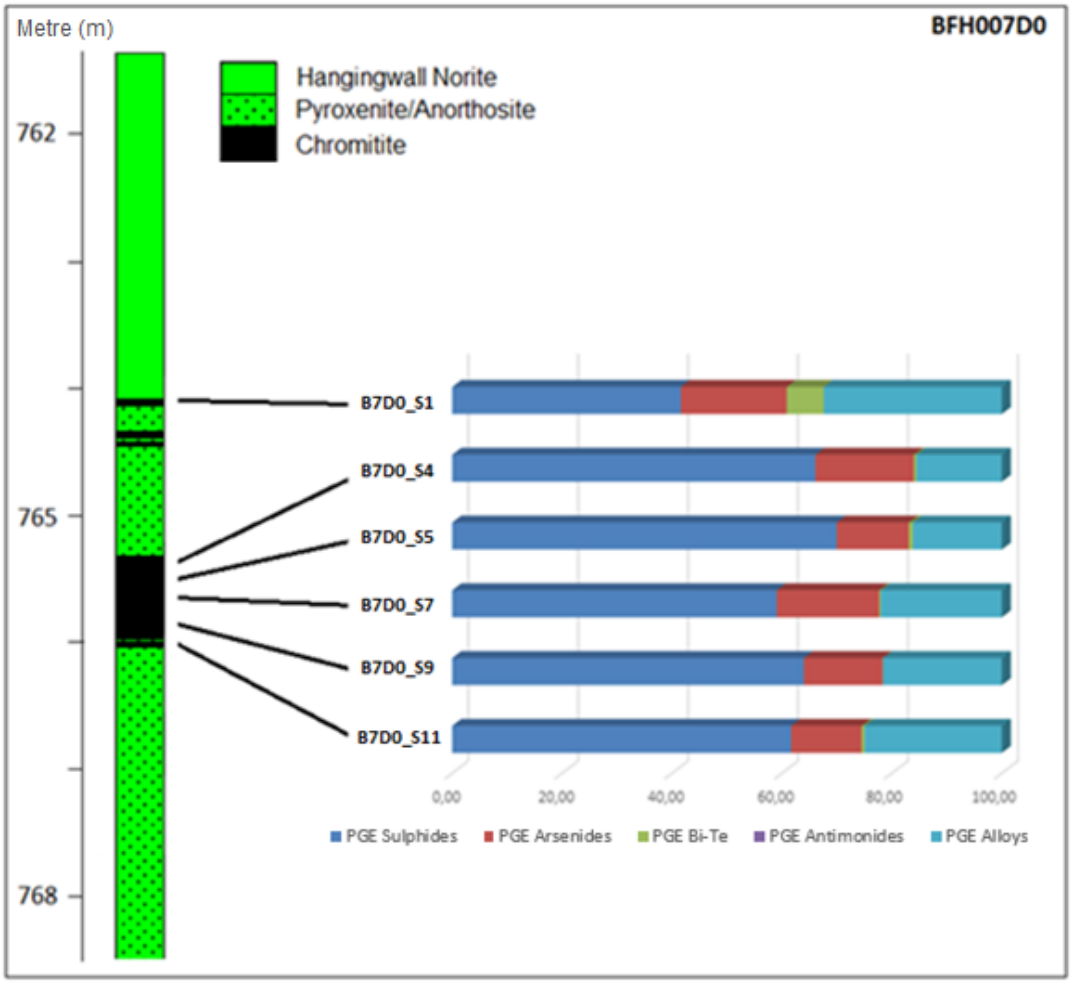

Figure 6.11: Stratigraphical distributions of the grouped PGM in the UG2 Normal Reef, borehole BFH007D0.

In borehole **BFH007D0** above, the PGM relative abundances are sporadic with PGE sulphides dominant followed by PGE alloys, PGE arsenides and PGE bismuth-tellurides (Bi-Te) respectively. From up the stratigraphy downward, the sample ***B7D0_S1*** comprises PGE sulphides (41.6%), PGE alloys (32.4%), PGE arsenides (19.3%) and PGE bismuth-tellurides (6.7%). ***B7D0_S4:*** PGE sulphides (66.1%), PGE arsenides (17.9), PGE alloys (15.5%) and PGE bismuth-tellurides (0.48%). ***B7D0_S5:*** PGE sulphides 69.9%, PGE alloys (16.2%), PGE arsenides (13.1%) and PGE bismuth-tellurides (0.76%). ***B7D0_S7:*** PGE sulphides (59.1%), PGE alloys (22%), PGE arsenides (18.6%) and PGE bismuth-tellurides (0.32%). ***B7D0_S9:*** PGE sulphides (64%), PGE alloys (21.5%), PGE arsenides (14.2%), PGE antimonides (0.15%) and PGE bismuth-tellurides (0.13%). ***B7D0_S11:*** PGE sulphides (61.7%), PGE alloys (24.9%), PGE arsenides (12.8%) and PGE bismuth-tellurides (0.58%).

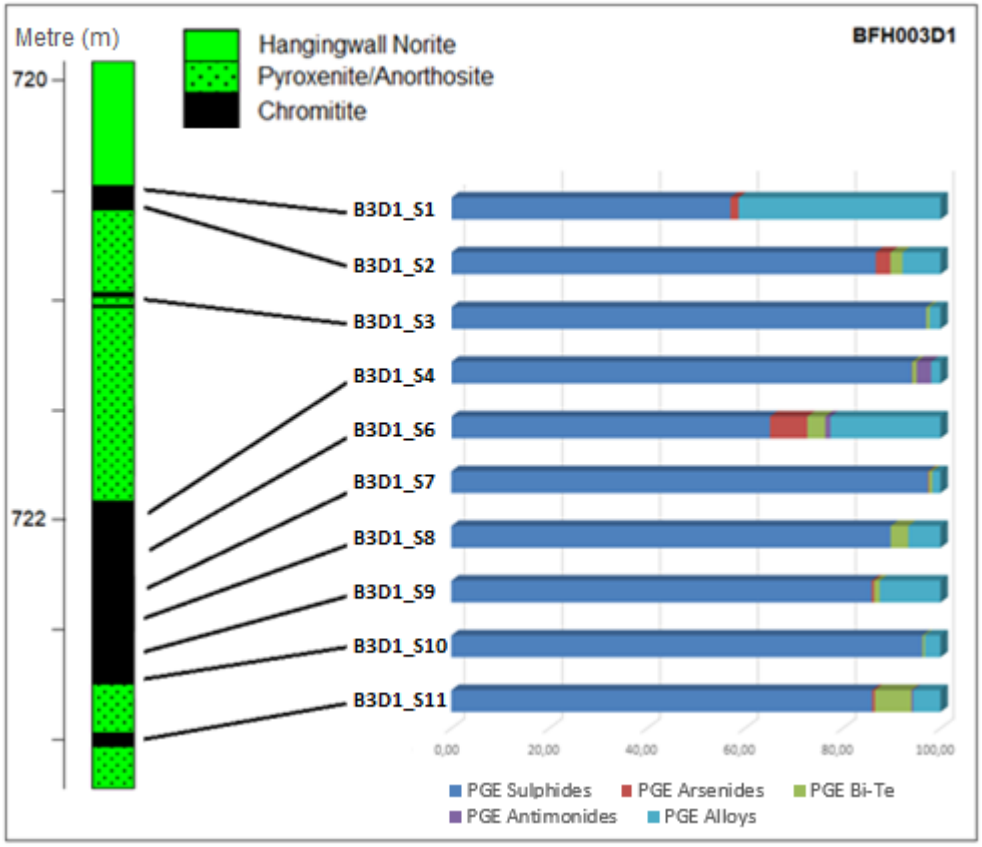

Figure 6.12: Stratigraphical distributions of the grouped PGM in the UG2 Split Reef, borehole BFH003D1.

In borehole **BFH003D1** above, the most abundant PGE sulphides and the second most abundant PGE alloys are present throughout the stratigraphy, however the least abundant PGM groups are not present in all the samples. The sample ***B3D1_S1*** comprises of PGE sulphides (57.1%), PGE alloys (41.2%) and PGE arsenides (1.7%). ***B3D1_S2:*** PGE sulphides (86.8%), PGE alloys (7.7%), PGE arsenides (3%) and PGE bismuth-tellurides (2.5%). ***B3D1_S3:*** PGE sulphides (97.1%), PGE alloys (2.2%), PGE bismuth-tellurides (0.7%). ***B3D1_S4:*** PGE sulphides (94.2%), PGE antimonides (3%), PGE alloys (1.9%), PGE bismuth-tellurides (0.8%) and PGE arsenides (0.1%). ***B3D1_S6:*** PGE sulphides (65.2%), PGE alloys (22.5%), PGE arsenides (7.6%), PGE bismuth-tellurides (3.6%) and

PGE antimonides (1.1%). ***B3D1_S7:*** PGE sulphides (97.45%), PGE alloys (1.6%), PGE bismuth-tellurides (0.7%), PGE arsenides (0.2%) and PGE antimonides (0.05%). ***B3D1_S8:*** PGE sulphides (89.8%), PGE alloys (6.6%) and PGE bismuth-tellurides (3.6%). ***B3D1_S9:*** PGE sulphides (85.9%), PGE alloys (12.4%), PGE bismuth-tellurides (1.2%) and PGE arsenides (0.5%). ***B3D1_S10:*** PGE sulphides (96.3%), PGE alloys (3.2%) and PGE bismuth-tellurides (0.5%). ***B3D1_S11:*** PGE sulphides (86.1%), PGE bismuth-tellurides (7.5%), PGE alloys (5.5%), PGE arsenides (0.5%) and PGE antimonides (0.4%).

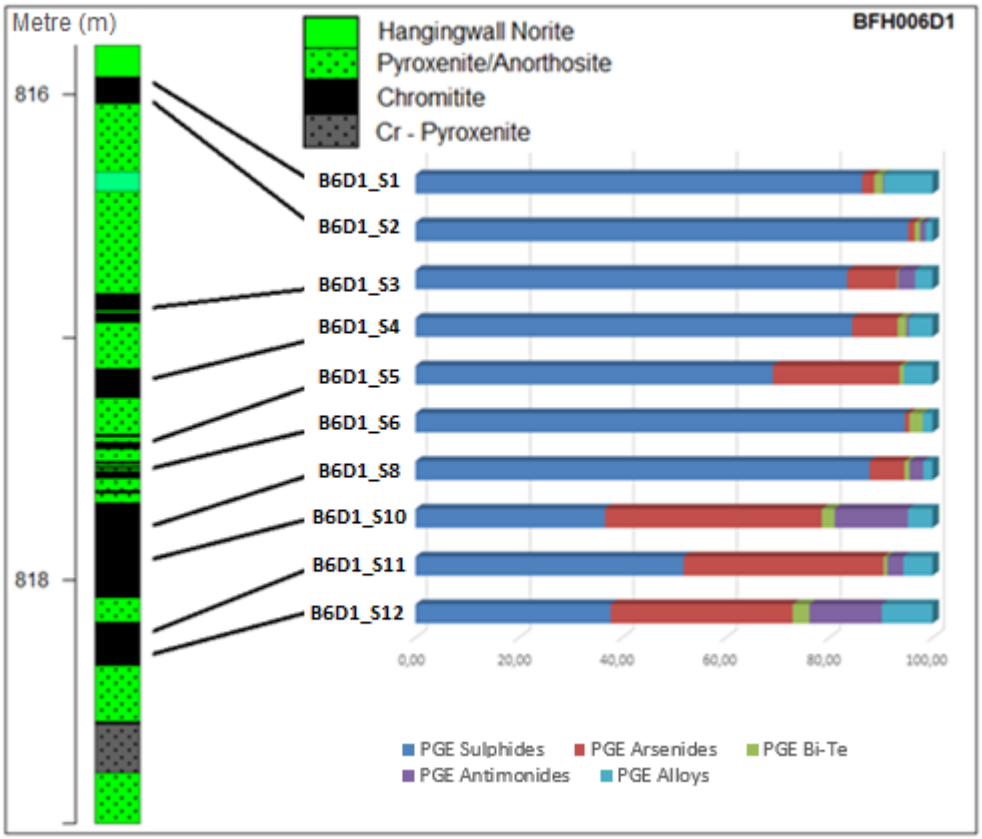

Figure 6.13: Stratigraphical distributions of the grouped PGM in the UG2 Multiple Split Reef, borehole BFH006D1.

From up the stratigraphy downward in **BFH006D1** the relative abundance of PGE arsenides generally increases with decreasing PGE sulphides. Borehole BFH006D1 have more PGE antimonides compared to BFH003D2, BFH007D0 and BFH003D1. The PGE antimonides in BFH006D1 is generally most abundant at the bottom of the stratigraphy. The sample ***B6D1_S1*** comprises PGE sulphides (86.4%), PGE alloys (9.4%), PGE arsenides (2.4%), PGE bismuth-tellurides (1.7%) and PGE antimonides (0.22%). ***B6D1_S2:*** PGE sulphides (95.3%), PGE alloys (1.3%), PGE arsenides (1.3%), PGE antimonides (1.07%) and PGE bismuth-tellurides (1.03%). ***B6D1_S3:*** PGE sulphides (83.5%), PGE arsenides (9.6%), PGE alloys (3.4%), PGE antimonides (3.3%) and PGE bismuth-tellurides (0.2%). ***B6D1_S4:*** PGE sulphides (84.4%), PGE arsenides (8.8%), PGE alloys (4.6%), PGE bismuth-tellurides (1.7%) and PGE antimonides (0.5%). ***B6D1_S5:*** PGE sulphides (6.1%), PGE arsenides (24.5%), PGE alloys (5.5%) and PGE bismuth-tellurides (0.9%). ***B6D1_S6:*** PGE sulphides (94.6%), PGE bismuth-telluride (2.6%), PGE alloys (1.9%) and PGE arsenides (0.9%). ***B6D1_S8:*** PGE sulphides (87.8%), PGE arsenides (6.8%), PGE antimonides (2.6%), PGE alloys (1.8%) and PGE bismuth-tellurides (1%). ***B6D1_S10***: PGE arsenides (41.9%), PGE sulphides (36.7%), PGE antimonides (14.1%), PGE alloys (4.8%) and PGE bismuth-tellurides (2.5%). ***B6D1_S11***: PGE sulphides (51.9%), PGE arsenides (38.7%), PGE alloys (5.6%), PGE antimonides (3.1%), and PGE bismuth-tellurides (0.7%). ***B6D1_S12:*** PGE sulphides (37.8%), PGE arsenides (35.2%), PGE antimonides (14%), PGE alloys (9.8%), and PGE bismuth-tellurides (3.2%).

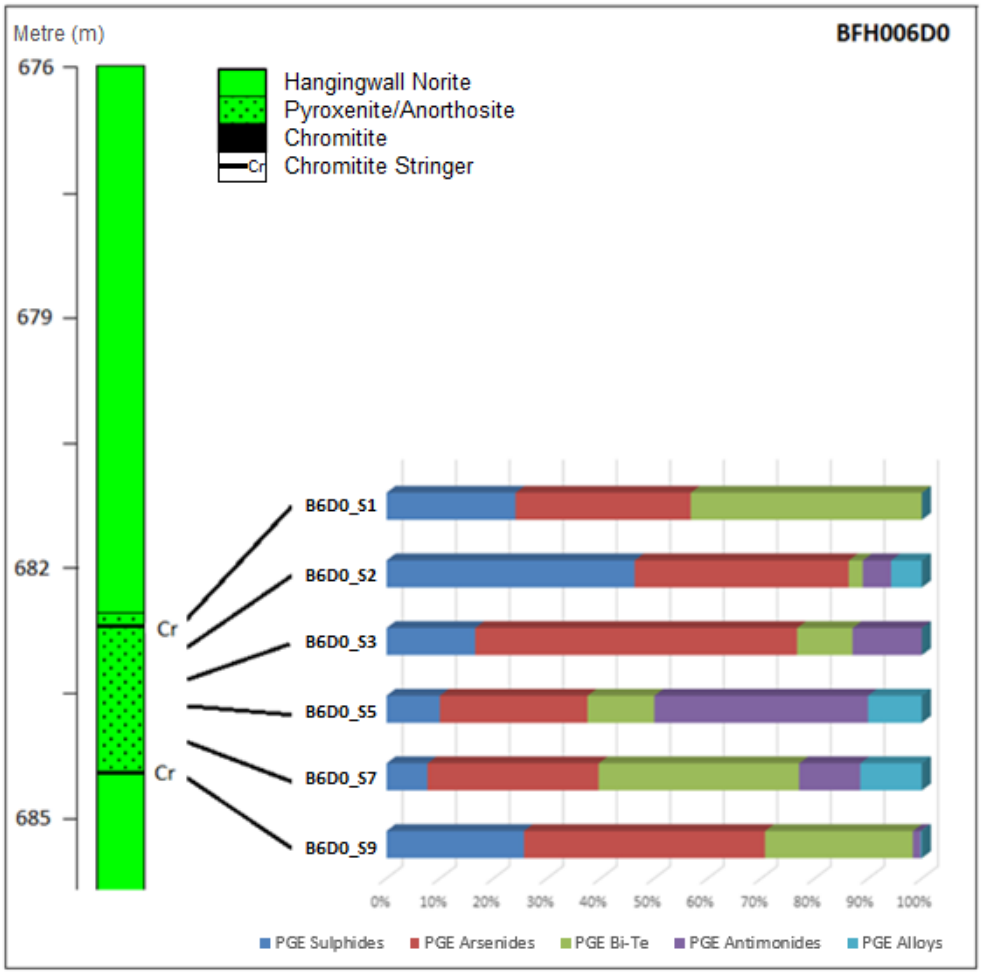

Figure 6.14: Stratigraphical distributions of the grouped PGM in the MR, borehole BFH006D0.

Borehole **BFH006D0** above, is generally dominated by PGE arsenides, with sporadic relative abundances of PGE sulphides and PGE bismuth-tellurides as the second and / or third most dominant. The PGE antimonides is present almost throughout the stratigraphy. The sample ***B6D0_S1*** comprises PGE bismuth-tellurides (43.2%), PGE arsenides (32.7%) and PGE sulphides (24.1%) only. **B6D0_S2:** PGE sulphides (46.4%), PGE arsenides (39.9%), PGE alloys (5.7%), PGE antimonides (5.3%) and PGE bismuth-tellurides (2.6%). **B6D0_S3:** PGE arsenides (60.1%), PGE sulphides (16.6%), PGE antimonides (12.9%) and PGE bismuth-tellurides (10.4%). **B6D0_S5:** PGE antimonides (39.9%), PGE arsenides

(27.6%), PGE bismuth-tellurides (12.5%), PGE alloys (10.1%) and PGE sulphides (9.9%). **B6D0_S7:** PGE bismuth-tellurides (37.4%), PGE arsenides (31.9%), PGE alloys (11.5%), PGE antimonides (11.4%) and PGE sulphides (7.7%). **B6D0_S9:** PGE arsenides (45%), PGE bismuth-tellurides (27.6%), PGE sulphides (25.7%), PGE antimonides (1.5%) and PGE alloys (0.2%).

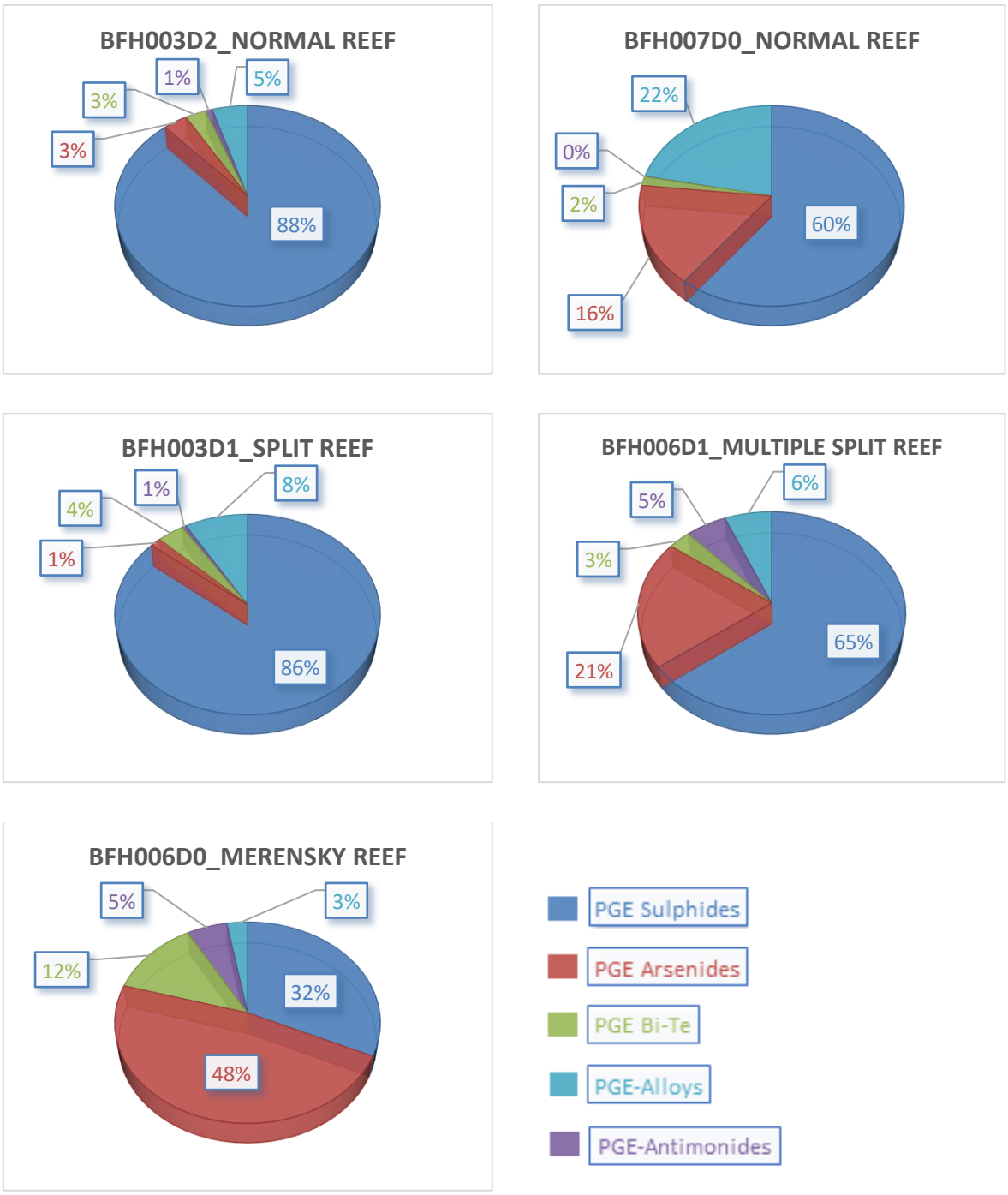

Figure 6.15: Pie chart showing abundances of the counted grains of the grouped PGM in each Reef type (UG2 Reef facies and MR).

The Figure 6.15 indicates that the most abundant group of PGM by the average number of grains in the UG2 Reef is the PGE sulphides (60 - 88%), followed by PGE alloys (5 - 22%), PGE arsenides (1 - 21%), PGE bismuth-tellurides (2 - 4%) and PGE antimonides (0-5%), with decreasing abundances respectively. In the MR, the most abundant PGM group by the average number of grains is the PGE arsenides (48%), followed by PGE sulphides (32%), PGE bismuth-tellurides (12%), PGE antimonides (5%) and PGE alloys (3%) with decreasing abundances respectively.

6.4. Platinum group mineral associations

Figures 6.16 to 6.20 illustrate the PGM associations for each sample in the various Reef types. The PGM in the UG2 Normal Reef (Figure 6.16) are mostly associated with pentlandite, chromite, amphibole and pumpellyite. The PGM in the UG2 Normal Reef of BFH007D0 (Figure 6.17) are mostly associated with pentlandite, chromite, chalcopyrite and amphibole. The PGM in the UG2 Split Reef (Figure 6.18) are mostly associated with pentlandite, chromite, pumpellyite and amphibole. The PGM in the UG2 Multiple Split Reef (Figure 6.19) are mostly associated with chromite, sulphides (pentlandite, chalcopyrite and other sulphide) and silicates (amphibole and chlorite). The PGM in the Merensky Reef (Figure 6.20) are mostly associated with silicates (amphibole, orthopyroxene and talc), and sulphides (pyrrhotite, pentlandite and chalcopyrite).

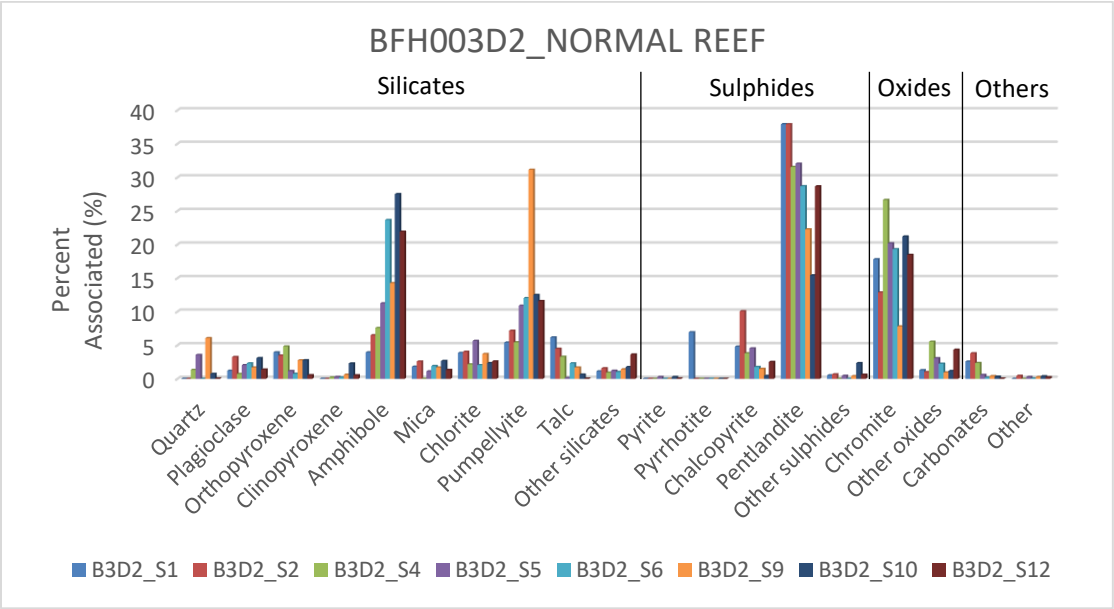

Figure 6.16: The PGM associations in the UG2 Normal Reef, for each sample in the borehole BFH003D2.

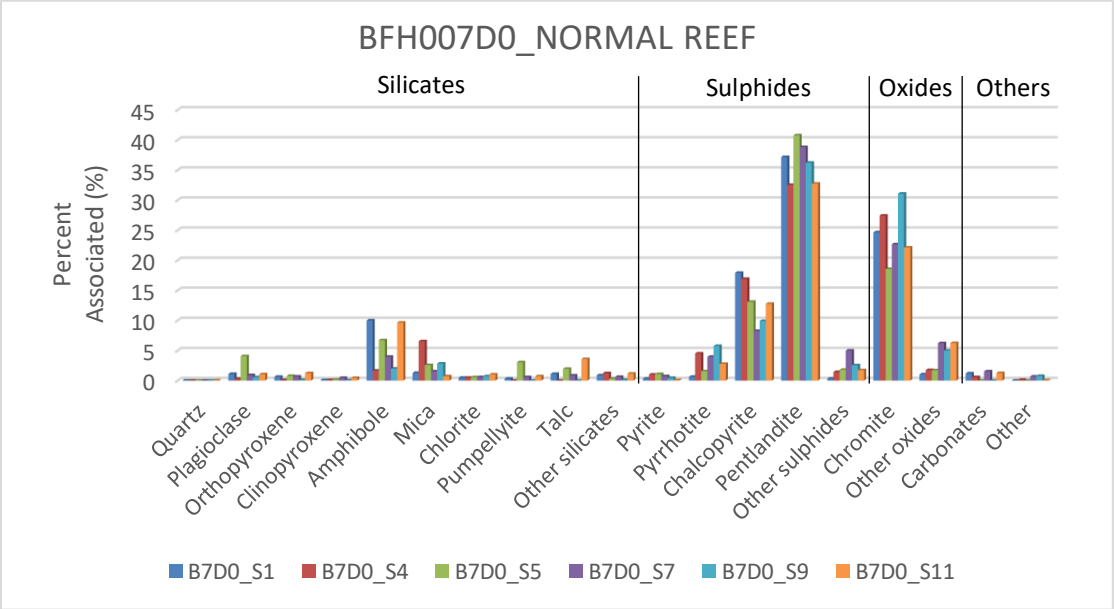

Figure 6.17: The PGM associations in the UG2 Normal Reef, for each sample in the borehole BFH007D0.

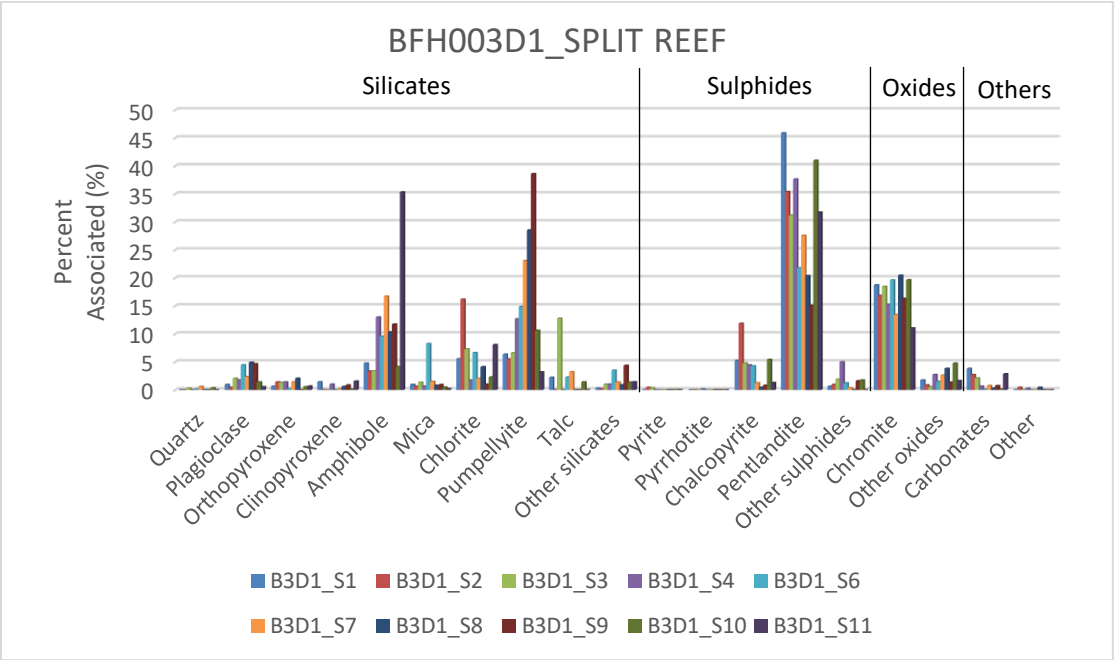

Figure 6.18: The PGM associations in the UG2 Split Reef, for each sample in the borehole BFH003D1.

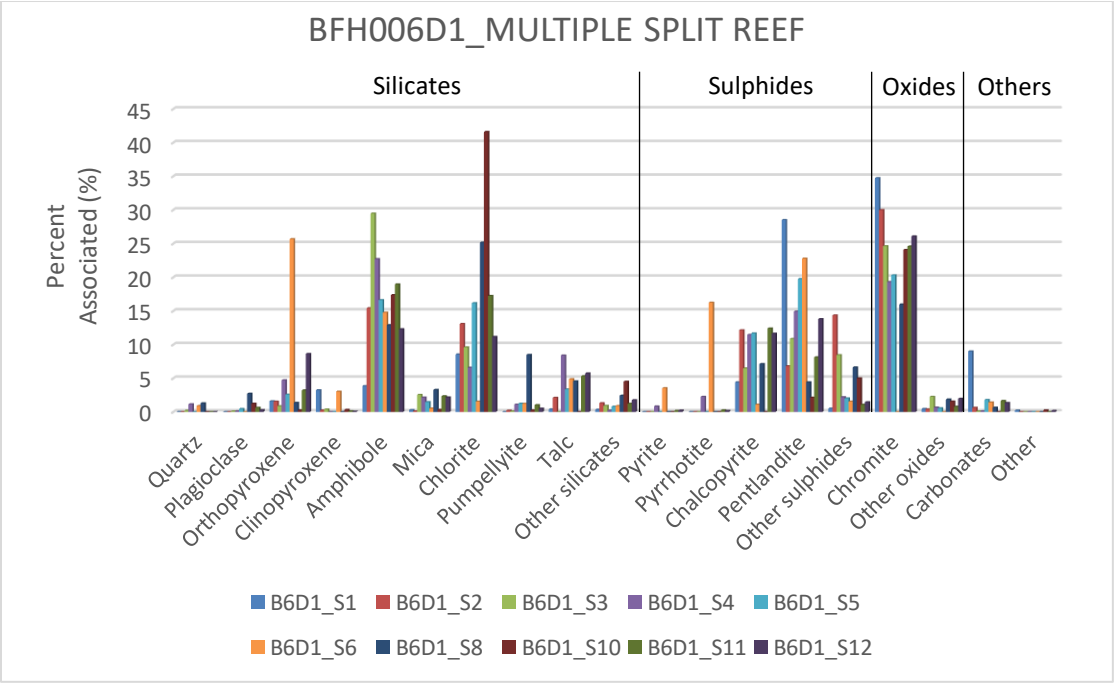

Figure 6.19: The PGM associations in the UG2 Multiple Split Reef, for each sample in the borehole BFH006D1.

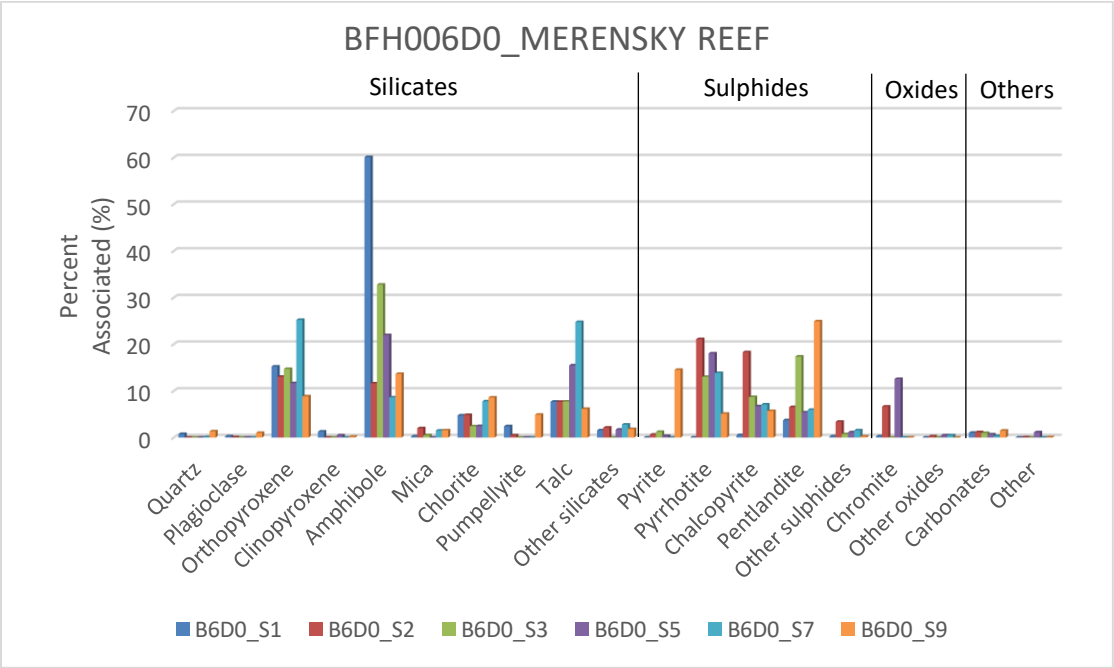

Figure 6.20: The PGM associations in the MR, for each sample in the borehole BFH006D0.

6.5. Platinum group mineral grain size distributions

The PGM grain sizes at Buffelshoek range from 0.87 to 53 microns (µm) from the samples, based on 80% passing through various sieve sizes, assuming the actual grain sizes does not exceed the diameter measured in two dimensions on the samples. The PGM grain sizes mostly range from 2 to 22 µm in the UG2 Reef and 2 to 32 µm in the MR (Figures 6.21 to 6.25). The UG2 Normal Reef (Figure 6.21) has most grain sizes distributed between 2 and 19 µm. The UG2 Normal Reef of BFH007D0 (Figure 6.22) has most grain sizes distributed between 2 and 16 µm. The UG2 Split Reef (Figure 6.23) has most grain sizes distributed between 1.75 and 22 µm, and some anomalous 53 µm sized grains. The UG2 Multiple Split Reef of (Figure 6.24) has most grain sizes distributed between 1.75 and 22 µm. The Merensky Reef (Figure 6.25) has most grain sizes distributed between 2 and 32 µm, and some anomalous 53 µm sized grains.

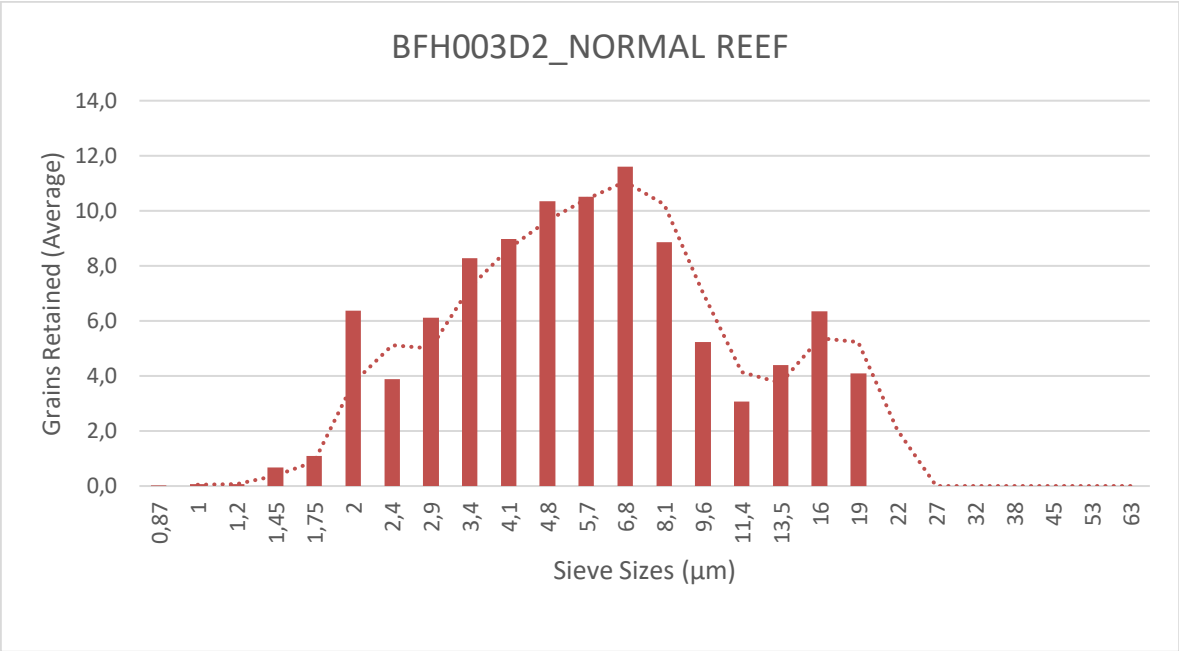

Figure 6.21: The PGM grain size distribution in the UG2 Normal Reef, borehole BFH003D2.

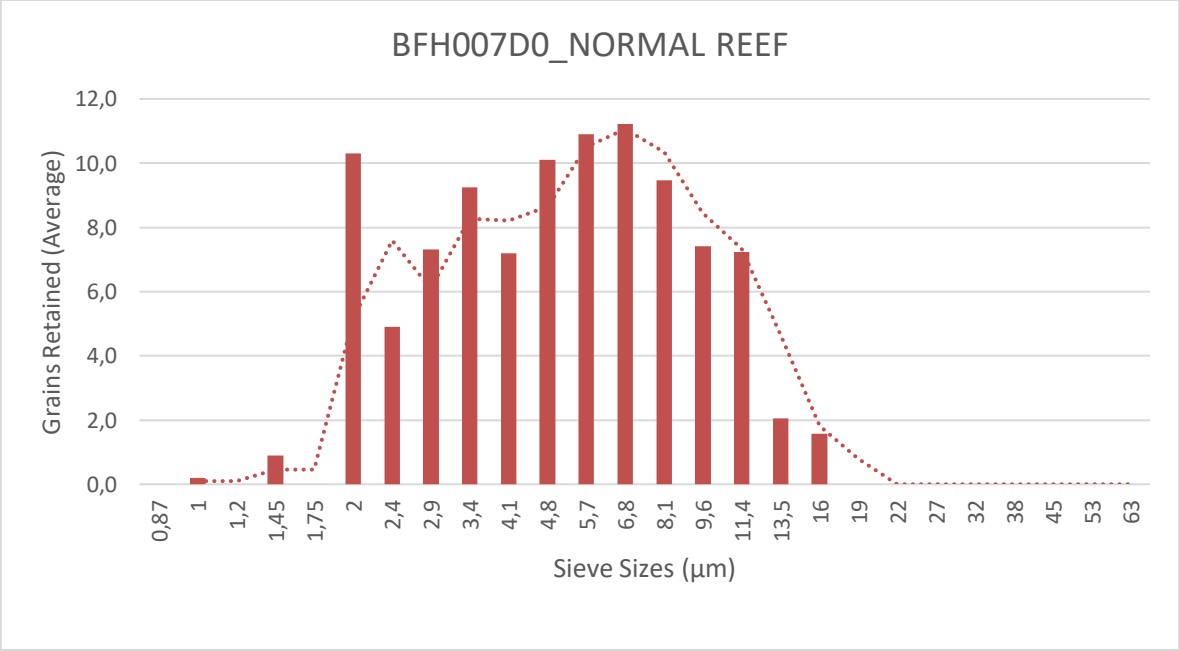

Figure 6.22: The PGM grain size distribution in the UG2 Normal Reef, borehole BFH007D0.

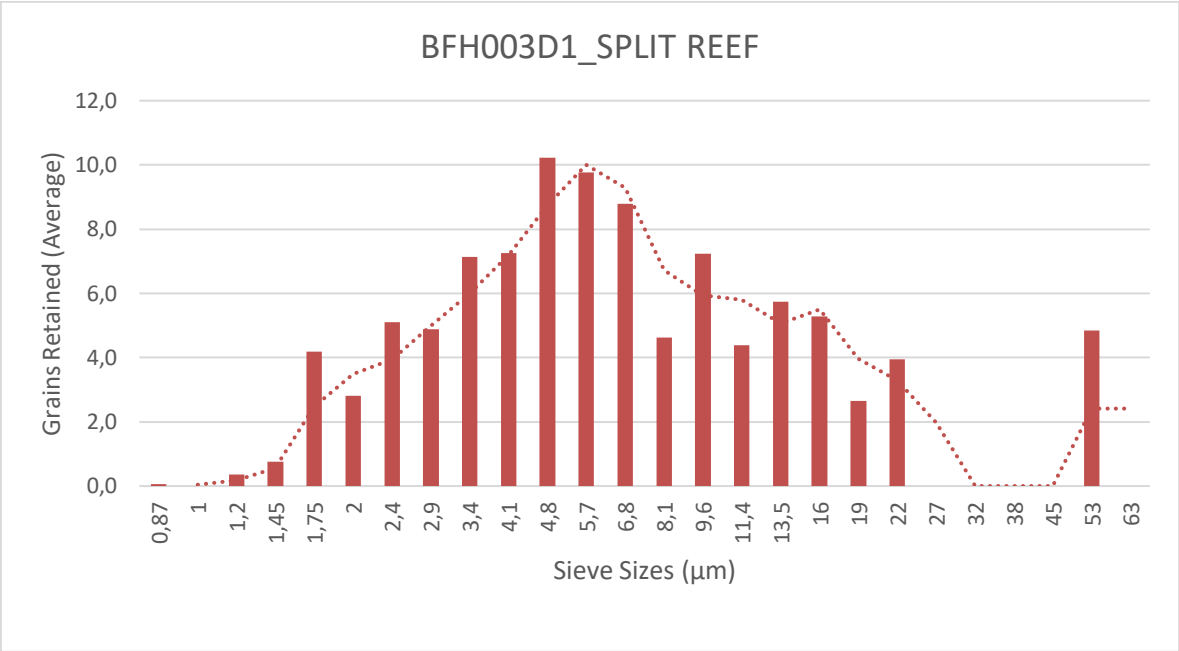

Figure 6.23: The PGM grain size distribution in the UG2 Split Reef, borehole BFH003D1.

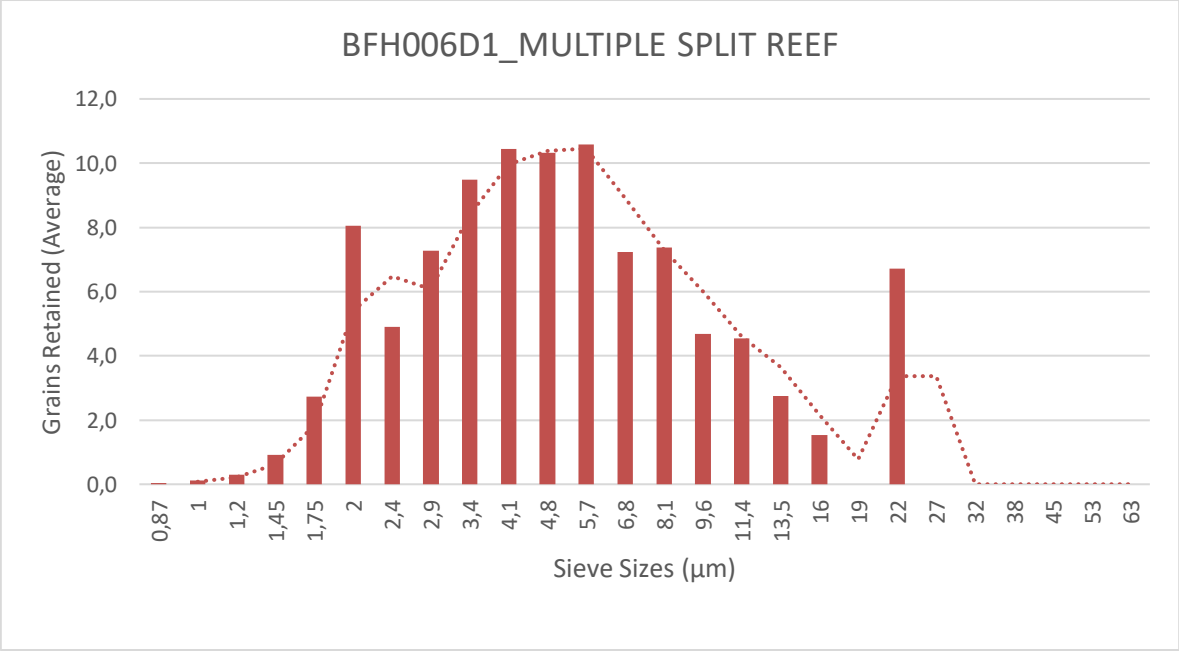

Figure 6.24: The PGM grain size distribution in the UG2 Multiple Split Reef, borehole BFH006D1.

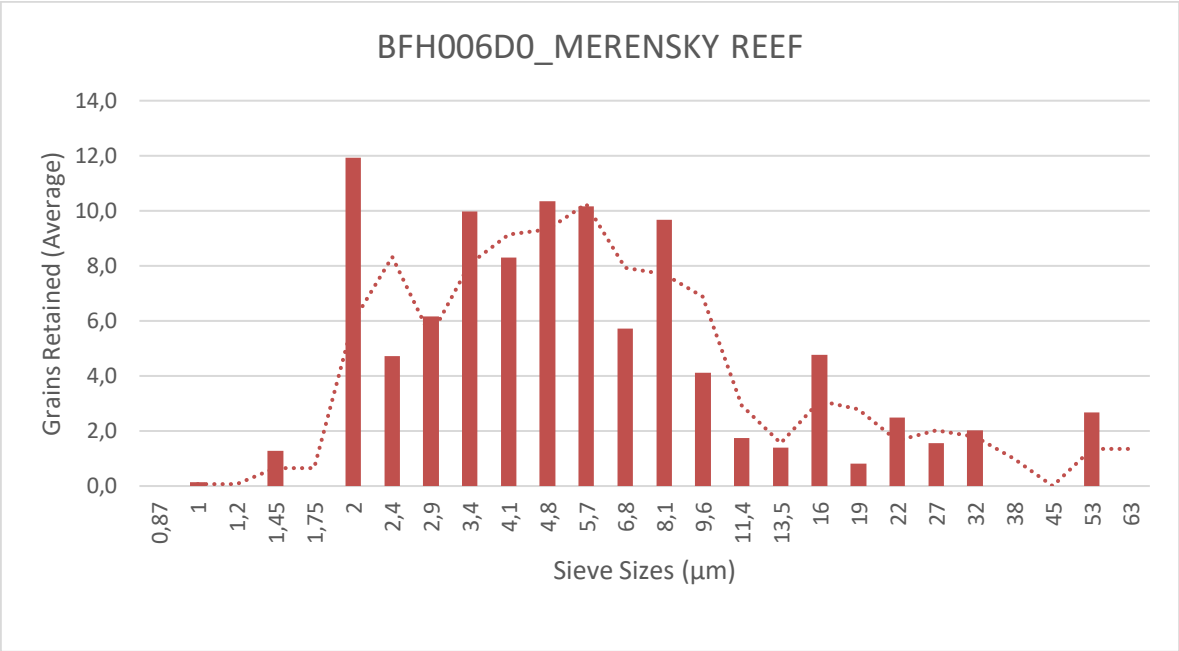

Figure 6.25: The PGM grain size distribution in the MR, borehole BFH006D0.

6.6. Deportments of palladium-platinum group elements

The palladium-PGE (PPGE) are the most dominant PGE with abundance up to 80% of total PGE content (Figure 6.1 to 6.5). Figures 6.26 to 6.28 represent the deportments (controls) of the PPGE in the PGM. Platinum (Pt) is mostly concentrated (deported) in the PGE sulphides (about 70.2 - 87.1%) in the UG2 Reef and mostly deported in the PGE arsenides (about 51.9%) and PGE sulphides (about 38.7%) in the MR (Figure 6.26). Palladium (Pd) is mostly deported in the PGE sulphides (about 55.4 - 69.7%) and PGE alloys (about 16 - 28 %) in the UG2 Normal, Split and Multiple Split Reefs, mostly deported in alloys (about 67.8%) in the UG2 Normal Reef of BFH007D0 (B7D0) and mostly deported in PGE antimonides (about 43%) and PGE bismuth-tellurides (Bi-Te) (about 38%) in the MR (Figure 6.27). Rhodium (Rh) is entirely deported in the PGE sulphides in UG2 Reef and deported in the PGE sulphide (about 86.5%) and PGE Bi-Te (about 13.5%) in the MR (Figure 6.28).

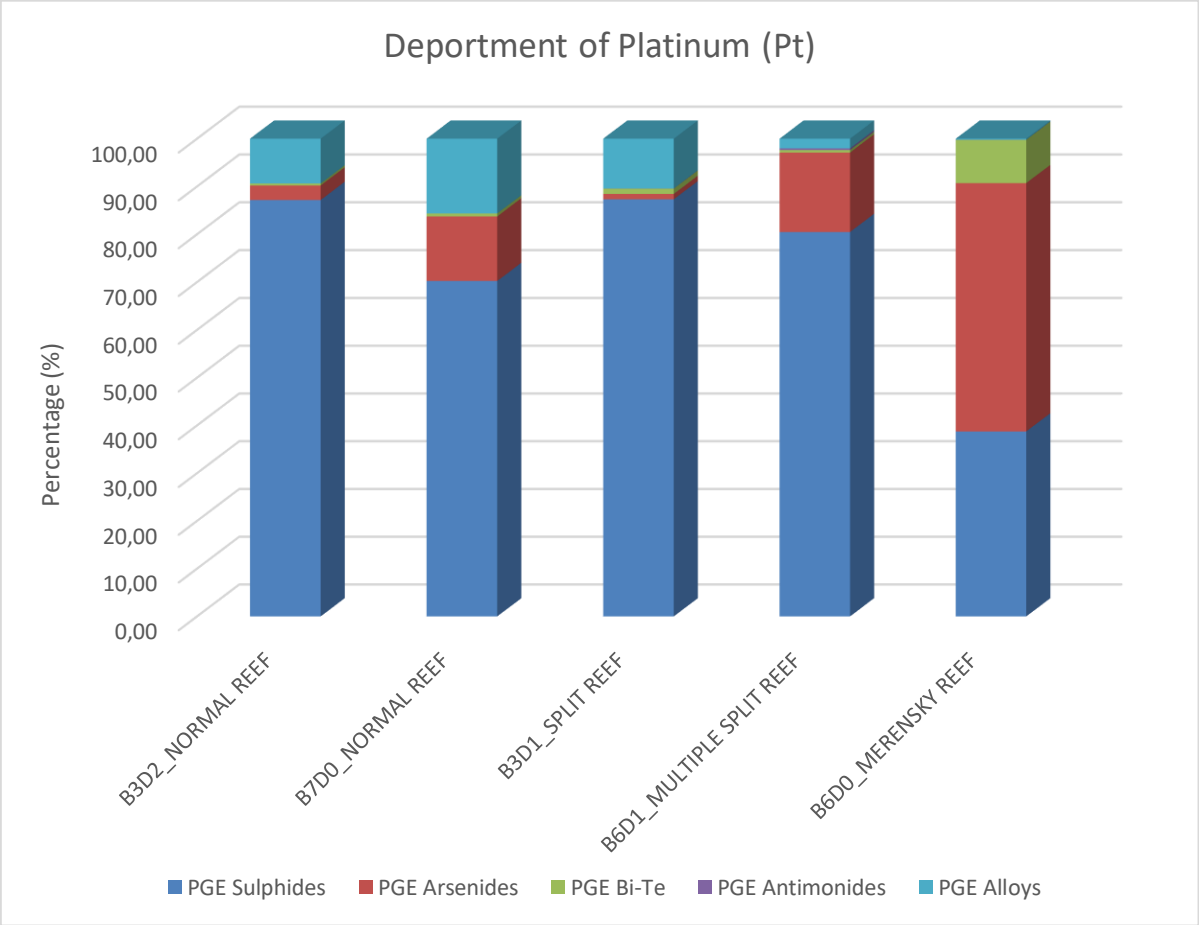

Figure 6.26: Deportment (control) of platinum in the PGM.

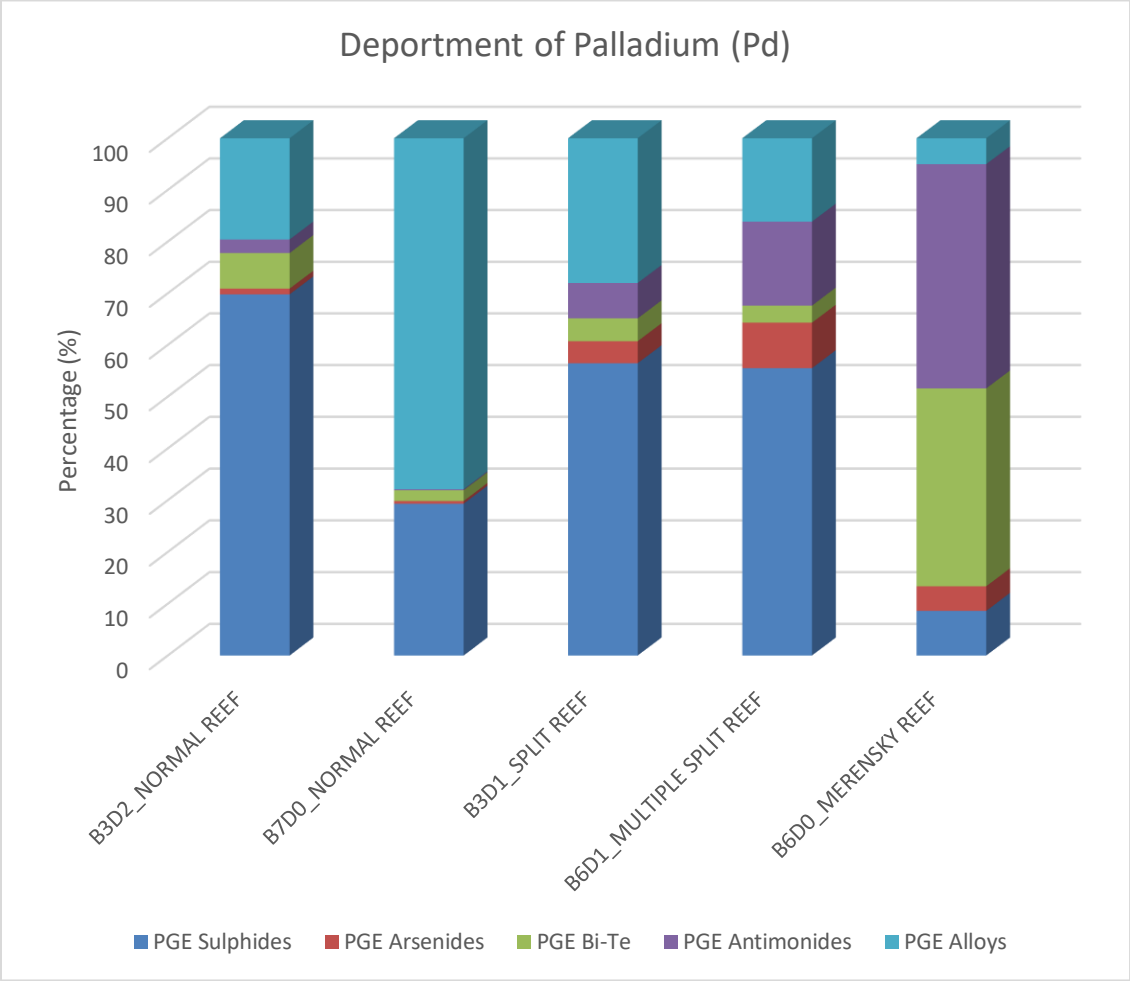

Figure 6.27: Deportment (control) of palladium in the PGM.

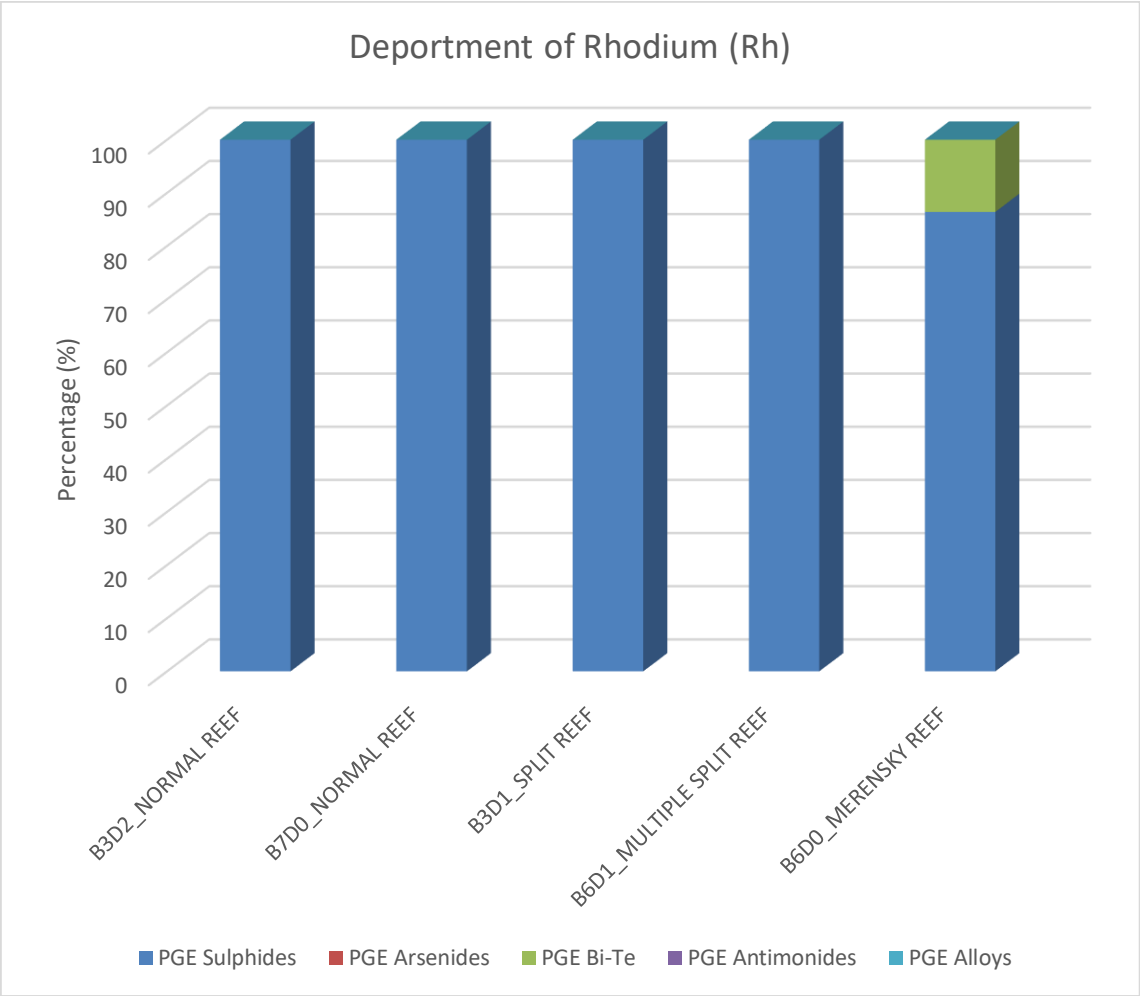

Figure 6.28: Deportment (control) of rhodium in the PGM.

CHAPTER 7 DISCUSSION AND CONCLUSION

7.1. The Upper Group 2 Chromitite and Merensky Reefs at Buffelshoek

The UG2 Reef at Buffelshoek can also be categorised into three Reef facies, (1) the Normal Reef (including internal pyroxenite, norite or anorthosite less than 10 cm thick), (2) the Split Reef (limited to one internal pyroxenite, norite or anorthosite equal or more than 10 cm thick) and (3) the Multiple Split Reef which generally has two or more internal pyroxenites, norites and / or anorthosites disruptions. The borehole data reveal that the UG2 Reef at the Buffelshoek is generally thinner than the UG2 Reef observed at the Dwarsrivier operations of TRP. The UG2 Reef at Buffelshoek has an average thickness of 0.7 m (Figures 2.3 to 2.6) which is within the 0.4 to 2.5 m reported by McLaren and De Villiers (1982), Schouwstra *et al.* (2000), Penberthy *et al.* (2000) and Barnes and Maier (2002).

The MLA based modal mineralogy indicates that the UG2 Reef at Buffelshoek is also characterised by predominately chromite (70-80%), plagioclase (5-15%) and orthopyroxene (6-8%), which agrees with McLaren and De Villiers (1982), Schouwstra *et al.* (2000), Penberthy *et al.* (2000) and Barnes and Maier (2002). Cramer (2001) indicated that in the UG2 Reef PGE grades vary from 3 to 8 g/t over a 0.65 to 1.5 m thick Reef. The assay data from TRP indicates that the UG2 Reef at Buffelshoek have PGE grade with a relatively wider range from 1.4 to 14.4 g/t over 0.1 m samples, however averages to 6.7 g/t over the 0.7 m thick Reef. The UG2 Reef at Buffelshoek is located about 130 m below the Merensky Reef (MR), comparable to the 140 m at the Dwarsrivier Farm reported by Mabuza (2007).

The MR at the Buffelshoek is generally a pyroxenite bounded by two chromitite stringers at the bottom and one at the top, and characterised predominately by orthopyroxene (about 55%), amphibole (about 15%) and sulphides (8%) based on

MLA data, which is not consistent with the general observations of Rose (2016) and Rose *et al*. (2018) at the TRP operation, where plagioclase and orthopyroxene are the most dominant minerals. The MR at Buffelshoek has a thickness of about 1.6 m (Figure 2.7) which is within the general 4 cm to 4 m thickness of MR reported by Cawthorn (1999) and Rose (2016). The PGE grades of the MR at Buffelshoek range from 0.15g/t to 29 g/t over 0.1 m samples, which averages to 15g/t over the 1.6 m thick Reef. The MR PGE grades vary from 3 to 9 g/t as reported by Cramer (2001) and 5 to 10 g/t reported by Barnes and Maier (2002a) and Cawthorn (2002), over a 0.6 to 3 m thick Reef.

Based on the theory of compatibility and incompatibility of PGE during fractionation, Harney *et al* (1990) indicated that the Pt and Pd are likely to be concentrated high up in the stratigraphy whereas IPGE (Ir, Ru and Os) and Rh are likely to be concentrated at the bottom in the stratigraphy. At Buffelshoek in the UG2 Reef the PGE are sporadically distributed through the stratigraphy, which is consistent with the UG2 Reef reported by Cawthorn (1999), Cramer (2001), Cawthorn (2011), MacCall (2016) and Rose et al. (2018). However, in the MR at Buffelshoek, there is a trend of Pt and Pd increasing down the stratigraphy, while the IPGE and Rh increases up the stratigraphy, which is rare compared to the sporadic mineralisation reported by Naldrett *et al*. (2009), Cawthorn (2011) and Rose *et al*. (2018). The total 6PGE (Pt, Pd, Rh, Ru, Ir and Os) concentrations are generally higher in the MR compared to the UG2 Reef at the Buffelshoek. The PGE chondrite normalised plot of the UG2 Reef and MR in Figure 7.1 of the Buffelshoek data indicates variable depletion and enrichment of the PGE, and this can be attributed to various stages of PGE mineralisation, which supports the proposal by Cawthorn (1999) where various geochemical models of PGE mineralisation were compared. This comparison argues that if the PGE were concentrated by a silicate magma (Merkle, 1992), the UG2 chromitite has limited silica but is enriched in PGE, similarly if the PGE were concentrated by chromite (Hiemstra, 1985), silica-rich Platreef has limited chromite

but is enriched in PGE. Furthermore, if sulphide immiscibility entirely concentrated the PGE (Naldrett, 1989), evidence should be seen in the geochemistry of the footwall and hanging-wall. Thus, these multiple models of PGE mineralisation suggest that hey must have been various stages or events of mineralisation resulting in variable contents of PGE across the Reefs (Cawthorn, 1999).

The textures observed from petrographic analysis are consistent with the several stages of mineralisation in the UG2 Reef and MR especially looking at minerals that are mostly associated or hosting the PGM such as BMS, as in Smith *et al*. (2014). Texturally, the BMS occur as interstitial to the silicates and chromites which is consistent with late-stage crystallisation of these sulphides. The fine grained BMS can be attributed to low diffusion at some stage of mineralisation compared to very coarse grained (high diffusion rates) at other stages. Similarly, scattered BMS can be attributed to lower diffusion rates during crystallisation compared to massive BMS. The BMS occurring as replacing phases can also be attributed to the late-stage mineralisation. The BMS exhibiting intergrowth textures can be attributed to the same stage of formations. The variable textures (grain shapes) of the BMS can also be attributed to several stages of sulphide mineralisation, e.g., euhedral grains can be attributed to good nucleation and diffusion during early-stage depositions resulting in well-formed crystals. Whereas subhedral, anhedral, irregular and interstitial grains, can be attributed to late-stage depositions, where grain shapes are controlled by pre-existing crystals / structures such as in fracture filling mineralisation (which is deposition post deformation).

The BMS observed from petrographic analysis in the UG2 Reef and MR are generally pentlandite, chalcopyrite and pyrrhotite, which agrees with Penberthy *et al.* (2000), Cawthorn *et al.* (2002) and Godel *et al.* (2010). In the UG2 Reef, the most dominant BMS is pentlandite followed by chalcopyrite and very rarely pyrrhotite

which is in line with the MLA results. In the MR the most dominant BMS are pentlandite and pyrrhotite followed by chalcopyrite.

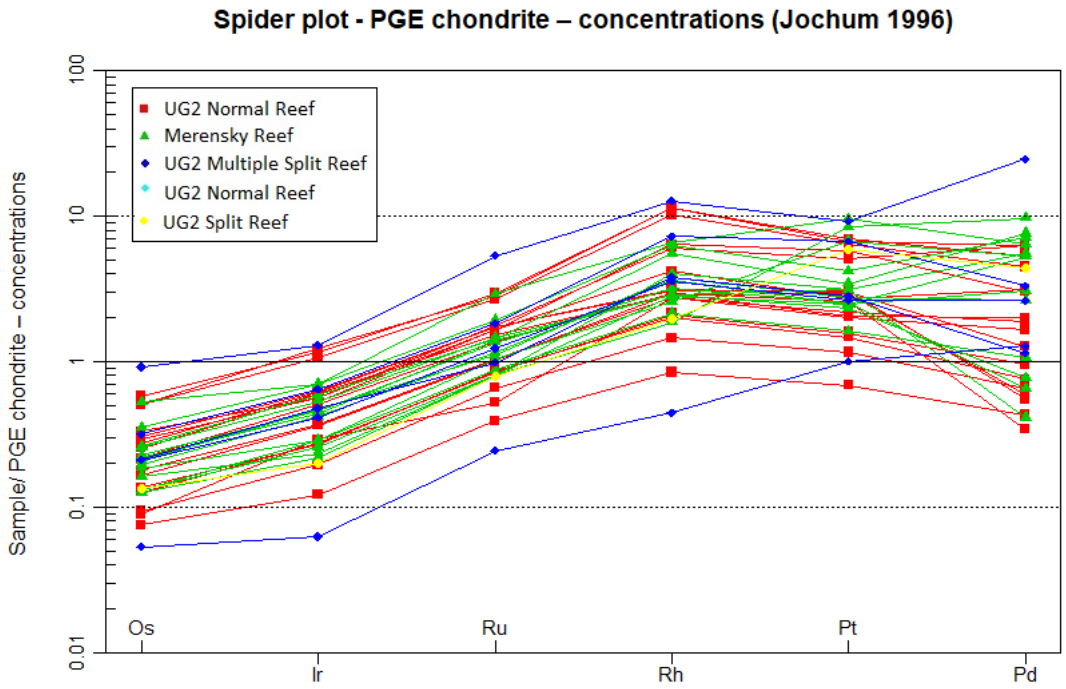

Figure 7.1: PGE chondrite normalised plot of the UG2 Reef and MR (normalised after Jochum, 1996).

Based on the geochemistry obtained from the MLA, the S contents in the UG2 Reef is less than 1% and greater than 1% in the MR, although a few samples in the UG2 Reef have S content greater than > 0.1% (Appendix D.1.2) which is not in agreement with the known geochemistry of the UG2 Reef by Cawthorn (1999), Naldrett *et al.* (2012) and Langa *et al.* (2020). The higher S content in the UG2 Reef can be attributed to massive BMS in smaller sample interval raising the S contents. The MR is characterised by low Cr, Fe, Al, Ti, V and Co (> 0.012) and high Mg#, Mg, Si and Cu (> 0.15) relative to the UG2 Reef. Generally, there is a great deal of overlaps in the chemistry composition of the various UG2 Reef facies (Normal, Split and Multiple

Split Reefs), which was also documented by Langa *et al.* (2020) while comparing the inferred UG2 Reef in the Platreef to that of the Eastern and Western Limbs. The chemistry of the UG2 Reef facies is noticeably distinct to that of the MR, however there are minor overlaps of other elements such as Ni between the UG2 Reef and MR.

7.2. Platinum group mineralogy and chemistry

The PGM in the UG2 Reef at Buffelshoek ranges from predominately PGE sulphides to non-sulphides, while the PGM in the MR ranges from predominately PGE arsenides and sulphides to other PGM. The MLA results for Buffelshoek suggest that there is a significant amount of S in the MR not related to PGE mineralisation given that the PGM are predominately arsenides. The high content of S and Cu in the MR can be attributed to concentrations of CuS phases in the MR which are not associated with PGE.

The Figure 7.2 summarises the distribution of PGM by Reef type at the Buffelshoek to indicate the relative abundances of the PGM in the various UG2 Reef facies and MR. The PGM are broadly grouped into PGE sulphides, PGE arsenides, PGE bismuth-tellurides, PGE antimonides and PGE alloys. The UG2 Reef is on average dominated by PGE sulphides (76.3%) followed by PGE alloys (11.3%), PGE arsenides (9.4%), PGE bismuth-tellurides (1.7%) and PGE antimonides (1.3%). The MR is dominated by PGE arsenides (39.6%) followed by PGE bismuth-tellurides (22.3%) and PGE sulphides (21.7%) and then PGE antimonides (11.8%) and PGE alloys (4.6%). These PGM distributions at Buffelshoek are to some extent comparable with Rose (2018) at the TRP operation where PGM are grouped as PGE sulphides, basemetal sulphides, alloys, sulpho-arsenides, tellurites, bismuthotellurides and others (see subgrouping in Table 6.1).

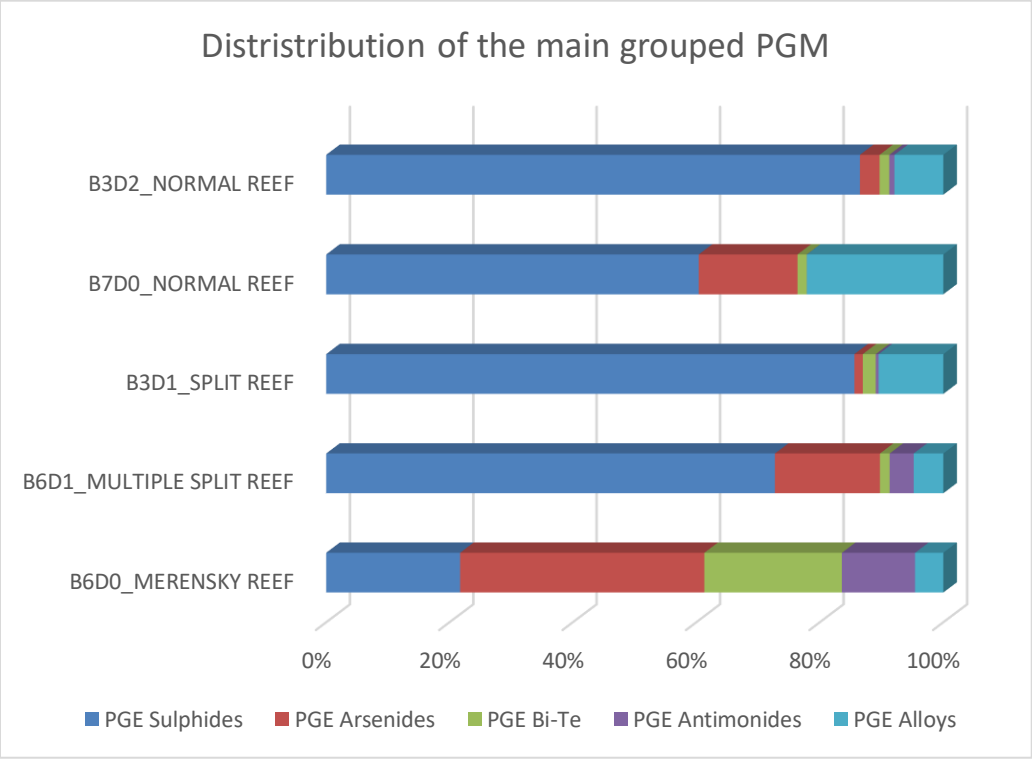

Figure 7.2: Correlation of the distribution of PGM by Reef type (UG2 Reef facies and MR).

Table 6.1 lists the PGM phases, and their relative abundances which were identified by the MLA, however sometimes the EDS spectra identify end-member minerals of the mineral groups with difficulty (Van der Merwe, 2011). The use of the EMPA, WDS spectra provide detailed end-member mineral chemistry. Table 5.1 summarise the various PGE mineral groups by detailed mineral chemistry, which are grouped into: PGE-Fe-S-Cu-Ni-Pb (Group 1), PGE-S-As (Group 2), PGE-As (Group 3), PGE-Bi-Te (Group 4), PGE-Cu-S (Group 5), PGE-Cu-Fe-S (Group 6), PGE-Ni-Fe-S (Group 7), PGE-Ni-S (Group 8), PGE-Fe-S (Group 9), PGE-S (Group 10) and PGE-Alloys / Complex (Group 11).

These PGE mineral groups are essentially PGM groups; PGE sulphides (Group 1, 2 and 10), PGE arsenides (Group 3), PGE bismuth-tellurides (Group 4), and PGE Antimonides and PGE alloys (Group 11), which indicates that somewhat the EMPA supports the MLA. The PGE sulphide, kharaelakhite (PtCuPbFeNiS) was identified using the MLA in the UG2 Reef and MR and confirmed using the EMPA in the UG2 Reef, yielding the quantitative chemistry Pt (32.47 wt%), Cu (8.57 wt%), Pb (23.83 wt%), Fe (7.48 wt%), Ni (7.02 wt%) and S (19.86 wt%). The list of the PGE minerals / PGM chemistry obtained using the EMPA for the identified PGM is found in Appendix C.1.1.

In general, the PGM are associated with pentlandite, chromite and amphibole (Figure 7.3). The PGM association can broadly be BMS (pentlandite, chalcopyrite and pyrrhotite), chromite and silicates (amphibole, chlorite, pumpellyite, orthopyroxene, talc, plagioclase, etc), which then agrees with Penberthy *et al.* (2000), Cawthorn *et al.* (2002), Godel *et al.* (2010) and Rose (2018). The BSE images in Figure 5.8 confirms a strong association of PGM with BMS, chromites and silicates to support the MLA results.

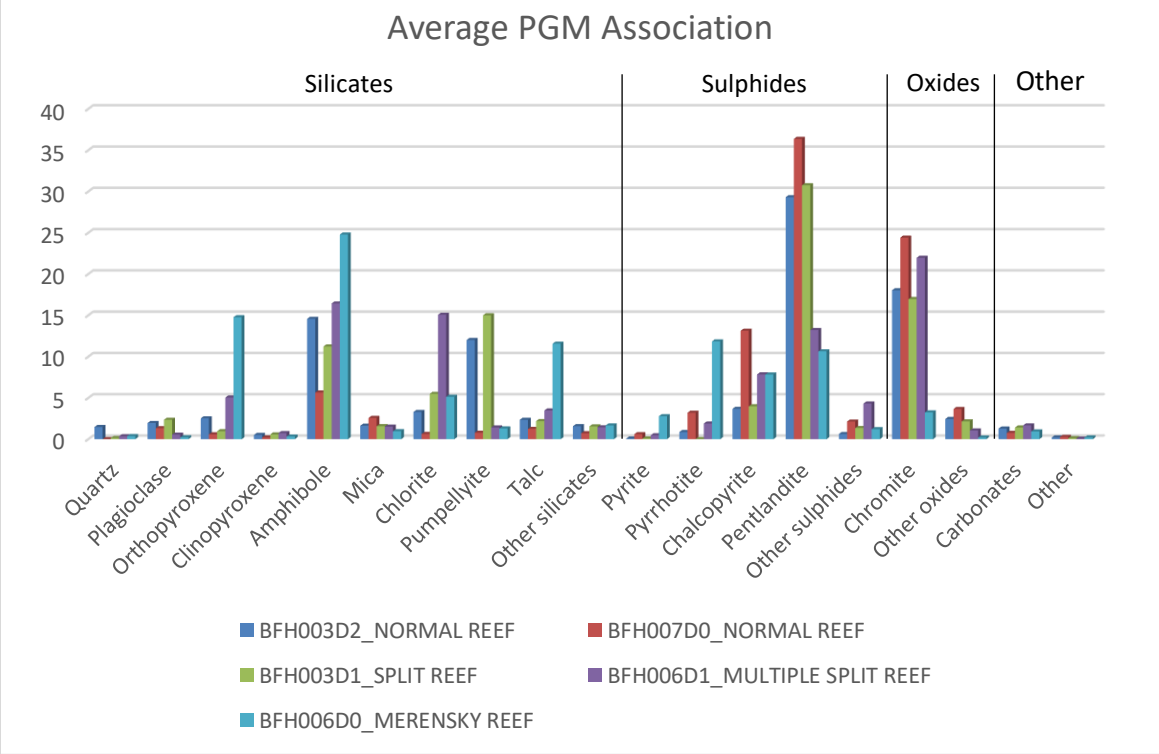

Figure 7.3: Correlation of the association of PGM by Reef type (UG2 Reef facies and MR).

Rose (2018) indicated that typically in the MR it is sufficient to mill ore to a grind size of 60 wt% passing 75 microns (µm), while in the UG2 Reef it is sufficient to mill ore to a grind size of 75 wt% passing 75 µm, which is controlled by the BMS grain size. Several authors Penberthy (2001), Osbahr *et al.* (2014) and Rose (2018) studied the grain size distribution of the BMS associated or hosting the PGM as opposed to the PGM grain size distribution in the UG2 Reef and MR of the Eastern Bushveld Complex. The grain size distribution of the PGM at Buffelshoek generally range from 2 to 22 µm with rare instances of grains of 53 µm in the UG2 Reef, and ranges from 2 to 32 µm also with some rare grains of 53 µm in the MR. Figure 7.4 shows the grain size distributions of the PGM in the various UG2 Reef facies and MR, which are fairly similar for the UG2 Reef facies and MR; approximately 80 wt% passing 13.5 µm, and more than 60 wt% of the grains are smaller than 6.8 µm. Generally, the PGM are smaller than 63 µm with 90% passing 22 µm in the UG2 Split Reef and

MR. To liberate most PGM (60 wt%) at Buffelshoek requires grind size up to 6.8 µm as indicated by the data in Figure 7.4.

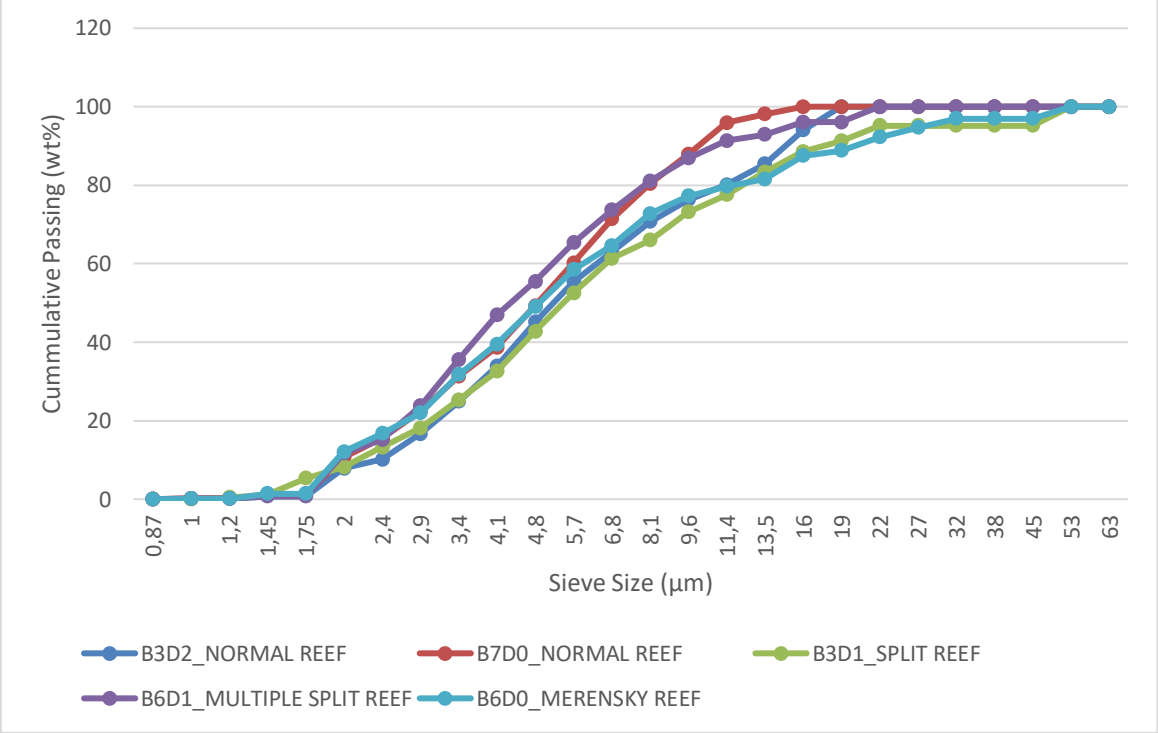

Figure 7.4: Correlation of the cumulative grain size distributions of PGM by Reef type (UG2 Reef facies and MR).

7.3. The effect of platinum group minerals on recovery

The PGE are largely dominated (up to 80% abundance) by palladium-PGE (PPGE), Pt, Pd and Rh. In the UG2 Reef Pt is mostly deported in PGE sulphides, about 70.2 - 87.1%, Pd is mostly deported in PGE sulphides, about 55.4 - 69.7% and PGE alloys, about 16 - 28%, whereas Rh is entirely deported in PGE sulphides. The concentrations of the PPGE, which are the most abundant is generally controlled by PGE sulphides in the UG2 Reef, as these PGE are mostly deported in the PGE sulphides. In the MR Pt is mostly deported in PGE arsenides, about 51.9% and PGE sulphides, about 38.7%, Pd is mostly deported in PGE antimonides (about 43%) and

PGE bismuth-tellurides (about 38%) and Rh is mostly deported in PGE sulphides, about 86.5% and PGE bismuth-tellurides, about 13.5%. The PPGE are controlled by various PGM groups in the MR.

Based on the deportment of PGE in the PGM, abundances and distributions of the PGM, association and grain size distributions of the PGM in this study and the work of Vermaak (2005) on recoverability of PGM summarised in Table 3.1; under normal flotation conditions, recovery at Buffelshoek is likely to be as follows: 76.4 - 89.6% of PGM will be recovered well (good), 7.9 - 22.1% variable and 1.5 - 2.4% poorly in the Normal Reef. In the Split and Multiple Split: 86.9 - 89.7% good, 2.5 - 5.46% poor and 4.8 - 10.5% variable recoveries of the PGM and in the MR: 61.3% good, 4.6% variable and 34.1% poor recoveries. These projections are based on grouping of the PGM according to their ease of recovery as indicated in Table 3.1, where PGE sulphides can be grouped with PGE arsenides, PGE bismuth-tellurides (Bi-Te) with PGE antimonides (Sb) and PGE alloys as an individual group (Figure 7.5).

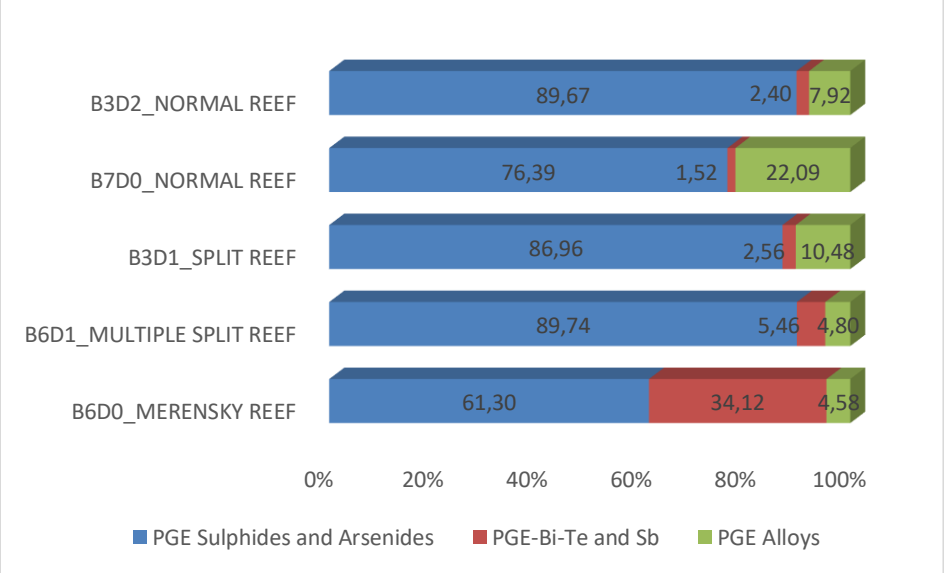

Figure 7.5: Distributions of the grouped PGM further simplified according to ease of PGE recovery after Vermaak (2005) outlined in Table 3.1. Note the PGE-Sb are grouped with Bi-Te to be conservative based on the study by Vermaak (2005).

7.4. Conclusion

The study at Buffelshoek have not only achieved the aim and objectives outlined in this dissertation, but also contributes the following to geology literature of the Bushveld Igneous Complex: (1) cryptic variation of sample geochemistry of the UG2 Reef and MR obtained from the MLA, (2) amongst the identified PGM which are mostly found in literature, the rare PGE sulphide, kharaelakhite was also identified for the first time in the UG2 Reef and MR using MLA and confirmed using the EMPA, and (3) PGM properties under reflected light microscopy.

From the study at the Buffelshoek the following conclusions were drawn:

The modal mineralogy of the UG2 Reef at the Buffelshoek obtained using MLA is fairly similar to that of the Dwarsrivier whereat the current TRP is operating. The PGM phases identified in the UG2 Reef and MR at Buffelshoek are broadly grouped into PGE sulphides, PGE arsenides, PGE bismuth-telluride, PGE antimonides and PGE alloys. The PGE sulphides are the most abundant PGM in the UG2 Reef and PGE arsenides are the most abundant in the MR. The sample geochemistry obtained using MLA shows higher content of Cu and S in the MR, attributed to CuS mineral phases with low concentrations of PGE (PGE not detected by MLA), which relates to the high sulphur content but less PGE in the MR.

The PGM in the UG2 Reef are closely associated with sulphides, chromite, and silicates in order of decreasing association. The PGM in the MR are mostly associated with silicates, sulphides and to some extent chromite, in order of decreasing association. The sulphides identified are mostly BMS, which occur interstitially to the major minerals such as chromite and silicates and indicative of late-stage formation of the BMS. The grains sizes generally range from 2 to 22 μm in the UG2 Reef and 2 to 32 μm in the MR.

The most abundant PGE are the PPGE and the PGM controls the PPGE as follows: Platinum (Pt) is mostly deported in the PGE sulphides in the UG2 Reef and deported in the PGE arsenides in the MR. Palladium (Pd) is mostly deported in the PGE-sulphides in the UG2 Normal, Split and Multiple Split Reefs, mostly deported in the PGE alloys in the UG2 Normal Reef with internal pyroxenite (< 10 cm) and mostly deported in PGE antimonides in the MR. Rhodium (Rh) is entirely deported in the PGE sulphides in the UG2 Reef and is mostly deported in the PGE sulphides and to some extent in the PGE bismuth-tellurides in the MR.

For the PGE recovery's process optimisation and efficiencies, the grouped PGM can be simplified based on their flotation rates as follows: The PGE sulphides and arsenides which would exhibit good recovery, the alloys which would exhibit variable recovery, and the bismuth-tellurides which may exhibit poor recovery (to be conservative the PGE antimonides are associated with poor recovery in this study). About 76 to 89% of PGM are PGE sulphides and arsenides in the UG2 Reef and 61.3% in the MR, which are likely to be well recovered. The remaining PGM will be variably to poorly recovered, however if suitable reagents are induced to encourage hydrophobicity of the PGE bismuth-tellurides (including PGE antimonides) and PGE alloys present in the UG2 Reef and MR at Buffelshoek the recovery will likely increase.

The information on the textural relationships of BMS (mostly associated with PGM) identified through petrographic analysis, the PGM phases and their abundances (with some PGM confirmed using the EMPA), the PGM associations and grain size distributions obtained using MLA can be used to assess the feasibility of the Buffelshoek prospect in relation to mineral processing (metallurgical throughput / flotation). Some of the main aspects of this study were presented at the Geological Society of South Africa REI Fund conference (Appendix E).

REFERENCES

Ashwal, L. D., Webb, S. J and Knoper, M. W. (2005). Magmatic stratigraphy in the Bushveld Northern Lobe: continuous geophysical and mineralogical data from the 2950 m Bellevue drillcore. South African Journal of Geology, **108**, 199-232.

Barnes, S. J and Maier, W. D. (2002). Platinum-group element distributions in the Rustenburg Layered Suite of the Bushveld Complex, South Africa. In: The Geology, Geochemistry, Mineralogy and Mineral Beneficiation of Platinum-Group Elements. In: Cabri, L. J. (Ed), Canadian Institute of Mining, Metallurgy and Petroleum, **54**, 431-458.

Barnes, S. J and Maier, W. D. (2002a). Platinum-group element distribution in the Merensky Reef, Impala Mine, Bushveld Complex. Journal of Petrology, **43**,103-128.

Boudreau, A. E and McCallum, I. S. (1992). Concentration of platinum-group elements by magmatic fluids in layered intrusions. Economic Geology, **87**, 1830-1848.

Buchanan, D. L., Nolan, J., Suddaby, P., Rouse, J. E., Viljoen, M. J and Davenport, J. W. J. (1981). The genesis of sulphide mineralisation in a portion of the Potgietersrus Limb of the Bushveld Complex. Economic Geology, **76**, 568-579.

Buchanan, D. L and Rouse, J. E. (1984). Role of contamination in the precipitation of sulphides in the Platreef of the Bushveld Complex. In: Buchanan, D. L and Jones, M. J. (Ed), Sulfide De-posits in Mafic and Ultramafic Rocks. Special Publication, Institution of Mining and Metallurgy, 141–146.

Buchanan, P. C., Reimold, W. U., Koeberl, C and Kruger, F. J. (2002). Geochemistry of intermediate to siliceous volcanic rocks of the Rooiberg Group, Bushveld

Magmatic Province, South Africa. Contributions to Mineralogy and Petrology, **144**, 131-143.

Buchanan, P. C., Koeberl, C and Reimold, W. U. (1999). Petrogenesis of Dullstroom Formation, Bushveld magmatic province, South Africa. Contributions to Mineralogy and Petrology, **137**, 133-146.

Buick, I. S., Maas, R and Gibson, R. (2001). Precise U-Pb titanite age constraints on the emplacement of the Bushveld Complex, South Africa. Journal of the Geological Society, London, **158**, 3-6.

Bye, A. R. (2003). The Development and Application of a 3D Geotechnical Model for Mining Optimisation, Sandsloot Open Pit Platinum Mine, South Africa. **PhD thesis,** University of Natal.

Cameca. (2018). Electron Probe Microanalysis. Manual Second Edition, Materials Analysis (AMETEK), 39p.

Cameron, E. N. (1978). The Lower Zone of the Eastern Bushveld Complex in the Olifants River trough. Journal of Petrology, **19**, 437-462.

Cawthorn, R. G. (1999). Platinum-group element mineralization in the in the Bushveld Complex – a critical reassessment of geochemical models. South African Journal of Geology, **102 (3)**, 268-281.

Cawthorn, R. G. (1999a). The platinum and palladium resources of the Bushveld Complex. South African Journal of Science, **95**, 481 – 48.9

Cawthorn, R. G. (2002). The role of magma mixing in the genesis of PGE mineralisation in the Bushveld Complex: Thermodynamic calculations and new interpretations – A discussion. Economic Geology, **97 (3)**, 663-666.

Cawthorn, R. G. (2011). Geological interpretations from the PGE distribution in the Bushveld Merensky and UG2 chromitite reefs. Journal of the Southern African Institute of Mining and Metallurgy, **111 (2)**, 67-79.

Cawthorn, R. G., Barton, J. M and Viljoen, M. J. (1985). Interaction of floor rocks with the Platreef on Overysel, Potgietersrus, norther Transvaal. Economic Geology, **80**, 988-1006.

Cawthorn, R. G and Walraven, F. (1998). Emplacement and crystallization time for the Bushveld Complex. Journal of Petrology, **39 (9)**, 437-462.

Cawthorn, R. G., Merkle, R. W. K and Viljoen, M. J. (2002). Platinum Group Element Deposits in the Bushveld Complex, South Africa. In: Cabri, L. J (Ed), The geology, geochemistry, mineralogy and mineral beneficiation of platinum-group elements. Canadian Institute of Mining, Metallurgy and Petroleum, Special Issue, **54**, 389-430.

Chatterjee, N. (2012). Electron Microprobe Analysis. Massachusetts Institute of Technology, from: http://web.mit.edu/e-probe/www/ (accessed 1 February 2020).

Chetty, D., Gryffenberg, L., Lekgetho, T. B and Molebale, I. J. (2009). Automated SEM study of PGM distribution across a UG2 flotation concentrate bank: Implications for understanding PGM floatability. Journal of the Southern African Institute of Mining and Metallurgy, **109 (10)**, 587-593.

Chief Surveyor General of South Africa. Cadastral data of South Africa, from: https://csggis.drdlr.gov.za/psv/ (accessed 2 July 2021).

Council for Geosciences. Geological data of South Africa at 1:1Million scale 2018 Edition, from: https://maps.geoscience.org.za/portal/apps/sites/ (accessed 2 July 2021).

Cramer, L. A. (2001). The extractive metallurgy of South Africa's platinum ores. Journal of the Minerals, Metals and Materials Society, **53 (10)**, 14-18.

Eales, H. V. (2002). Caveats in defining the magmas parental to the mafic rocks of the Bushveld Complex, and the manner of their emplacement: review and commentary. Mineralogical Magazine, **66 (6)**, 815-882.

Eales, H. V and Cawthorn, R. G. (1996). The Bushveld Complex. In: Cawthorn, R. G. (Ed), Layered intrusions. Elsevier, Amsterdam, 181-230.

Eales, H. V., Marsh, J. S., Mitchell, A. A., De Klerk, W. J., Kruger, F. J and Field, M. (1986). Some geochemical constraints upon models for the crystallization of the Upper Critical Zone-Main Zone interval, northwestern Bushveld Complex. Mineralogical Magazine, **50**, 567-582.

Eriksson, P. G., Schreiber, U. M and Van der Neut. (1991). A review of the sedimentology of the Early Proterozoic Pretoria Group, Transvaal Sequence, South Africa: implications for tectonic setting. Journal of African Earth Sciences, **13 (1)**, 107-119.

Eriksson, P. G., Hattingh, P. J and Altermann, W. (1995). An overview of the geology of the Transvaal Sequence and Bushveld Complex. Mineralium Deposita, **30**, 98-111.

Esterhuizen, A. (2014). Unique fall-of-ground prevention strategy implemented at Two Rivers Platinum Mine. Journal of the Southern African Institute of Mining and Metallurgy, **114 (10)**, 785-788.

Fandrich, R., Gu, Y., Burrows, D and Moeller, K. (2007). Modern SEM-based Mineral Liberation Analysis. International Journal of Mineral Processing, **84**, 310-320.

Gain, S. B and Mostert, A. B. (1982). The geological setting of the platinoids base metal sulphide mineralization in the Platreef of the Bushveld Complex on Drenthe, north of Potgietersrus. Economic Geology, **77**, 1395-1404.

Godel, B., Barnes, S. J., Barnes, S. J and Maier, W. D. (2010). Platinum ore in three dimensions: Insights from high-resolution X-ray computed tomography. Geology, **38 (12)**, 1127-1130.

Godel, B., Maier, W. D and Barnes, S. J. (2008). Platinum-group elements in the Merensky and J-M Reefs: A review of recent studies. Journal Geological Society of India, **72**, 595-609.

Google Earth Pro 7.0.2.8415. (13 May 2021). Local generalised geology of the Buffelshoek 368 KT Farm showing the boundary of the farm and locations of the boreholes studied. 30.033126, -24.979886, eye alt 17.43km. RSA1M_Lithocronostratigraphic_polygons. http://www.google.com/earth/ index.html/ (accessed 2 July 2021).

Grobler, D. F., Brits, J. A. N., Maier, W. D and Crossingham, A. (2018). Litho- and chemostratigraphy of the Flatreef PGE deposit, Northern Bushveld Complex. Mineralium Deposita (2019), **54**, 3-28.

Gu, Y. (2003). Automated Scanning Electron Microscope based Mineral Liberation Analysis. Journal of Minerals and Materials Characterization and Engineering, **2 (1)**, 33-41.

Hahn, U. F and Ovendale, B. (1994). UG2 Chromitite layer potholes at Wildebeestfontein North Mine, Impala Platinum Limited. Proceedings from 15th CMMI Congress, SAIMM, **3**, 195-200.

Harris, C and Chaumba, J. B. (2001). Crustal contamination and fluid-rock interaction during the formation of the Platreef, Northern Limb of the Bushveld Complex, South Africa. Journal of Petrology, **42 (7)**, 1321-1347.

Harney, D. M. W., Merkle, R. K. W and Von Gruenewaldt, G. (1990). Platinum-group element behavior in the lower part of the upper zone, eastern Bushveld

Complex; implications for the formation of the main magnetite layer. Economic Geology, **85 (8)**, 1777-1789.

Hatton, C. J. and Von Gruenewaldt, G. (1987). The geological setting and petrogenesis of the Bushveld chromitite layers. In: Stowe, C. W. (Ed), Evolution of Chromium Ore Fields. New York: Van Nostrand Reinhold, 109-143.

Hiemstra, S. A. (1979). The role of collectors in the formation of platinum deposits in the Bushveld. Canadian Mineralogist, **17**, 469-482.

Hiemstra, S. A. (1985). The distribution of some platinum-group elements in the UG-2 chromitite layer of the Bushveld Complex. Economic Geology, **80**, 944-957.

Holwell, D. A., Armitage, P. E. B and McDonald, I. (2005). Observations on the relationship between the Platreef and its hangingwall. Applied Earth Science, Transactions of the Institute of Mining and Metallurgy B, **114**, 199-207.

Holwell, D. A., McDonald, I and Armitage, P. E. B. (2006). Platinum-group mineral assemblages in the Platreef at the Sandsloot Mine, Northern Bushveld Complex, South Africa. Mineralogical Magazine, **70**, 83-101.

Hulbert, L. J and Von Gruenewaldt, G. (1982). Nickel, copper, and platinum mineralization in the Lower Zone of the Bushveld Complex, South of Potgietersrus. Economic Geology, **77**, 1296-1306.

Hutchison, D and Kinnaird, J. A. (2005). Complex multistage genesis for the Ni-Cu-PGE mineralization in the southern region of the Platreef, Bushveld Complex, South Africa. Applied Earth Science, Transitions of the Institute of Mining and Metallurgy B, **114**, 208-224.

Jochum, K. P. (1996). Rhodium and other platinum-group elements in carbonaceous chondrites. Geochimica et Cosmochimica Acta, **60**, 3353-3357.

Johnson, M. R., Anhaeusser, C. R and Thomas, R. J. (2006). The Geology of South Africa. Geological Society of South Africa and Council for Geoscience. 691p.

Kawatra, S. (2011). Fundamental principles of froth flotation. Michigan Technological University, from: http://www.chem.mtu.edu/chem_eng/ faculty/kawatra/Flotation_Fundamentals.pdf (accessed 11 February 2021).

Kinnaird, J. A. (2005). The Bushveld large igneous province. Review Paper, the University of the Witwatersrand, Johannesburg, from: http://www.largeigneousprovinces.org/sites/default/files/BushveldLIP.pdf (accessed 16 April 2020).

Kinnaird, J. A., Hutchison, D., Schurmann, L. W., Nex, P. A. M and De Lange, R. (2005). Petrology and mineralisation of the southern Platreef: Northern Limb of the Bushveld Complex, South Africa. Mineralium Deposita, **40**, 576-597.

Langa, M. M., Petro, J. J., Leybourne, M. I., Grobler, D. F., Adetunji, J and Skogby, H. (2020). Chromite chemistry of a massive chromitite seam in the northern limb of the Bushveld Igneous Complex, South Africa: correlation with the UG-2 in the eastern and western limbs and evidence of variable assimilation of footwall rocks. Mineralium Deposita, **56 (1)**, 31-44.

Mabuza, M. (2007). Two Rivers Platinum Mine: the orebody, the mining method-a perfect match. The Journal of the South African Institute of Mining and Metallurgy, **107 (1)**, 43-46.

MacCall, M. J. (2016). Mineralogical and geochemical variations in the UG2 reef at Booysendal and Zondereinde mines, with implications for beneficiation of PGM. **MSc dissertation**, University of Stellenbosch.

Maier, W. D. (2005). Platinum-group element (PGE) deposit and occurrences: Mineralization styles, genetic concept and exploration criteria. Journal of African Earth Sciences, **41**, 165-191.

Maier, W. D and Barnes, S. J. (2008). Platinum-group elememts in the UG1 and UG2 chromitites, and the Bastard Reef, at Impala platinum mine, Bushveld complex, South Africa: evidence for late magmatic cumulate instability and reef constitution. South African Journal of Geology, **111**, 159-176.

Maier, W. D and Eales, H. V. (1997). Correlation of the UG-2 – Merensky Reef interval of the Western Bushveld Complex, based on geochemical, mineralogical and petrological data. Council for Geosciences, Bulletin of the Geological Survey of South Africa, **120**, 1-56.

Maier, W. D., De Klerk, L. J., Blaine, J., Manyeruke, T and Barnes S. J., Stevens, M. V. A and Mavrogenes, J. A. (2008). Petrogenesis of contact-style PGE mineralization in the northern lobe of the Bushveld Complex: comparison of data from the farms Rooipoort, Townlands, Drenthe and Nonnenwerth. Mineralium Deposita, **43**, 255-280.

McLaren, C. H and De Villiers, J. P. R. (1982). The platinum-group chemistry and mineralogy of the UG-2 chromitite layer of the Bushveld Complex. Economic Geology, **77**, 1348-1366.

Merkle, R. K. W. (1992). Platinum-group minerals in the middle group of chromitite layers at Marikana, western Bushveld Complex: indications for collection mechanisms and post-magmatic modification. Canadian Journal of Earth Sciences, **29**, 209-221.

Michaud, D. (2021). Flotation. Copper froth flotation process, from: https://www.911metallurgist.com/blog/froth-flotation-process (accessed 1 July 2021).

Miller, J. D., Li, J., Davidtz, J. C and Vos, F. (2005). A review of pyrrhotite flotation chemistry in the processing of PGM ores. Minerals Engineering, **18 (8)**, 855-865.

Mitchell, A. A., Eales, H. V and Kruger, F. J. (1998). Magma replenishment, and the significance of poikilitic textures, in the Lower Main Zone of the western Bushveld Complex, South Africa. Mineralogical Magazine, **62**, 435-450.

Molyneux, T. G. (1974). A geological investigation of the Bushveld Complex in Sekhukhune land and part of the Steelpoort valley. Transactions of the Geological Society of South Africa, **77**, 329-338.

Nadeau, J. L and Davidson, M. W. (2012). Optical Microscopy. Optical imaging and spectroscopy, from: https://doi.org/10.1002/0471266965. com056.pub2 (accessed 7 May 2020).

Naldrett, A. J. (1989). Stratiform PGE deposits in layered intrusions. Economic Geology, **4**, 135-166.

Naldrett, A. J. (2004). Magmatic sulfide deposits: Geology, geochemistry and exploration. New York, Springer-Verlag, 727p.

Naldrett, A. J and Lehmann, J. (1988). Spinel non-stoichiometry as the explanation for Ni-, Cu- and PGE-enriched sulfides in chromitites. In: Prichard, H., Potts, P., Bowles, J and Cribb, S (Ed). Geo-platinum, Elsevier, London, **87**, 93-110.

Naldrett, A. J., Kinnaird, J., Wilson, A and Chunnett, G. (2008). Concentration of PGE in the Earth's crust with special reference to the Bushveld Complex. Earth Science Frontiers, **15 (2)**, 264-297.

Naldrett, A. J., Kinnaird, J. A., Wilson, A., Yudovskaya, M., McQuade, S., Chunnett, G and Stanley, C. (2009). Chromite composition and PGE content of Bushveld chromitites: Part I – the Lower and Middle Groups. Applied Earth

Science, Transactions of the Institution of Mining and Metallurgy, B, **118**, 131-161.

Naldrett, A. J., Wilson, A., Kinnaird, J., Yudovskaya, M and Chunnett, G. (2012). The origin of chromitites and related PGE mineralization in the Bushveld Complex: new mineralogical and petrological constraints. Mineralium Deposita, **47**, 209-232.

Newell, A. J. H., Clark, D. W and Gumede, H. N. (2000). Process for recovery of copper, nickel, and platinum-group metal bearing minerals, from: https://www.google.com/patents/US6044978 (accessed 21 November 2020).

Osbahr, I., Klemd, R., Oberthur, T., Bratz, H and Schouwstra, R. (2013). Platinum-group element distribution in base-metal sulfides of the Merensky Reef from the eastern and western Bushveld Complex, South Africa. Mineralium Deposita (2013), **48**, 211-232.

Osbahr, I., Oberthur, T., Klemd R and Josties A. (2014). Platinum-group element distribution in base-metal sulfides of the UG2 chromitite, Bushveld Complex, South Africa – a reconnaissance study. Mineralium Deposita (2014), **49**, 655-665.

Osbahr, I., Krause, J., Bachmann, K and Gutzmer, J. (2015). Efficient and Accurate Identification of Platinum-Group Minerals by a Combination of Mineral Liberation and Electron Probe Microanalysis with a New Approach to the Offline Overlap Correction of Platinum-Group Element Concentrations. Cambridge University Press, **21 (5)**, 1080-1095.

Page, P., Barnes, S. J., Bedard, J. H and Zientek, M. L. (2011). In situ determination of Os, Ir, and Ru in chromites formed from komatiite, tholeiite and boninite magma: implications for chromite control of OS, Ir and Ru during partial

melting and crystal fractionation. Elsevier Science, Chemical Geology, **302-303**, 3-15.

Penberthy, C. J. (2001). The effect of mineralogical variation in the UG-2 chromitite on recovery of platinum-group elements. **PhD thesis**, University of Pretoria.

Penberthy, C. J and Merkle, R. K. W. (1999). Lateral variations in the platinum-group element content and mineralogy of the UG2 chromitite layer, Bushveld Complex. South African Journal of Geology, **102 (3)**, 240-250.

Penberthy, C. J., Oosthuyzen, E. J and Merkle, R. K. W. (2000). The recovery of platinum group elements from the UG-2 chromitite, Bushveld Complex – a mineralogical perspective. Mineralogy and Petrology, **68**, 213-222.

Pienaar, D., Guy, B. M., Pienaar, C and Viljoen, K. S. (2017). A geometallurgical characterization study of the Crystalkop Reef at the Great Noligwa mine, Klerksdorp Goldfield, South Africa. South African Journal of Geology, **120 (3)**, 303-322.

Pszonka, J and Sala, D. (2018). Application of the Mineral Liberation Analysis (MLA) for extraction of grain size and shape measurements in siliciclastic sedimentary rocks. 4th International Conference of Applied Geophysics, **66**.

Reynolds, I. M. (1985). The nature and origin of titaniferous magnetite-rich layers in the Upper Zone of the Bushveld Complex - A review and synthesis. Economic Geology, **80**,1089-1108.

Rinaldi, R and Llovet, X. (2015). Electron probe microanalysis: A review of the past, present and future. Microscopy and Microanalysis, **21 (5)**, 1053-1069.

Robb, L. (2005). Introduction to ore forming processes. Malden, Maryland, published by Blackwell, from: https://kursatozcan.com/ders_notlari/Introduction_to_Ore_Forming_Processes.pdf (accessed 23 February 2021).

Rose, D. H., Viljoen, F., Knoper, M and Rajesh, H. (2011). Detailed assessment of platinum-group minerals associated with chromitite stringers in the Merensky Reef of the Eastern Bushveld Complex, South Africa. The Canadian Mineralogist, **49**, 1385-1396.

Rose, D. H. (2016). A process mineralogical investigation of the Merensky Reef and UG-2 at the Two Rivers Platinum Mine with emphasis on ore characterization. **PhD Thesis**, University of Johannesburg.

Rose, D. H, Viljoen, K. S and Mulaba-Bafubiandi, A. (2018). A mineralogical perspective on the recovery of platinum group elements from Merensky Reef and UG2 at the Two Rivers mine on the Eastern Limb of the Bushveld Complex in South Africa. Mineralogy and Petrology, **112**, 881-902.

Schouwstra, R. P., Kinloch, E. D. and Lee, C. A. (2000). A short geological review of the Bushveld Complex. Platinum Metals Review, **44 (1)**, 33-39.

Schulz, B., Merker, G and Gutzmer, J. (2019). Automated SEM Mineral Liberation Analysis (MLA) with Generically Labelled EDX Spectra in the Mineral Processing of Rare Earth Element Ores. Minerals, **9**, 1-18.

Scoon, R. N and Teigler, B. (1995). New LG-6 chromitite reserve at Eerste Geluk in the boundary zone between the central and southern sectors of the Eastern Bushveld Complex. Economic Geology, **90**, 969-982.

Scoon, R. N and Mitchell, A. A. (2004). The platiniferous dunite pipes in the eastern Limb of the Bushveld Complex: Review and comparison with unmineralized discordant ultramafic bodies. South African journal of Geology, **107**, 505-520.

Seabrook, C. L. (2005). The Upper Critical and Lower Main Zones of the Eastern Bushveld Complex. **PhD thesis**, University of Witwatersrand.

Shackleton, N. J. (2007). Surface characterisation and flotation behaviour of the platinum and palladium arsenide, telluride and sulphide mineral species. **PhD thesis**, University of Cape Town.

Short, M. N. (1931). Microscopic determination of the ore minerals. Geological Survey, **Bulletin 825**.

Smith, J. W., Holwell, I and McDonald. (2014). Precious and base metal geochemistry and mineralogy of the Grasvally Norite-Pyroxenite-Anorthosite (GNPA) member, northern Bushveld Complex, South Africa: implications for a multistage emplacement. Mineralium Deposita, **49**, 667-692.

South African Committee for Stratigraphy (SACS). (1980). Stratigraphy of South Africa. Part 1. In: Kent, L. E and Comp. (Ed), Lithostratigraphy of the Republic of South Africa, South West Africa/Namibia, and the Republics of Bophuthatswana, Transkei and Venda. Handbook of the Geological Survey of South Africa, **8**.

TRP (Two Rivers Platinum Mine). (2016). Two Rivers Platinum Mine Facts Sheet, from: https://www.implats.co.za/pdf/fact-sheets/two-rivers-fact-sheet-nov-2016.pdf (accessed 17 May 2020).

Van der Merwe, F. (2011). MLA-based mineralogical investigation of PGE mineralisation at Lonmin's Akanani Platinum Group Metal Project, northern Limb of the Bushveld Complex. **MSc Dissertation**, University of Johannesburg.

Vermaak, C. F. (1976). The Merensky Reef-thoughts on its environment and genesis. Economic Geology, **71**, 1270-1298.

Vermaak, C. F. (1995). The platinum group metals: a global perspective. Mintek, Randburg, 247p.

Vermaak, M. K. G. (2005). Fundamentals of the flotation behaviour of Palladium Bismuth Tellurides. **PhD Thesis**, University of Pretoria.

Viljoen, M. J and Scoon, R. N. (1985). The distribution and main geologic features of discordant bodies of Iron-Rich Ultramafic Pegmatite in the Bushveld Complex. Economic Geology, **80**, 1109-1128.

Viljoen, F., Knoper, M., Rajesh, H., Rose, D and Greeff, T. (2012). Application of a Field Emission Mineral Liberation Analyser to the in-Situ Study of Platinum-Group Element Mineralisation in the Merensky Reef of the Bushveld Complex, South Africa. Proceedings of the 10th International Congress for Applied Mineralogy (ICAM), 757-764.

Von Gruenewaldt, G. (1973). The Main and Upper Zones of the Bushveld Complex in the Roossenekal area, eastern Transvaal. Transaction of the Geological Society of South Africa, **76**, 207-227.

Von Gruenewaldt, G., Sharpe, M. R., and Hatton, C. J. (1985). The Bushveld Complex: Introduction and review. Economic Geology, **80**, 803-812.

Von Gruenewaldt, G., Horsch, H., Dickst, D and De Wet, J. (1990). PGE mineralization in the western sector of the eastern Bushveld Complex. Mineralogy and Petrology, **42**, 71-95.

Voordouw, R., Gutzmer, J and Beukes, N. J. (2010). Zoning of platinum group mineral assemblages in the UG-2 chromitite determined through in situ SEM-EDS-based image analysis. dithiophosphate, **45**, 147-159.

Walraven, F. (1997). Geochronology of the Rooiberg Group, Transvaal Supergroup, South Africa. University of Witwatersrand. Economic Geology Research Unit Information Circular, **316**, 21p.

Walraven, F., Armstrong, R. A and Kruger, F. J. (1990). A chrono-stratigraphic framework for the north-central Kaapvaal craton, the Bushveld Complex and Vredefort structure. Tectonophysics, **171**, 23-48.

White, J. A. (1994). The Potgietersrus project geology and exploration history: Proceedings, 15th CMMI Congress. South African Institute of Mining and Metallurgy, 173-182.

Willemse, J. (1969). The Geology of the Bushveld Complex, the largest repository of magmatic ore deposits in the world. Economic Geology Monograph, **4**, 1-22.

Zientek, M. L., Causey, J. D., Parks, H. L., and Miller, R. J. (2014). Platinum-group elements in southern Africa—Mineral inventory and an assessment of undiscovered mineral resources: U.S. Geological Survey Scientific Investigations Report 2010–5090–Q, 126 p. and GIS data, http://dx.doi.org/10.3133/sir20105090Q.

APPENDICES

Appendix A: Samples and Analysis Selection

A.1.1: Table of the list of samples indicating the type of Reef, the analytical technique used and the total PGE+Au grades.

REEF TYPE	SAMPLE_ID	DEPTH FROM	DEPTH TO	PETROGRAPHY	MLA	EMPA	6PGE+Au
UG2 NORMAL REEF	B3D2_S1	720,58	720,60	X	x		3,301
UG2 NORMAL REEF	B3D2_S2	720,65	720,68	x	x		3,301
UG2 NORMAL REEF	B3D2_S3	721,00	721,30	x	x		1,408
UG2 NORMAL REEF	B3D2_S4	721,60	721,80	x			1,408
UG2 NORMAL REEF	B3D2_S5	721,97	721,99	x	x	x	4,558
UG2 NORMAL REEF	B3D2_S6	722,06	722,08	x	x	x	5,419
UG2 NORMAL REEF	B3D2_S7	722,20	722,23	x			5,419
UG2 NORMAL REEF	B3D2_S8	722,27	722,29	x			11,151
UG2 NORMAL REEF	B3D2_S9	722,36	722,38	x	x	x	11,151
UG2 NORMAL REEF	B3D2_S10	722,51	722,53	x	x	x	4,499
UG2 NORMAL REEF	B3D2_S11	722,61	722,63	x			12,912
UG2 NORMAL REEF	B3D2_S12	722,73	722,75	x	x	x	12,912
UG2 NORMAL REEF	B7D0_S1	764,34	764,36	x	x		3,156
UG2 NORMAL REEF	B7D0_S2	764,65	764,67	x	x		1,865
UG2 NORMAL REEF	B7D0_S3	765,04	765,06	x			1,865
UG2 NORMAL REEF	B7D0_S4	765,31	765,33	x	x	x	4,422
UG2 NORMAL REEF	B7D0_S5	765,39	765,41	x	x	x	5,773
UG2 NORMAL REEF	B7D0_S6	765,55	765,57	x			5,773
UG2 NORMAL REEF	B7D0_S7	765,60	765,62	x	x		11,067
UG2 NORMAL REEF	B7D0_S8	765,71	765,73	x	x		11,067
UG2 NORMAL REEF	B7D0_S9	765,78	765,80	x	x	x	6,553
UG2 NORMAL REEF	B7D0_S10	765,91	765,93	x			6,553
UG2 NORMAL REEF	B7D0_S11	765,99	766,01	x	x		14,474

A.1.1. (continued): Table of the list of samples indicating the type of Reef, the analytical technique used and the total PGE+Au grades.

REEF TYPE	SAMPLE_ID	DEPTH FROM	DEPTH TO	PETROGRAPHY	MLA	EMPA	6PGE+Au
UG2 SPLIT REEF	B3D1_S1	720,54	720,56	x	x		2,924
UG2 SPLIT REEF	B3D1_S2	720,62	720,64	x	x		2,924
UG2 SPLIT REEF	B3D1_S3	720,96	720,98	x	x		2,293
UG2 SPLIT REEF	B3D1_S4	721,95	721,97	x	x		4,85
UG2 SPLIT REEF	B3D1_S5	722,07	722,09	x			5,085
UG2 SPLIT REEF	B3D1_S6	722,17	722,19	x	x		5,085
UG2 SPLIT REEF	B3D1_S7	722,27	722,29	x	x		9,785
UG2 SPLIT REEF	B3D1_S8	722,31	722,33	x	x		9,785
UG2 SPLIT REEF	B3D1_S9	722,55	722,57	x	x		3,827
UG2 SPLIT REEF	B3D1_S10	722,68	722,70	x	x		14,246
UG2 SPLIT REEF	B3D1_S11	723,01	723,03	x	x		4,96
UG2 MULTTIPLE SPLIT REEF	B6D1_S1	815,99	816,01	x	x		4,634
UG2 MULTTIPLE SPLIT REEF	B6D1_S2	816,13	816,15	x	x		4,458
UG2 MULTTIPLE SPLIT REEF	B6D1_S3	817,16	817,18	x	x	x	5,081
UG2 MULTTIPLE SPLIT REEF	B6D1_S4	817,39	817,42	x	x	x	7,688
UG2 MULTTIPLE SPLIT REEF	B6D1_S5	817,51	817,53	x	x	x	6,603
UG2 MULTTIPLE SPLIT REEF	B6D1_S6	817,69	817,71	x	x		5,729
UG2 MULTTIPLE SPLIT REEF	B6D1_S7	817,77	817,80	x			5,788
UG2 MULTTIPLE SPLIT REEF	B6D1_S8	817,84	817,86	x	x	x	5,788
UG2 MULTTIPLE SPLIT REEF	B6D1_S9	817,90	817,92	x			5,788
UG2 MULTTIPLE SPLIT REEF	B6D1_S10	818,02	818,05	x	x		5,773
UG2 MULTTIPLE SPLIT REEF	B6D1_S11	818,22	817,24	x	x		10,903
UG2 MULTTIPLE SPLIT REEF	B6D1_S12	818,33	818,35	x	x		9,828

A.1.1. (continued): Table of the list of samples indicating the type of Reef, the analytical technique used and the total PGE+Au grades.

REEF TYPE	SAMPLE_ID	DEPTH FROM	DEPTH TO	PETROGRAPHY	MLA	EMPA	6PGE+Au
MERENSKY REEF	B6D0_S1	682,77	682,79	x	x	x	2,293
MERENSKY REEF	B6D0_S2	682,84	682,87	x	x	x	11,108
MERENSKY REEF	B6D0_S3	682,92	682,94	x	x		15,631
MERENSKY REEF	B6D0_S4	683,65	683,69	x			0,156
MERENSKY REEF	B6D0_S5	683,22	683,24	x	x	x	10,009
MERENSKY REEF	B6D0_S6	683,27	683,30	x			10,009
MERENSKY REEF	B6D0_S7	684,33	684,36	x	x	x	17,797
MERENSKY REEF	B6D0_S8	684,40	684,42	x			30,092
MERENSKY REEF	B6D0_S9	684,46	684,48	x	x	x	30,092
MERENSKY REEF	B6D0_S10	684,49	684,51	x	x		30,092

Appendix B: Photomicrographs

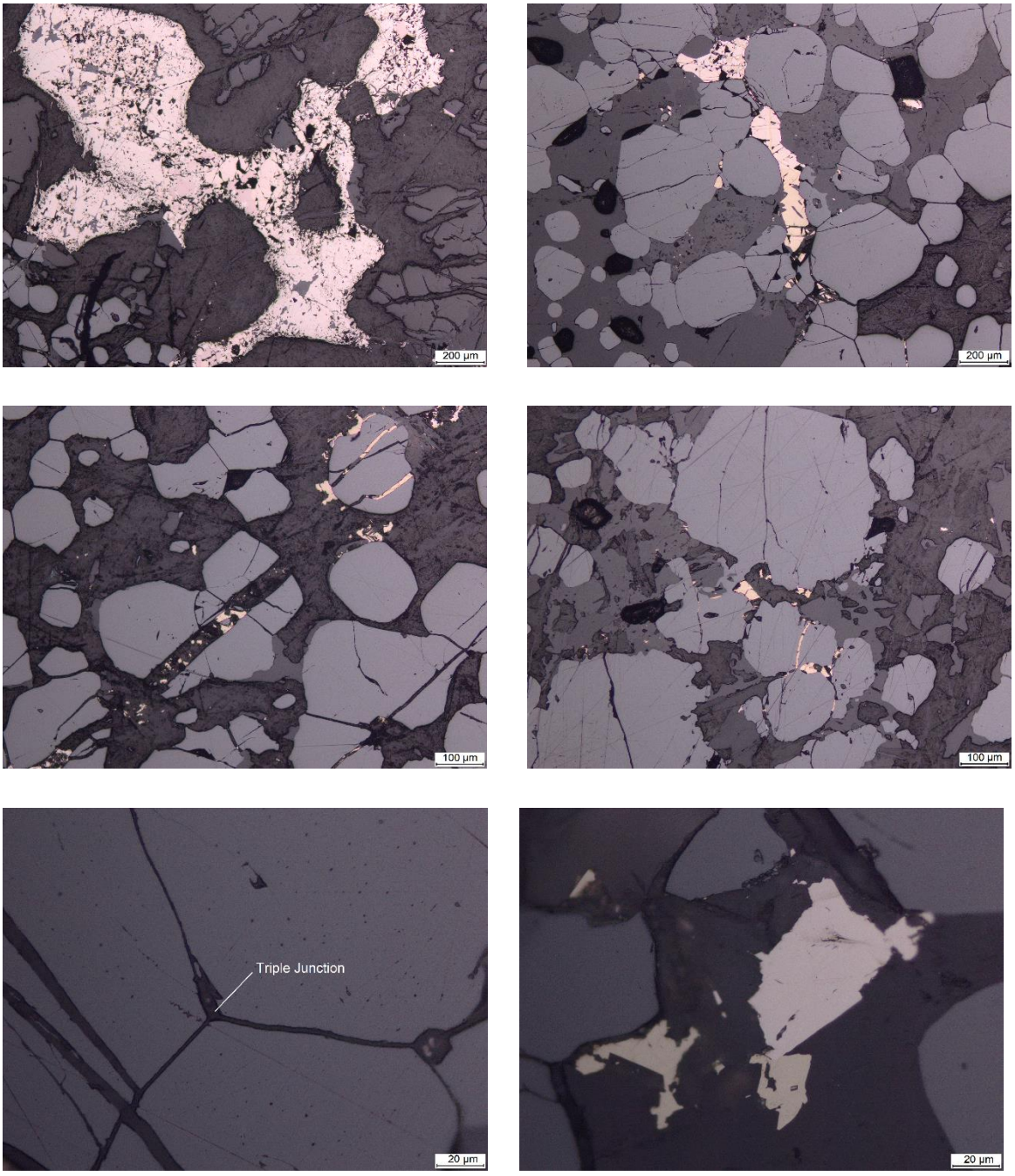

B.1.1: Photomicrographs of the textures observed in the UG2 Reef.

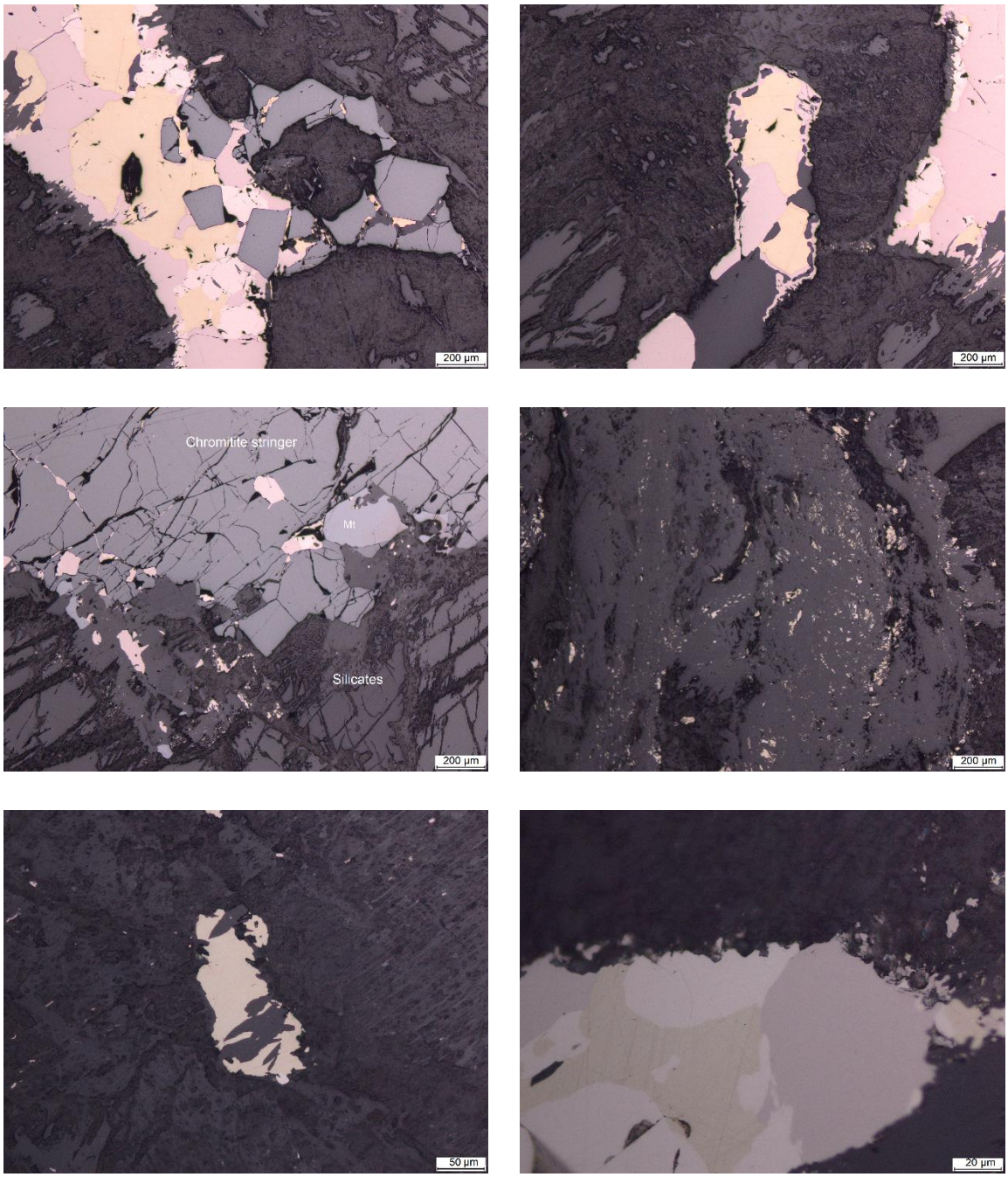

B.1.2: Photomicrographs of the textures observed in the Merensky Reef.

Appendix C: Electron Microprobe Results

C.1.1: Table of PGM chemistry obtained from the EMPA also indicating specifically targeted minerals.

The PGM are classified into eleven groups based on the dominant metal. The metals (elements) used to classify or group the minerals are indicated in **bold**. Group 1: PGE-Fe-S-Cu-Ni-Pb, Group 2: PGE-S-As, Group 3: PGE-As, Group 4: PGE-Bi-Te, Group 5: PGE-Cu-S, Group 6: PGE-Cu-Fe-S, Group 7: PGE-Ni-Fe-S, Group 8: PGE-Ni-S, Group 9: PGE-Fe-S, Group 10: PGE-S and Group 11: PGE-Alloys / Complex; 11A: PGE-Bi-Te-As-Ni-S, 11B: PGE-Bi-Te-As, 11C: PGE-Cu-Fe-Ni-S, 11D: PGE-Sb-Cu-Fe-As and 11E: PGE-Fe. The total wt% composition indicated with ** are the original total elements abundances which were renormalised to 100 wt% by subtracting Cr and O from the original total, to allow for mineral classification and grouping. UG2 – Upper Group 2 chromitite, MR – Merensky Reef.

Group	Ag	As	Au	Bi	Co	Cu	Fe	Hg	Ir	Ni	Os	Pb	Pd	Pt	Rh	Ru	S	Sb	Se	Sn	Te	Si	Zn	Total	Total	Reef	Mineral
1	0,24	0,03	0,00	0,00	0,08	**9,30**	**10,05**	0,00	0,16	**9,42**	0,00	**12,84**	0,12	45,65	0,00	0,00	**11,90**	0,00	0,20	0,00	0,00	0,00	0,00	100	74,2**	UG2	
	0,26	0,05	0,16	0,00	0,05	**9,15**	**9,77**	0,06	0,21	**7,88**	0,06	**25,52**	0,01	29,01	0,06	0,00	**17,65**	0,00	0,10	0,00	0,00	0,00	0,00	100	81,46**	UG2	
	0,26	0,02	0,06	0,01	0,02	**8,24**	**8,93**	0,01	0,00	**6,84**	0,02	**22,73**	0,00	34,23	0,00	0,01	**18,43**	0,00	0,15	0,02	0,00	0,00	0,00	100	87,1**	UG2	
	0,09	0,00	0,00	0,00	0,04	**8,38**	**8,20**	0,02	0,09	**7,48**	0,00	**23,70**	0,00	32,32	0,02	0,01	**19,51**	0,00	0,14	0,00	0,00	0,00	0,00	100	95,37**	UG2	
	0,00	0,00	0,00	0,07	0,00	**8,36**	**7,94**	0,00	0,00	**7,30**	0,00	**23,90**	0,03	32,71	0,08	0,00	**19,55**	0,00	0,00	0,00	0,00	0,06	0,00	100	97,02**	UG2	
	0,16	0,00	0,00	0,00	0,90	**11,12**	**6,18**	0,00	3,88	**3,61**	0,05	**15,15**	0,01	31,77	1,96	0,00	**23,83**	0,00	0,03	0,00	0,02	0,00	0,00	98,67		UG2	
	0,00	0,00	0,00	0,03	0,00	**8,20**	**7,90**	0,00	0,00	**7,43**	0,00	**23,44**	0,01	32,40	0,04	0,00	**19,21**	0,04	0,00	0,00	0,00	0,00	0,02	98,72		UG2	
	0,20	0,00	0,00	0,02	0,03	**8,00**	**8,17**	0,02	0,08	**7,00**	0,02	**24,00**	0,00	30,76	0,05	0,01	**20,56**	0,00	0,08	0,02	0,01	0,00	0,00	99,03		UG2	
	0,00	0,00	0,00	0,08	0,00	**8,18**	**7,87**	0,00	0,00	**7,21**	0,00	**23,84**	0,03	32,39	0,03	0,00	**19,47**	0,02	0,00	0,00	0,00	0,00	0,02	99,14		UG2	
	0,00	0,00	0,00	0,04	0,00	**8,11**	**7,92**	0,00	0,00	**7,12**	0,00	**24,02**	0,02	32,18	0,10	0,00	**19,74**	0,00	0,00	0,00	0,00	0,04	0,02	99,31		UG2	
	0,15	0,00	0,00	0,00	0,01	**8,57**	**7,48**	0,02	0,06	**7,02**	0,03	**23,83**	0,01	32,47	0,06	0,02	**19,86**	0,00	0,17	0,00	0,00	0,00	0,00	99,76		UG2	Kharaelakhite
	0,00	0,00	0,00	0,03	0,00	**7,51**	**8,96**	0,00	0,00	**9,09**	0,00	**22,29**	0,00	30,48	0,07	0,00	**21,28**	0,01	0,00	0,00	0,00	0,32	0,01	100,05		UG2	
	0,09	0,01	0,05	0,00	0,18	**7,04**	**10,77**	0,08	0,13	**11,55**	0,01	**20,37**	0,01	28,43	0,03	0,02	**21,30**	0,00	0,18	0,00	0,03	0,00	0,00	100,28		UG2	
2	0,00	**46,30**	0,00	0,00	0,00	0,85	1,26	0,00	0,00	0,43	0,00	0,00	0,30	18,59	4,51	0,00	**27,62**	0,00	0,00	0,00	0,00	0,11	0,04	100	53,05**	UG2	
	0,00	**46,30**	0,00	0,00	0,00	0,91	2,10	0,00	0,00	2,71	0,00	0,02	0,12	22,91	4,83	0,00	**20,05**	0,00	0,00	0,00	0,05	0,00	0,02	100	59,44**	UG2	
	0,00	**46,12**	0,00	0,00	0,00	0,89	2,03	0,00	0,00	2,58	0,00	0,00	0,13	23,19	4,89	0,00	**20,16**	0,00	0,00	0,00	0,00	0,02	0,00	100	59,73**	UG2	
	0,00	**45,54**	0,00	0,00	0,00	0,87	1,98	0,00	0,00	2,59	0,00	0,00	0,15	23,49	5,08	0,00	**20,29**	0,00	0,00	0,00	0,00	0,00	0,03	100	60,63**	UG2	
	0,00	**2,76**	0,01	0,00	0,04	0,00	2,36	0,00	8,20	0,43	5,69	0,00	0,54	0,34	0,21	43,91	**36,03**	0,01	0,02	0,01	0,00	0,00	0,00	100,56		UG2	PtIrRuOsSAs
3	0,00	**38,60**	0,08	0,01	0,55	0,00	3,89	0,00	0,00	3,05	0,02	0,14	0,43	**48,72**	0,01	0,01	2,63	0,06	0,31	0,04	1,44	0,00	0,00	100	95,95**	MR	
	0,00	**41,98**	0,02	0,00	0,00	0,21	1,12	0,00	0,79	0,01	0,05	0,10	0,00	**53,47**	0,03	0,03	0,34	0,87	0,17	0,02	0,01	0,00	0,00	99,22		MR	Sperrylite

C.1.1: (continued) Table of PGM chemistry obtained from the EMPA also indicating specifically targeted minerals.

Group	Ag	As	Au	Bi	Co	Cu	Fe	Hg	Ir	Ni	Os	Pb	Pd	Pt	Rh	Ru	S	Sb	Se	Sn	Te	Si	Zn	Total	Total	Reef	Mineral
4	0,00	0,24	0,00	**4,81**	0,14	1,98	8,44	0,00	0,39	5,14	0,17	0,02	0,01	34,15	0,31	0,15	7,24	0,02	0,01	0,00	**36,80**	0,00	0,00	100	95,9**	UG2	
	0,00	0,05	0,01	**11,52**	0,02	0,11	0,46	0,00	0,02	0,15	0,07	0,01	0,02	39,14	0,00	0,02	0,01	1,36	0,00	0,00	**47,01**	0,00	0,00	100	96,9**	MR	
	0,00	0,27	0,00	**4,73**	0,14	1,74	9,31	0,05	0,43	5,95	0,14	0,02	0,00	32,09	0,29	0,16	9,14	0,00	0,01	0,02	**35,51**	0,00	0,00	100	97,14**	UG2	
	0,00	0,05	0,00	**11,49**	0,02	0,05	0,52	0,00	0,00	0,39	0,09	0,01	0,04	38,08	0,01	0,01	0,04	1,31	0,01	0,00	**47,88**	0,00	0,00	100	97,85**	MR	
	0,00	0,13	0,08	**12,96**	0,03	0,00	0,56	0,07	0,02	3,18	0,07	0,00	7,40	21,86	0,00	0,00	0,00	0,01	0,00	0,00	**52,70**	0,00	0,00	99,07		MR	
	0,04	0,05	0,04	**13,25**	0,00	0,00	0,64	0,04	0,00	3,17	0,04	0,00	7,32	21,61	0,02	0,01	0,01	0,02	0,00	0,04	**53,36**	0,00	0,00	99,66		MR	
	0,01	0,00	0,03	**11,08**	0,01	0,04	1,15	0,02	0,00	2,44	0,04	0,05	6,87	23,59	0,00	0,00	0,04	0,04	0,00	0,03	**54,26**	0,00	0,00	99,7		MR	
	0,00	0,01	0,02	**6,44**	0,00	0,29	0,73	0,00	0,15	0,05	0,06	0,06	0,11	39,22	0,06	0,06	0,07	0,00	0,02	0,00	**52,51**	0,00	0,00	99,86		MR	
	0,00	0,00	0,00	**30,69**	0,00	0,02	0,94	0,00	0,00	0,79	0,00	0,84	39,27	0,00	0,00	0,00	0,03	0,01	0,00	0,00	**27,69**	0,08	0,02	100,38		UG2	PdBiTe
5	0,00	0,00	0,00	0,00	0,00	**12,87**	1,38	0,00	0,00	0,47	0,00	0,07	0,08	38,32	18,36	0,00	**28,40**	0,00	0,00	0,00	0,00	0,05	0,00	100	97,02**	UG2	
	0,01	0,01	0,00	0,00	2,19	**12,71**	0,83	0,00	3,69	0,54	0,28	0,06	0,00	36,23	13,13	0,91	**29,37**	0,02	0,02	0,00	0,00	0,00	0,00	100	97,41**	UG2	
	0,00	0,00	0,00	0,00	4,70	**12,51**	1,00	0,00	7,57	0,92	0,34	0,05	0,00	37,58	6,56	0,21	**28,24**	0,03	0,01	0,00	0,00	0,00	0,00	99,72		UG2	
	0,00	0,00	0,02	0,00	5,54	**12,51**	2,23	0,00	0,79	3,72	0,03	0,07	0,00	39,29	6,38	0,01	**29,40**	0,03	0,02	0,03	0,01	0,00	0,00	100,08		UG2	
6	0,04	0,00	0,15	0,00	0,00	**2,33**	**2,08**	0,15	0,00	0,59	0,00	0,13	0,00	78,14	0,07	0,03	**16,25**	0,00	0,02	0,00	0,00	0,00	0,00	100	97,02**	UG2	
	0,03	0,00	0,00	0,00	1,01	**6,78**	**6,01**	0,00	4,07	8,40	0,02	0,11	0,91	35,93	9,20	0,04	**26,01**	0,04	0,01	0,00	0,00	0,00	0,00	98,57		UG2	
	0,00	0,01	0,08	0,00	0,06	**7,06**	**17,44**	0,00	0,00	2,61	0,03	0,07	0,00	57,41	0,04	0,10	**13,85**	0,00	0,00	0,01	0,04	0,00	0,00	98,81		UG2	
	0,03	0,00	0,00	0,00	1,45	**6,54**	**12,89**	0,00	2,29	18,10	0,04	0,04	0,06	19,44	7,67	0,10	**30,72**	0,02	0,02	0,00	0,00	0,00	0,00	99,41		UG2	
	0,00	0,00	0,00	0,00	0,00	**34,00**	**30,44**	0,01	0,04	0,01	0,01	0,02	0,03	0,03	0,00	0,01	**34,99**	0,00	0,00	0,00	0,00	0,00	0,00	99,59		UG2	
	0,00	0,01	0,00	0,03	0,00	**11,24**	**17,20**	0,00	0,00	0,11	0,03	0,04	0,00	59,05	0,00	0,00	**12,91**	0,00	0,00	0,01	0,00	0,00	0,00	100,63		UG2	
7	0,00	0,00	0,00	0,09	0,14	0,28	**17,55**	0,00	0,00	**6,54**	0,00	0,00	0,00	59,51	0,15	0,00	**15,75**	0,00	0,00	0,00	0,00	0,00	0,00	100	80**	UG2	
	0,01	0,00	0,04	0,00	0,20	0,09	**20,18**	0,04	0,00	**10,85**	0,03	0,06	0,59	53,96	0,04	0,03	**13,85**	0,00	0,00	0,02	0,00	0,00	0,00	100	96,81**	UG2	
	0,01	0,01	0,03	0,00	3,35	0,00	**23,61**	0,00	0,00	**38,51**	0,02	0,04	0,00	0,03	0,01	0,00	**34,34**	0,00	0,04	0,00	0,00	0,00	0,00	100	97,38**	UG2	
	0,00	0,03	0,00	0,00	1,69	0,09	**23,93**	0,02	0,00	**39,77**	0,02	0,00	0,55	0,00	0,00	0,01	**33,88**	0,00	0,00	0,00	0,00	0,00	0,00	100	97,7**	UG2	
	0,00	0,00	0,00	0,00	0,00	0,00	**26,09**	0,00	0,00	**38,35**	0,00	0,07	0,53	0,00	0,94	0,00	**32,49**	0,00	0,00	0,00	0,00	0,03	0,00	98,5		UG2	
	0,00	0,01	0,02	0,00	0,53	0,00	**31,60**	0,04	0,00	**33,42**	0,01	0,00	0,07	0,00	0,01	0,00	**33,83**	0,00	0,01	0,00	0,00	0,00	0,00	99,55		UG2	
	0,00	0,00	0,06	0,00	1,57	0,00	**23,90**	0,02	0,00	**40,75**	0,01	0,00	0,03	0,01	0,00	0,00	**33,47**	0,02	0,00	0,02	0,00	0,00	0,00	99,86		UG2	
	0,00	0,01	0,05	0,02	0,55	0,02	**33,58**	0,06	0,00	**31,76**	0,01	0,00	0,46	0,00	0,30	0,00	**33,72**	0,00	0,00	0,00	0,00	0,00	0,00	100,54		UG2	
	0,03	0,00	0,00	0,01	0,64	0,01	**33,65**	0,08	0,04	**32,41**	0,01	0,00	0,29	0,00	0,14	0,01	**33,33**	0,00	0,01	0,01	0,00	0,00	0,00	100,67		UG2	
	0,00	0,00	0,00	0,00	0,57	0,01	**33,88**	0,03	0,03	**31,93**	0,01	0,01	0,40	0,00	0,05	0,06	**33,45**	0,00	0,01	0,01	0,00	0,00	0,00	100,45		UG2	
	0,00	0,01	0,00	0,00	0,49	0,02	**32,83**	0,00	0,07	**31,33**	0,01	0,01	0,48	0,00	0,18	0,02	**33,41**	0,00	0,00	0,00	0,01	0,00	0,00	98,87		UG2	

C.1.1: (continued) Table of PGM chemistry obtained from the EMPA also indicating specifically targeted minerals.

Group	Ag	As	Au	Bi	Co	Cu	Fe	Hg	Ir	Ni	Os	Pb	Pd	Pt	Rh	Ru	S	Sb	Se	Sn	Te	Si	Zn	Total	Total	Reef	Mineral
8	0,11	0,89	0,05	0,01	0,02	0,05	2,19	0,00	0,00	**6,81**	0,00	0,27	15,00	53,58	0,00	0,04	**20,86**	0,03	0,08	0,00	0,01	0,00	0,00	100	92,35**	UG2	
	0,16	0,02	0,02	0,00	0,01	0,00	1,60	0,02	0,07	**10,68**	0,10	0,10	36,33	24,37	0,30	2,04	**24,12**	0,04	0,00	0,00	0,00	0,00	0,00	100	97,21**	UG2	
	0,00	0,00	0,00	0,04	0,14	0,04	3,43	0,02	0,00	**4,30**	0,04	0,11	1,01	72,09	0,04	0,00	**18,63**	0,00	0,06	0,04	0,00	0,00	0,00	100	97,8**	UG2	
	0,00	0,00	0,00	0,00	0,02	0,00	1,65	0,03	0,00	**11,49**	0,04	0,10	3,41	62,54	0,06	0,01	**20,63**	0,01	0,00	0,00	0,00	0,00	0,00	100	97,92**	UG2	
	0,02	0,00	0,03	0,00	0,01	0,13	1,24	0,00	0,00	**4,02**	0,04	0,00	2,51	74,51	0,03	0,00	**17,46**	0,00	0,00	0,00	0,00	0,00	0,00	100	98,06**	UG2	
	0,51	0,00	2,30	0,00	0,02	0,55	1,45	0,00	0,00	**7,45**	0,00	0,07	28,75	37,23	0,03	0,02	**20,45**	0,00	0,00	0,00	0,00	0,00	0,00	98,83		UG2	
	0,01	0,02	0,06	0,00	0,02	0,29	1,26	0,00	0,00	**8,20**	0,02	0,00	10,92	58,44	0,00	0,02	**19,64**	0,00	0,00	0,02	0,00	0,00	0,00	98,92		UG2	
	0,00	0,00	0,00	0,00	0,00	0,14	1,38	0,00	0,00	**3,99**	0,00	0,10	7,22	69,00	0,01	0,00	**17,94**	0,00	0,00	0,00	0,00	0,21	0,00	100		UG2	
	0,00	0,00	0,00	0,06	0,00	0,10	1,31	0,00	0,00	**4,33**	0,00	0,19	12,50	62,63	0,06	0,00	**17,73**	0,01	0,00	0,00	0,06	0,00	0,00	98,98		UG2	
	0,00	0,00	0,00	0,06	0,00	0,00	1,23	0,00	0,00	**4,04**	0,00	0,14	13,34	62,38	0,05	0,00	**17,65**	0,02	0,00	0,00	0,00	0,18	0,00	99,09		UG2	
	0,09	0,33	0,00	0,00	0,00	0,01	1,25	0,02	0,86	**4,33**	0,19	0,08	18,97	50,74	0,17	1,77	**20,65**	0,00	0,00	0,00	0,01	0,00	0,00	99,47		UG2	
	0,06	0,01	0,05	0,00	0,01	0,04	0,66	0,04	0,00	**7,55**	0,01	0,03	23,56	48,22	0,00	0,02	**19,75**	0,02	0,03	0,00	0,00	0,00	0,00	100,06		UG2	
	0,00	0,00	0,03	0,02	1,84	0,00	0,60	0,04	0,00	**62,09**	0,04	0,00	0,00	0,02	0,01	0,01	**35,58**	0,00	0,06	0,00	0,03	0,00	0,00	100,37		UG2	
	0,01	0,01	0,00	0,00	1,87	0,00	0,79	0,06	0,01	**61,91**	0,02	0,01	0,00	0,00	0,00	0,03	**35,73**	0,00	0,04	0,00	0,00	0,00	0,00	100,49		UG2	
	0,00	0,01	0,00	0,00	0,05	0,15	1,50	0,06	0,13	**8,84**	0,06	0,09	20,70	48,41	0,12	0,01	**20,58**	0,04	0,04	0,01	0,00	0,00	0,00	100,8		UG2	
9	0,00	0,00	0,00	0,00	0,00	0,02	**32,18**	0,00	0,00	0,19	0,00	0,00	0,00	0,00	2,44	0,00	**65,13**	0,02	0,00	0,00	0,00	0,05	0,00	100	63,2**	UG2	
	0,06	0,09	0,00	0,05	0,09	0,01	**13,01**	0,02	4,69	0,40	3,88	0,00	0,19	0,01	3,34	34,24	**39,86**	0,01	0,02	0,02	0,00	0,00	0,00	100	85,72**	UG2	
	0,00	0,03	0,03	0,00	0,19	0,00	**60,73**	0,04	0,00	2,88	0,00	0,00	0,00	0,04	0,01	0,02	**36,03**	0,00	0,00	0,00	0,00	0,00	0,00	100	96,61**	UG2	
	0,02	0,01	0,08	0,00	0,09	0,46	**14,74**	0,00	0,00	4,80	0,05	0,06	0,06	72,01	0,10	0,19	**5,89**	0,00	0,00	0,01	0,00	0,00	0,00	98,57		UG2	
	0,05	0,00	0,00	0,00	0,01	0,05	**6,14**	0,00	0,00	2,08	0,05	0,03	0,15	69,76	0,00	0,00	**20,56**	0,00	0,00	0,00	0,00	0,00	0,00	98,88		UG2	
	0,00	0,00	0,04	0,00	1,49	0,00	**24,10**	0,01	0,02	39,50	0,01	0,03	0,04	0,02	0,14	0,00	**33,26**	0,00	0,03	0,00	0,00	0,00	0,00	98,69		UG2	
	0,00	0,31	0,08	0,00	0,08	0,00	**12,11**	0,04	4,15	0,43	2,10	0,00	0,53	0,02	1,64	37,65	**40,66**	0,05	0,01	0,00	0,00	0,00	0,00	99,86		UG2	
11A	0,08	**2,07**	0,00	**4,86**	0,84	0,08	1,45	0,00	0,56	**34,94**	0,68	0,26	1,26	8,41	2,62	5,88	**27,22**	0,65	0,08	0,03	**8,02**	0,00	0,00	100	95,14**	UG2	
11B	0,61	**16,07**	0,02	**9,41**	0,02	0,01	1,54	0,00	0,03	1,74	0,01	0,00	4,86	29,26	0,12	0,00	0,11	0,02	0,04	0,00	**36,12**	0,00	0,00	100	97,26**	MR	
11C	0,01	0,01	0,05	0,00	1,75	**3,29**	**3,31**	0,04	1,58	**2,84**	0,03	0,29	0,01	56,36	1,91	0,03	**28,49**	0,00	0,00	0,00	0,01	0,00	0,00	100	79,26**	UG2	
	0,00	0,02	0,02	0,00	0,83	**3,74**	**14,99**	0,02	5,65	**13,77**	0,37	0,12	0,09	31,58	0,38	0,00	**28,31**	0,00	0,01	0,05	0,03	0,00	0,00	100	96,64**	UG2	
11D	0,31	2,49	0,03	0,00	0,00	2,02	2,72	0,01	0,00	0,02	0,00	0,02	65,43	0,04	0,00	0,00	2,20	**24,13**	0,01	0,00	0,00	0,00	0,00	99,43		MR	
11E	0,08	0,06	0,05	0,00	0,01	0,30	**12,71**	0,00	0,02	0,15	0,00	0,00	0,00	86,31	0,03	0,05	0,21	0,01	0,00	0,01	0,00	0,00	0,00	100	87,39**	UG2	Alloy

C.1.1: (continued) Table of PGM chemistry obtained from the EMPA also indicating specifically targeted minerals.

Group	Ag	As	Au	Bi	Co	Cu	Fe	Hg	Ir	Ni	Os	Pb	Pd	Pt	Rh	Ru	S	Sb	Se	Sn	Te	Si	Zn	Total	Total	Reef	Mineral
10	0,00	0,16	0,00	0,07	0,00	0,02	2,87	0,00	0,00	0,67	0,00	0,56	2,92	60,08	0,62	0,07	**31,92**	0,04	0,00	0,00	0,00	0,00	0,00	100	44,89**	UG2	
	0,00	0,06	0,00	0,02	0,02	0,06	3,54	0,00	0,00	0,44	0,04	0,05	0,95	82,80	0,00	0,00	**11,96**	0,00	0,00	0,05	0,00	0,00	0,00	100	80,42**	UG2	
	0,02	0,00	0,00	0,00	0,02	0,15	3,32	0,05	3,00	0,05	4,26	0,00	0,38	0,02	0,17	**53,48**	**35,02**	0,01	0,03	0,00	0,00	0,00	0,00	100	86,63**	UG2	Laurite
	0,00	0,06	0,11	0,00	0,00	1,16	4,04	0,20	0,00	0,92	0,00	2,42	0,75	72,77	0,08	0,01	**17,45**	0,00	0,02	0,00	0,00	0,00	0,00	100	87,03**	MR	
	0,00	0,59	0,00	0,00	0,02	0,01	2,52	0,00	2,96	0,22	6,10	0,03	0,31	0,00	0,22	**51,89**	**35,08**	0,00	0,03	0,00	0,01	0,00	0,00	100	87,97**	UG2	Laurite
	0,07	0,00	0,00	0,00	0,03	0,11	1,12	0,00	0,00	0,96	0,08	0,00	2,71	80,22	0,00	0,00	**14,68**	0,01	0,00	0,00	0,00	0,00	0,00	100	88,53**	UG2	
	0,00	0,02	0,06	0,00	0,00	0,19	**2,50**	0,01	0,00	**2,05**	0,00	0,19	**3,81**	**71,10**	0,08	0,03	**19,96**	0,00	0,00	0,00	0,00	0,00	0,00	100	90,27**	UG2	Cooperite
	0,04	0,04	0,03	0,00	0,03	0,11	**1,81**	0,00	0,00	**0,93**	0,00	0,16	**1,57**	**76,75**	0,04	0,00	**18,42**	0,00	0,04	0,01	0,00	0,00	0,00	100	90,28**	UG2	Cooperite
	0,00	0,04	0,08	0,00	0,00	0,26	**1,18**	0,00	0,00	**0,95**	0,00	0,01	**1,14**	**79,86**	0,01	0,00	**16,30**	0,03	0,05	0,01	0,08	0,00	0,00	100	92,41**	UG2	Cooperite
	0,00	0,06	0,06	0,00	0,04	0,03	2,88	0,00	0,96	0,72	0,18	0,00	1,65	72,68	0,18	3,14	**17,37**	0,01	0,00	0,00	0,00	0,00	0,00	100	92,57**	UG2	
	0,00	0,00	0,00	0,00	0,00	0,01	**1,28**	0,00	0,00	**0,94**	0,00	0,02	**0,81**	**81,31**	0,00	0,00	**14,87**	0,00	0,00	0,00	0,00	0,73	0,00	100	94,66**	UG2	Cooperite
	0,02	0,01	0,00	0,00	0,01	0,03	2,02	0,00	0,00	2,44	0,01	0,00	0,23	78,30	0,00	0,02	**16,88**	0,01	0,00	0,02	0,00	0,00	0,00	100	96,62**	UG2	
	0,00	0,00	0,00	0,00	0,00	0,00	1,60	0,00	0,00	0,68	0,00	0,32	2,69	74,61	0,09	0,00	**19,58**	0,00	0,00	0,00	0,00	0,39	0,02	100	96,65**	UG2	
	0,00	0,00	0,01	0,00	0,01	0,00	1,89	0,06	0,00	1,21	0,01	0,05	0,28	**78,06**	0,00	0,24	**18,11**	0,06	0,00	0,01	0,00	0,00	0,00	100	97,73**	UG2	
	0,01	0,01	0,00	0,00	0,02	0,01	0,87	0,04	0,00	1,37	0,06	0,00	0,00	81,55	0,00	0,00	**16,05**	0,00	0,00	0,00	0,01	0,00	0,00	100	97,87**	UG2	
	0,04	0,01	0,02	0,00	0,03	0,11	0,99	0,06	0,00	1,04	0,06	0,12	4,10	77,03	0,06	0,00	**16,33**	0,00	0,00	0,00	0,00	0,00	0,00	100		UG2	
	0,00	0,01	0,00	0,00	0,04	0,01	3,19	0,00	0,00	1,90	0,04	0,00	0,00	75,74	0,04	0,00	**19,00**	0,03	0,00	0,00	0,00	0,00	0,00	100		UG2	
	0,00	0,00	0,00	0,00	0,00	0,00	0,72	0,00	0,00	0,67	0,00	0,03	1,62	79,67	0,00	0,00	**15,78**	0,01	0,00	0,00	0,00	0,00	0,01	98,51		UG2	
	0,06	0,00	0,04	0,00	0,00	0,03	1,37	0,02	0,00	0,53	0,02	0,20	0,12	80,43	0,02	0,00	**15,78**	0,02	0,00	0,00	0,03	0,00	0,00	98,67		UG2	
	0,00	0,01	0,00	0,00	0,00	0,67	1,14	0,00	0,00	1,00	0,03	0,00	0,00	80,05	0,00	0,03	**15,82**	0,00	0,00	0,01	0,00	0,00	0,00	98,76		MR	
	0,00	0,00	0,00	0,03	0,00	0,03	1,13	0,00	0,00	1,39	0,00	0,08	0,12	80,13	0,02	0,00	**15,83**	0,01	0,00	0,00	0,00	0,00	0,02	98,79		UG2	
	0,00	0,00	0,06	0,00	0,00	0,02	1,31	0,00	0,00	0,38	0,05	0,00	2,22	78,92	0,02	0,01	**16,04**	0,03	0,01	0,00	0,00	0,00	0,00	99,07		MR	
	0,02	0,00	0,02	0,00	0,05	0,03	2,74	0,00	0,00	2,11	0,21	0,07	0,10	75,80	0,08	0,36	**17,51**	0,00	0,00	0,03	0,00	0,00	0,00	99,13		UG2	
	0,03	0,00	0,00	0,00	0,01	0,05	1,45	0,00	0,00	0,91	0,03	0,00	0,41	80,33	0,02	0,00	**15,97**	0,02	0,02	0,02	0,04	0,00	0,00	99,31		MR	
	0,03	0,43	0,02	0,00	0,02	0,50	1,12	0,00	0,00	1,31	0,04	0,02	0,00	79,85	0,00	0,04	**15,97**	0,00	0,00	0,00	0,00	0,00	0,00	99,35		MR	
	0,00	0,00	0,00	0,00	0,00	0,00	0,77	0,00	0,00	0,42	0,00	0,11	11,11	70,39	0,01	0,00	**16,61**	0,00	0,00	0,00	0,00	0,00	0,01	99,43		UG2	
	0,00	0,00	0,00	0,00	0,00	0,65	0,87	0,00	0,00	0,49	0,03	0,00	0,00	81,97	0,00	0,02	**15,70**	0,04	0,00	0,01	0,01	0,00	0,00	99,79		UG2	
	0,01	0,00	0,00	0,00	0,02	0,42	1,86	0,00	0,00	1,41	0,00	0,13	0,15	77,16	0,00	0,00	**18,64**	0,04	0,00	0,00	0,00	0,00	0,00	99,84		UG2	
	0,02	0,00	0,04	0,00	0,00	0,03	0,78	0,00	0,00	0,23	0,00	0,00	2,50	80,08	0,00	0,00	**16,18**	0,02	0,00	0,00	0,00	0,00	0,00	99,88		MR	
	0,02	0,00	0,01	0,00	0,06	0,04	6,51	0,02	0,00	1,68	0,05	0,17	0,00	68,20	0,00	0,13	**22,98**	0,04	0,00	0,00	0,00	0,00	0,00	99,91		UG2	
	0,01	0,00	0,07	0,01	0,04	0,08	**1,11**	0,00	0,00	**1,75**	0,00	0,28	**0,88**	**77,01**	0,11	0,04	**17,23**	0,01	0,05	0,00	0,02	0,00	0,00	98,7		UG2	Cooperite
	0,02	0,00	0,08	0,00	0,00	1,33	**1,62**	0,00	0,00	**0,80**	0,02	0,01	**1,07**	**79,30**	0,01	0,01	**15,91**	0,00	0,00	0,00	0,00	0,00	0,00	100,18		MR	Cooperite
	0,00	0,09	0,01	0,00	0,02	0,24	1,21	0,02	2,93	0,13	5,23	0,00	0,57	0,03	0,86	**51,57**	**37,63**	0,03	0,03	0,00	0,00	0,00	0,00	100,6		UG2	Laurite
	0,00	0,26	0,05	0,00	0,03	0,01	2,75	0,00	4,60	0,33	7,14	0,01	0,55	0,01	0,82	**48,03**	**36,06**	0,00	0,01	0,00	0,00	0,00	0,00	100,66		UG2	Laurite

Appendix D: Mineral Liberation Analyser Results

D.1.1: List of mapped PGM

PGM	MINERAL FORMULA
Cooperite	$(Pt_{2.2}, Pd_{0.1}, Ni_{0.1}, Fe_{0.1})S_{0.5}$
Braggite	$(Pt_{1.9}, Pd, Ni_{0.3})S$
Kharaelakhite	$Pt_{0.5}Cu_{2.5}Pb_{1.5}Fe_{2+0.75}Ni_{0.25}S_8$
Vysotskite	$Pd_{0.75}Pt_{0.05}Ni_{0.25}S$
PtRhCuS (unnamed)	$PtRh_{0.5}CuS_3Fe_{0.2}Co_{0.2}$
Platarsite	$Pt_{0.6}Rh_{0.3}Ru_{0.1}AsS$
Hollingworthite	(Rh, Pt, Pd)AsS
PtSnS	PtSnS
PdSSe	$PdSSe_{0.2}$
PtPdSAs	$PtPd_2SAs$
PtAsRhS	PtAsSRh
PtAsRhS2	$RhPt_{0.25}AsS_2$
PtIrRuOsSAs	$Pt_{0.5}Ir_{0.6}RuOs_{0.2}S_3As_{1.2}$
PtSAgRh	PtSAgRh
Sperrylite	$PtAs_2$
Atheneite	$Pd_{2.25}Hg_{0.75}As$
Palladoarsenide	Pd_2As
PdAsNi	PdNiAs
PtSbAs	PtSbAs
PtPdAsSb	$PtPd_2AsSb$
Moncheite	$Pt_{0.75}Pd_{0.25}Te_{1.5}Bi_{0.5}$
Maslovite	PtBiTe
Merenskyite	$Pd_{0.9}Pt_{0.1}Te_{1.8}Bi_{0.2}$
Kotulskite	$PdTe_{0.75}Bi_{0.25}$
Michenerite	$(Pd_2, Pt_{0.5})BiTe$
PdTeBi	PdBiTe
PtBiTe	$Pt_{0.6}BiTe_{0.3}$
Temagamite	Pd_3HgTe_3
Pasavaite	PdTePb
Keithconnite	$Pd_{2.8}Te$
Stibiopalladinite	Pd_5Sb_2
Mertieite	$Pd_8Sb_{2.9}As_{0.5}$
Geversite	$PtSb_{1.84}$
PdPtSb	$Pd_2Pt_{0.4}Sb$
Isoferroplatinum	$Pt_3FeCu_{0.1}$
Rustenburgite	$(Pt_2, Pd_{0.6})_3Sn_{1.3}$
Sobolevskite	PdBi

PGM (continued)	Mineral Formula
Plumbopalladinite	Pd_3Pb_2
Potarite	PdHg
Native Au	$AuAg_{0.2}$
Native Pt	Pt
Native Pd	Pd
Zvyagintsevite	Pd_3Pb
Polarite	$PdBi_{0.75}Pb_{0.25}$
Froodite	$PdBi_2$
Atokite	$Pd_{2.25}Pt_{0.75}Sn$
Ferronickelplatinum	Pt_2NiFe
Insizwaite	$PtBi_2$
Skaergaardite	$Pd_{0.96}Au_{0.02}Pt_{0.01}Cu_{0.82}Fe_{0+0.12}Zn_{0.03}Sn_{0.01}Te_{0.004}Pb_{0.003}$
PtPdSn	$Pt_{0.1}Pd_2Sn_{0.5}$
PtPd	PtPd
PdPbAu	Pd_3PbAu
PdPtBi	$Pt_{0.5}PdBi$
Laurite	RuS_2
Erlichmanite	$Os_{0.5}Ru_{0.5}S_2$
Irarsite	$Ir_{0.4}Ru_{0.3}Rh_{0.2}Pt_{0.1}AsS$
RuOs	RuOs

D.1.2: Geochemical Data

SAMPLE_ID	Al	C	Ca	Cl	Co	Cr	Cu	F	Fe	H	K	Mg	Mn	Na	Ni	O	P	Pb	S	Sb	Si	Sn	Ti	V	Zn	Zr	Unknown	Total
UG2 NORMAL REEF																												
B3D2_S1	9,053	0,038	1,919	0,002	0,017	20,863	0,007	0,009	17,437	0,035	0,046	6,779	0,110	0,097	0,098	35,471	0,000	0,000	0,023	0,000	7,268	0,000	0,460	0,102	0,056	0,000	0,111	**100,00**
B3D2_S2	8,912	0,056	1,851	0,003	0,016	20,223	0,006	0,017	17,079	0,049	0,098	7,080	0,109	0,095	0,088	35,858	0,000	0,000	0,016	0,000	7,743	0,000	0,441	0,099	0,054	0,000	0,105	**100,00**
B3D2_S4	10,016	0,013	1,302	0,000	0,022	26,741	0,006	0,010	21,044	0,017	0,036	4,883	0,104	0,060	0,119	32,230	0,000	0,000	0,016	0,000	2,574	0,000	0,535	0,131	0,072	0,000	0,070	**100,00**
B3D2_S5	9,609	0,009	0,803	0,000	0,022	27,087	0,007	0,007	21,235	0,017	0,030	5,417	0,109	0,041	0,119	32,076	0,001	0,000	0,018	0,000	2,392	0,000	0,731	0,133	0,073	0,000	0,062	**100,00**
B3D2_S6	10,723	0,007	2,478	0,000	0,018	22,641	0,010	0,017	17,945	0,021	0,092	4,899	0,094	0,157	0,104	34,622	0,001	0,000	0,022	0,000	5,548	0,000	0,404	0,111	0,061	0,000	0,025	**100,00**
B3D2_S9	10,124	0,004	2,963	0,000	0,015	18,426	0,006	0,015	15,381	0,021	0,071	6,198	0,101	0,192	0,083	36,944	0,000	0,000	0,014	0,000	8,974	0,000	0,299	0,090	0,049	0,000	0,030	**100,00**
B3D2_S10	8,934	0,008	1,954	0,000	0,016	19,451	0,002	0,006	16,520	0,024	0,023	7,393	0,116	0,125	0,083	36,326	0,000	0,000	0,007	0,000	8,548	0,000	0,299	0,095	0,052	0,000	0,019	**100,00**
B3D2_S12	9,855	0,008	1,052	0,001	0,022	27,303	0,006	0,006	21,465	0,019	0,016	4,927	0,105	0,049	0,124	31,897	0,001	0,002	0,020	0,000	2,128	0,000	0,715	0,134	0,074	0,000	0,072	**100,00**
B7D0_S1	9,168	0,029	1,993	0,001	0,018	22,203	0,007	0,003	18,634	0,034	0,015	6,097	0,103	0,076	0,102	34,603	0,000	0,000	0,019	0,000	6,194	0,000	0,482	0,109	0,060	0,000	0,051	**100,00**
B7D0_S4	8,829	0,011	0,384	0,001	0,021	26,008	0,007	0,041	20,890	0,020	0,315	6,492	0,116	0,016	0,125	32,504	0,003	0,000	0,037	0,000	3,370	0,000	0,570	0,127	0,070	0,000	0,044	**100,00**
B7D0_S5	10,206	0,008	2,328	0,002	0,018	22,242	0,008	0,028	18,076	0,024	0,195	5,299	0,096	0,130	0,105	34,676	0,012	0,000	0,027	0,000	5,906	0,000	0,411	0,109	0,060	0,000	0,033	**100,00**
B7D0_S7	9,530	0,004	0,857	0,001	0,022	26,749	0,010	0,015	21,184	0,014	0,105	5,462	0,108	0,043	0,123	32,187	0,004	0,000	0,029	0,000	2,710	0,000	0,599	0,131	0,072	0,000	0,041	**100,00**
B7D0_S9	9,528	0,002	0,282	0,000	0,024	29,112	0,004	0,009	22,625	0,007	0,062	5,264	0,112	0,013	0,132	30,958	0,002	0,000	0,020	0,000	0,995	0,000	0,589	0,143	0,078	0,000	0,039	**100,00**
B7D0_S11	7,981	0,004	0,887	0,000	0,018	21,986	0,004	0,004	18,670	0,017	0,024	7,819	0,125	0,039	0,104	34,732	0,000	0,000	0,024	0,000	6,782	0,000	0,574	0,107	0,059	0,001	0,040	**100,00**
UG2 SPLIT REEF																												
B3D1_S1	9,053	0,038	1,919	0,002	0,017	20,863	0,007	0,009	17,437	0,035	0,046	6,779	0,110	0,097	0,098	35,471	0,000	0,000	0,023	0,000	7,268	0,000	0,460	0,102	0,056	0,000	0,111	**100,00**
B3D1_S2	10,069	0,085	1,811	0,002	0,020	24,120	0,007	0,015	19,309	0,043	0,072	5,287	0,105	0,093	0,112	33,686	0,001	0,000	0,023	0,000	4,204	0,000	0,590	0,118	0,065	0,000	0,167	**100,00**
B3D1_S3	9,704	0,048	2,066	0,001	0,017	21,085	0,010	0,033	17,164	0,050	0,196	6,187	0,103	0,110	0,097	35,423	0,001	0,000	0,022	0,000	6,856	0,000	0,538	0,103	0,057	0,000	0,131	**100,00**
B3D1_S4	10,016	0,013	1,302	0,000	0,022	26,741	0,006	0,010	21,044	0,017	0,036	4,883	0,104	0,060	0,119	32,230	0,000	0,000	0,016	0,000	2,574	0,000	0,535	0,131	0,072	0,000	0,070	**100,00**
B3D1_S6	10,250	0,011	2,004	0,001	0,018	22,692	0,008	0,078	18,098	0,033	0,278	5,571	0,098	0,125	0,098	34,458	0,001	0,000	0,015	0,000	5,551	0,000	0,372	0,111	0,061	0,002	0,064	**100,00**
B3D1_S7	9,509	0,008	2,805	0,000	0,014	17,304	0,012	0,014	14,847	0,022	0,062	7,046	0,109	0,177	0,084	37,501	0,000	0,000	0,027	0,000	9,947	0,000	0,326	0,084	0,046	0,000	0,054	**100,00**
B3D1_S8	10,270	0,010	2,768	0,000	0,016	20,103	0,014	0,012	16,439	0,021	0,047	5,734	0,100	0,171	0,093	35,986	0,000	0,000	0,028	0,000	7,577	0,000	0,399	0,098	0,054	0,000	0,061	**100,00**
B3D1_S9	12,405	0,012	4,616	0,001	0,015	18,657	0,016	0,018	14,736	0,027	0,058	3,485	0,074	0,289	0,082	36,931	0,000	0,000	0,021	0,000	8,084	0,000	0,273	0,091	0,050	0,000	0,058	**100,00**
B3D1_S10	9,509	0,003	0,277	0,000	0,024	29,276	0,004	0,011	22,726	0,010	0,029	5,160	0,112	0,008	0,140	30,794	0,001	0,000	0,025	0,000	0,733	0,000	0,825	0,143	0,079	0,000	0,110	**100,00**
B3D1_S11	10,607	0,034	5,126	0,001	0,012	14,683	0,007	0,007	12,705	0,024	0,034	5,432	0,082	0,267	0,062	38,824	0,000	0,000	0,010	0,000	11,502	0,000	0,402	0,072	0,039	0,000	0,067	**100,00**

D.1.2 (continued): Geochemical Data

Sample Id	Al	C	Ca	Cl	Co	Cr	Cu	F	Fe	H	K	Mg	Mn	Na	Ni	O	P	Pb	S	Sb	Si	Sn	Ti	V	Zn	Zr	Unknown	
UG2 MULTIPLE SPLIT REEF																												
B6D1_S1	9,102	0,082	0,415	0,000	0,023	28,275	0,007	0,000	22,033	0,020	0,001	5,930	0,116	0,000	0,132	31,405	0,000	0,000	0,023	0,000	1,649	0,000	0,427	0,138	0,076	0,002	0,144	**100,00**
B6D1_S2	8,839	0,001	0,957	0,000	0,022	27,026	0,020	0,000	21,244	0,030	0,001	6,030	0,106	0,006	0,123	32,064	0,000	0,000	0,029	0,000	2,877	0,000	0,385	0,132	0,073	0,000	0,033	**100,00**
B6D1_S3	9,503	0,003	1,161	0,001	0,021	26,263	0,023	0,004	21,248	0,047	0,015	5,424	0,102	0,033	0,123	32,366	0,000	0,000	0,034	0,001	2,967	0,000	0,431	0,129	0,071	0,000	0,031	**100,00**
B6D1_S4	8,647	0,004	2,197	0,003	0,016	19,948	0,082	0,007	17,161	0,056	0,050	6,950	0,099	0,089	0,193	35,603	0,000	0,000	0,361	0,000	8,049	0,000	0,300	0,097	0,054	0,000	0,033	**100,00**
B6D1_S5	8,977	0,006	2,396	0,005	0,014	17,756	0,013	0,008	15,451	0,052	0,043	7,448	0,106	0,134	0,085	37,272	0,000	0,000	0,027	0,000	9,752	0,000	0,293	0,087	0,048	0,000	0,028	**100,00**
B6D1_S6	10,341	0,007	2,091	0,001	0,019	23,141	0,036	0,020	18,687	0,041	0,073	5,129	0,093	0,122	0,148	34,098	0,000	0,000	0,239	0,000	5,113	0,000	0,373	0,113	0,062	0,000	0,054	**100,00**
B6D1_S8	10,248	0,003	2,572	0,000	0,017	20,927	0,014	0,007	17,205	0,047	0,032	5,551	0,093	0,145	0,099	35,528	0,000	0,000	0,024	0,000	6,944	0,000	0,358	0,102	0,056	0,000	0,026	**100,00**
B6D1_S10	9,771	0,001	1,401	0,000	0,019	23,285	0,002	0,004	19,465	0,133	0,023	5,968	0,089	0,164	0,111	34,024	0,000	0,003	0,011	0,000	4,744	0,002	0,530	0,114	0,063	0,000	0,075	**100,00**
B6D1_S11	7,660	0,004	1,931	0,004	0,014	17,588	0,012	0,025	16,040	0,130	0,102	8,747	0,100	0,037	0,081	37,123	0,001	0,000	0,022	0,000	9,881	0,000	0,334	0,086	0,047	0,003	0,029	**100,00**
B6D1_S12	7,749	0,002	1,256	0,011	0,016	19,352	0,022	0,006	17,463	0,129	0,039	8,483	0,108	0,018	0,116	36,160	0,001	0,000	0,061	0,000	8,496	0,000	0,332	0,094	0,052	0,000	0,035	**100,00**
MERENSKY REEF																												
B6D0_S1	2,881	0,001	3,284	0,003	0,000	0,229	0,184	0,002	8,616	0,245	0,007	14,990	0,129	0,103	0,367	44,669	0,000	0,000	1,006	0,000	23,107	0,000	0,071	0,000	0,000	0,000	0,108	**100,00**
B6D0_S2	2,262	0,001	0,839	0,002	0,003	3,963	0,179	0,019	9,737	0,106	0,052	16,113	0,155	0,024	0,164	43,160	0,000	0,000	1,346	0,000	21,498	0,000	0,248	0,018	0,011	0,000	0,099	**100,00**
B6D0_S3	1,465	0,000	1,727	0,002	0,000	0,328	0,295	0,052	9,630	0,147	0,132	16,140	0,149	0,053	0,237	43,514	0,000	0,000	2,219	0,000	23,475	0,000	0,038	0,000	0,000	0,090	0,306	**100,00**
B6D0_S5	1,315	0,001	2,106	0,002	0,000	0,497	0,168	0,035	9,016	0,080	0,086	16,418	0,164	0,025	0,076	44,313	0,012	0,000	1,384	0,001	24,190	0,000	0,025	0,001	0,002	0,000	0,081	**100,00**
B6D0_S7	1,626	0,001	2,123	0,001	0,000	0,527	0,162	0,032	9,233	0,142	0,099	16,272	0,145	0,020	0,249	43,688	0,000	0,000	2,040	0,000	23,439	0,000	0,053	0,001	0,001	0,006	0,141	**100,00**
B6D0_S9	2,208	0,002	1,947	0,003	0,000	0,176	0,304	0,008	17,049	0,220	0,019	10,717	0,075	0,029	3,449	32,859	0,000	0,000	13,461	0,000	17,275	0,000	0,047	0,000	0,000	0,000	0,153	**100,00**

D.1.3: Modal Mineralogy

Minerals	B3D2_NORMAL REEF	B7D0_NORMAL REEF	B3D1_SPLIT REEF	B6D1_MULTIPLE SPLIT REEF	B6D0_MERENSKY REEF
Quartz	0,03	0,01	0,04	0,03	0,95
Plagioclase	11,38	5,83	15,77	6,99	0,65
Orthopyroxene	8,07	7,05	6,83	6,82	55,17
Clinopyroxene	0,11	0,20	0,53	0,99	2,62
Amphibole	2,22	3,32	1,78	4,58	15,55
Mica	0,55	1,32	0,91	0,39	0,70
Chlorite	0,72	0,19	0,76	2,95	6,56
Pumpellyite	0,74	0,25	1,22	0,93	0,09
Talc	0,88	0,50	0,78	2,70	6,65
Other silicates	0,23	0,10	0,36	0,20	0,17
Pyrite	0,00	0,00	0,00	0,06	3,57
Pyrrhotite	0,00	0,01	0,00	0,00	1,91
Chalcopyrite	0,02	0,02	0,03	0,06	0,62
Pentlandite	0,03	0,05	0,03	0,07	2,20
Other sulphides	0,00	0,00	0,00	0,01	0,01
Chromite	74,52	80,66	70,32	72,95	2,34
Other oxides	0,29	0,35	0,31	0,10	0,08
Carbonates	0,15	0,08	0,22	0,10	0,01
Other	0,06	0,06	0,09	0,05	0,16
Total	**100,00**	**100,00**	**100,00**	**100,00**	**100,00**

% contributions

D.1.4: PGM Associations

SAMPLE_ID	Quartz	Plagioclase	Orthopyroxene	Clinopyroxene	Amphibole	Mica	Chlorite	Pumpellyite	Talc	Other silicates	Pyrite	Pyrrhotite	Chalcopyrite	Pentlandite	Other sulphides	Chromite	Other oxides	Carbonates	Other	Total
UG2 NORMAL REEF																				
B3D2_S1	0,00	1,20	3,94	0,00	3,94	1,80	3,85	5,39	6,16	1,11	0,00	6,93	4,79	37,93	0,51	17,81	1,28	2,57	0,00	100,00
B3D2_S2	0,00	3,24	3,47	0,00	6,49	2,57	4,03	7,16	4,47	1,57	0,00	0,00	10,07	37,92	0,67	12,86	1,01	3,80	0,45	100,00
B3D2_S4	1,33	0,72	4,82	0,20	7,58	0,00	2,15	5,43	3,28	0,92	0,00	0,00	3,79	31,56	0,00	26,64	5,53	2,36	0,00	100,00
B3D2_S5	3,56	2,04	1,16	0,27	11,24	1,11	5,64	10,89	0,13	1,20	0,27	0,00	4,53	32,04	0,44	20,18	3,07	0,58	0,27	100,00
B3D2_S6	0,00	2,31	0,75	0,20	23,66	1,90	2,04	12,03	2,31	1,02	0,00	0,00	1,77	28,69	0,00	19,31	2,24	0,20	0,07	100,00
B3D2_S9	6,05	1,68	2,76	0,61	14,26	1,68	3,70	31,14	1,68	1,41	0,00	0,00	1,48	22,26	0,40	7,80	0,94	0,40	0,27	100,00
B3D2_S10	0,74	3,08	2,76	2,28	27,51	2,66	2,34	12,48	0,64	1,75	0,27	0,00	0,42	15,40	2,34	21,19	1,17	0,32	0,37	100,00
B3D2_S12	0,06	1,38	0,54	0,52	21,91	1,32	2,59	11,58	0,04	3,63	0,06	0,00	2,51	28,67	0,62	18,46	4,33	0,04	0,24	100,00
UG2 NORMAL REEF																				
B7D0_S1	0,00	1,11	0,63	0,08	9,98	1,27	0,48	0,32	1,11	0,87	0,32	0,63	17,91	37,16	0,32	24,64	1,03	1,19	0,00	100,00
B7D0_S4	0,00	0,28	0,09	0,09	1,66	6,53	0,47	0,00	0,00	1,23	0,99	4,50	16,90	32,53	1,42	27,41	1,75	0,57	0,14	100,00
B7D0_S5	0,00	4,05	0,78	0,16	6,70	2,57	0,55	3,04	1,95	0,31	1,09	1,56	13,09	40,76	1,79	18,55	1,72	0,00	0,00	100,00
B7D0_S7	0,00	0,90	0,68	0,45	3,95	1,52	0,56	0,56	0,85	0,62	0,73	3,95	8,25	38,81	4,97	22,66	6,21	1,52	0,68	100,00
B7D0_S9	0,00	0,55	0,11	0,06	1,99	2,82	0,72	0,00	0,00	0,11	0,44	5,76	9,91	36,21	2,55	31,06	4,98	0,00	0,78	100,00
B7D0_S11	0,04	1,05	1,23	0,43	9,63	0,70	1,01	0,72	3,57	1,15	0,08	2,77	12,76	32,73	1,74	22,12	6,24	1,25	0,04	100,00
UG2 SPLIT REEF																				
B3D1_S1	0,00	0,95	0,64	1,43	4,76	0,95	5,56	6,35	2,22	0,32	0,00	0,00	5,24	45,87	0,64	18,73	1,75	3,81	0,00	100,00
B3D1_S2	0,00	0,43	1,40	0,00	3,34	0,65	16,18	5,50	0,00	0,22	0,43	0,00	11,87	35,38	0,97	16,83	0,86	2,70	0,43	100,00
B3D1_S3	0,28	2,04	1,33	0,00	3,37	1,33	7,30	6,60	12,78	0,98	0,35	0,00	4,78	31,18	1,90	18,47	0,56	2,11	0,00	100,00
B3D1_S4	0,00	1,75	1,40	1,01	12,98	0,66	1,71	12,68	0,00	1,01	0,00	0,13	4,43	37,63	5,00	15,26	2,72	0,66	0,26	100,00
B3D1_S6	0,19	4,45	0,19	0,00	9,56	8,24	6,63	14,87	2,27	3,50	0,00	0,00	4,26	21,78	1,23	19,60	1,52	0,09	0,00	100,00
B3D1_S7	0,61	2,36	1,40	0,20	16,70	1,49	2,04	23,08	3,21	1,37	0,00	0,00	1,25	27,57	0,38	13,44	2,62	0,76	0,06	100,00
B3D1_S8	0,00	4,91	2,05	0,59	10,34	0,81	4,11	28,52	0,00	0,88	0,00	0,00	0,44	20,38	0,00	20,45	3,81	0,29	0,44	100,00
B3D1_S9	0,00	4,65	0,00	0,87	11,72	0,93	0,99	38,58	0,00	4,34	0,00	0,00	0,81	15,07	1,61	16,31	1,37	0,74	0,00	100,00
B3D1_S10	0,35	1,40	0,54	0,11	4,14	0,48	2,28	10,61	1,40	1,37	0,05	0,00	5,42	40,98	1,75	19,63	4,75	0,11	0,00	100,00
B3D1_S11	0,00	0,54	0,68	1,56	35,30	0,20	8,06	3,18	0,00	1,42	0,00	0,00	1,29	31,71	0,00	11,04	1,63	2,85	0,00	100,00

D.1.4 (continued): PGM Associations

SAMPLE_ID	Quartz	Plagioclase	Orthopyroxene	Clinopyroxene	Amphibole	Mica	Chlorite	Pumpellyite	Talc	Other silicates	Pyrite	Pyrrhotite	Chalcopyrite	Pentlandite	Other sulphides	Chromite	Other oxides	Carbonates	Other	Total
UG2 MULTIPLE SPLIT REEF																				
B6D1_S1	0,00	0,00	1,59	3,23	3,85	0,28	8,55	0,00	0,40	0,34	0,00	0,00	4,41	28,52	0,51	34,75	0,45	9,00	0,23	100,00
B6D1_S2	0,00	0,00	1,53	0,23	15,41	0,10	13,08	0,20	2,10	1,30	0,00	0,00	12,14	6,80	14,34	29,99	0,40	0,63	0,00	100,00
B6D1_S3	0,19	0,10	0,86	0,38	29,48	2,54	9,60	0,10	0,00	0,91	0,00	0,00	6,48	10,85	8,45	24,63	2,26	0,10	0,00	100,00
B6D1_S4	1,15	0,11	4,72	0,00	22,71	2,14	6,58	1,10	8,39	0,22	0,82	2,25	11,46	14,92	2,19	19,31	0,66	0,11	0,00	100,00
B6D1_S5	0,00	0,45	2,58	0,00	16,61	1,46	16,16	1,23	3,37	0,79	0,00	0,00	11,67	19,75	2,02	20,31	0,56	1,80	0,00	100,00
B6D1_S6	0,90	0,00	25,67	3,02	14,76	0,51	1,54	1,22	4,88	0,90	3,53	16,24	1,09	22,79	1,54	0,00	0,00	1,41	0,00	100,00
B6D1_S8	1,28	2,71	1,35	0,00	12,90	3,28	25,16	8,48	4,56	2,42	0,00	0,00	7,13	4,42	6,63	15,97	1,85	0,64	0,00	100,00
B6D1_S10	0,00	1,23	0,25	0,33	17,36	0,33	41,61	0,25	0,00	4,50	0,00	0,00	0,00	2,13	5,00	24,08	1,56	0,00	0,25	100,00
B6D1_S11	0,00	0,64	3,21	0,12	18,95	2,34	17,24	1,01	5,32	1,21	0,17	0,26	12,41	8,13	1,07	24,59	0,78	1,65	0,00	100,00
B6D1_S12	0,00	0,28	8,63	0,06	12,29	2,16	11,15	0,51	5,73	1,76	0,23	0,17	11,64	13,79	1,45	26,09	1,96	1,33	0,17	100,00
MERENSKY REEF																				
B6D0_S1	0,77	0,26	15,22	1,28	60,10	0,26	4,73	2,43	7,67	1,53	0,00	0,00	0,51	3,71	0,26	0,26	0,00	1,02	0,00	100,00
B6D0_S2	0,00	0,07	13,02	0,00	11,61	2,00	4,85	0,46	7,67	2,13	0,61	21,10	18,28	6,54	3,38	6,64	0,27	1,14	0,06	100,00
B6D0_S3	0,00	0,00	14,70	0,00	32,77	0,48	2,41	0,00	7,71	0,00	1,20	13,01	8,67	17,35	0,72	0,00	0,00	0,96	0,00	100,00
B6D0_S5	0,00	0,00	11,65	0,45	21,95	0,00	2,46	0,00	15,45	1,68	0,34	18,03	6,72	5,37	1,12	12,54	0,45	0,67	1,12	100,00
B6D0_S7	0,11	0,00	25,21	0,00	8,61	1,47	7,76	0,00	24,76	2,78	0,00	13,82	7,08	5,95	1,53	0,00	0,45	0,34	0,00	100,00
B6D0_S9	1,33	1,00	8,83	0,19	13,64	1,54	8,58	4,90	6,13	1,82	14,51	5,10	5,68	24,91	0,24	0,01	0,00	1,48	0,07	100,00

D.1.5: PGM Grains Size Distributions

Sieve Size	B3D2_NORMAL REEF	B7D0_NORMAL REEF	B3D1_SPLIT REEF	B6D1_MULTIPLE SPLIT REEF	B6D0_MERENSKY REEF
0,87	0,01	0,00	0,07	0,04	0,00
1	0,07	0,19	0,00	0,11	0,13
1,2	0,08	0,00	0,36	0,31	0,00
1,45	0,68	0,90	0,76	0,93	1,29
1,75	1,10	0,00	4,18	2,73	0,00
2	6,36	10,31	2,80	8,06	11,94
2,4	3,89	4,90	5,10	4,90	4,73
2,9	6,13	7,31	4,89	7,28	6,17
3,4	8,28	9,25	7,13	9,49	9,97
4,1	8,97	7,19	7,26	10,44	8,30
4,8	10,34	10,10	10,23	10,32	10,34
5,7	10,52	10,91	9,77	10,59	10,15
6,8	11,59	11,22	8,79	7,23	5,73
8,1	8,86	9,47	4,62	7,37	9,66
9,6	5,22	7,42	7,24	4,67	4,13
11,4	3,07	7,24	4,38	4,54	1,74
13,5	4,40	2,06	5,74	2,76	1,39
16	6,36	1,58	5,28	1,54	4,77
19	4,09	0,00	2,65	0,00	0,83
22	0,00	0,00	3,94	6,72	2,50
27	0,00	0,00	0,00	0,00	1,55
32	0,00	0,00	0,00	0,00	2,02
38	0,00	0,00	0,00	0,00	0,00
45	0,00	0,00	0,00	0,00	0,00
53	0,00	0,00	4,84	0,00	2,69
63	0,00	0,00	0,00	0,00	0,00

Average grain size distributions of boreholes (by Reef type)

D.1.6: BSE Images of Some Samples

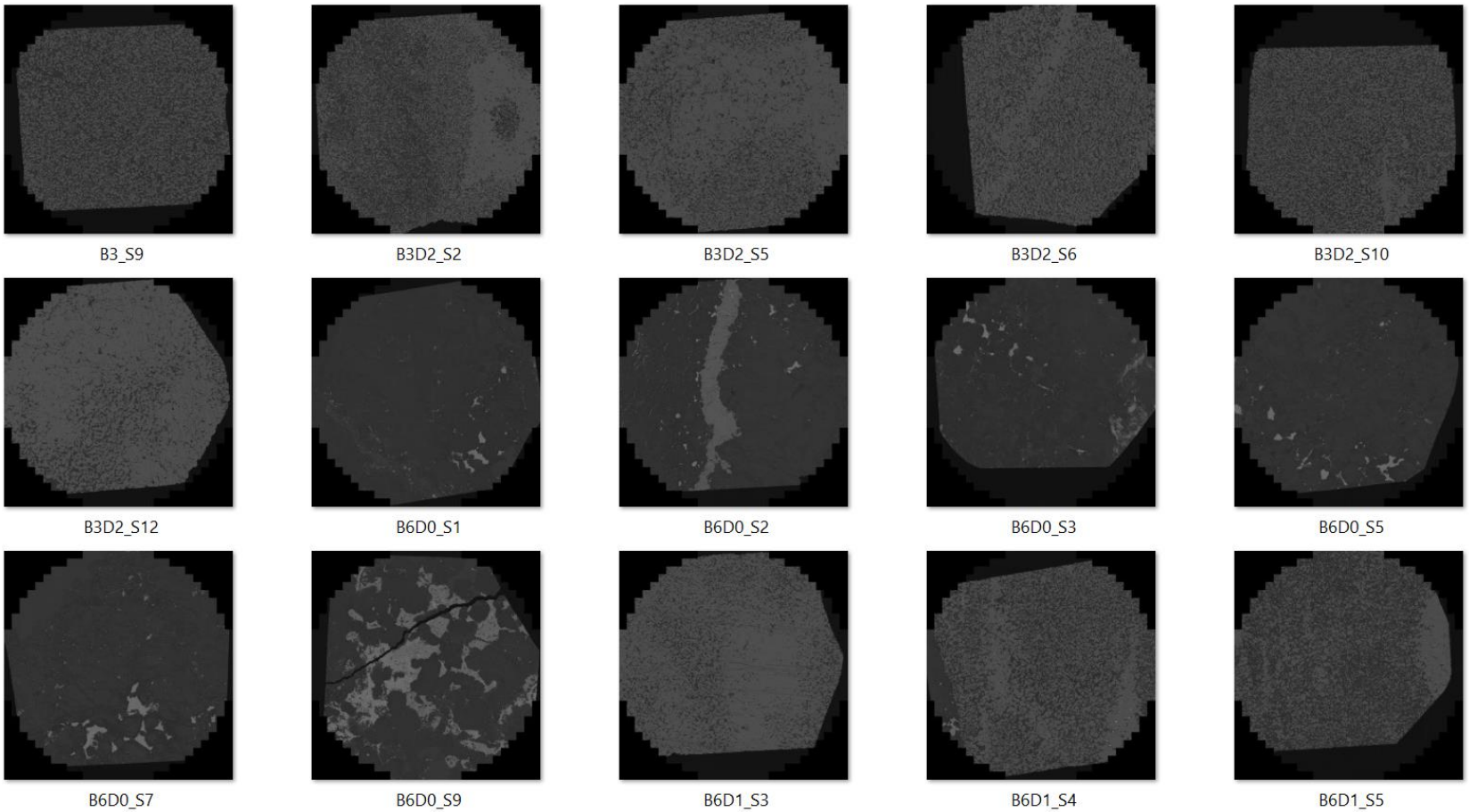

D.1.6 (continued): BSE Images of Some Samples

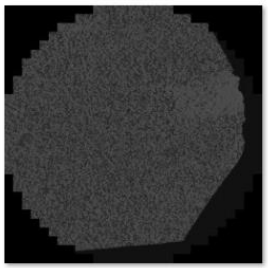
B6D1_S8

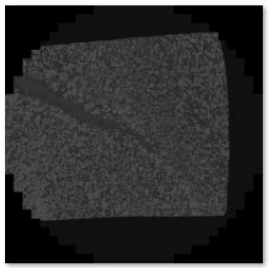
B6D1_S11

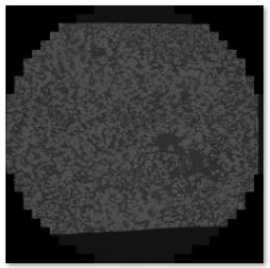
B6D1_S12

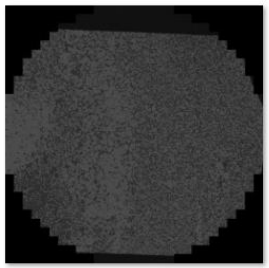
B7D0_S1

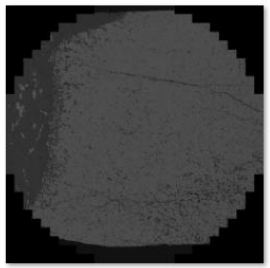
B7D0_S4

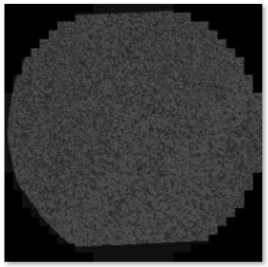
B7D0_S5

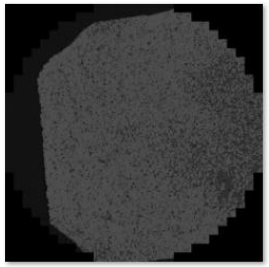
B7D0_S7

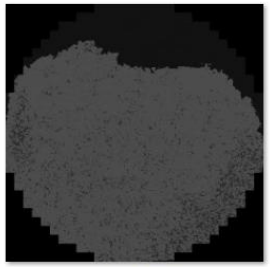
B7D0_S9

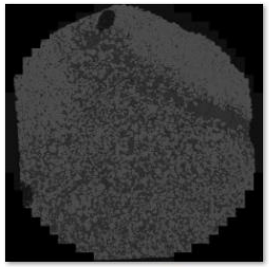
B7D0_S11

Appendix E: Conference presentation from this study

E.1.1: Conference Abstract

ABSTRACTS

Charles Pheeha and Dr NQ Hammond

Mineralogical characterisation of platinum-group elements in the UG-2 chromitites at Buffelshoek farm, Eastern Bushveld Complex

IThe Buffelshoek farm located in the Eastern Bushveld Complex is a new acquisition of the Two Rivers Platinum Mine (TRP) which targets Platinum-Group Elements (PGE) in the Upper Group 2 (UG-2) chromitite. The PGE mineralogical distribution in the UG-2 chromitite varies considerably along the strike including at the TRP and these variations are still not well understood. At the TRP the UG-2 chromitite is disrupted and can be classified as Normal-, Split- and Multiple Split-Reefs differentiated with; undisrupted chromitite, one pyroxenite lens within the chromitite and multiple pyroxenite lenses within the chromitite, respectively. The study is conducted with the aim of using Mineral Liberation Analyser (MLA) to investigate detailed PGE mineralogical characteristics such as PGM phases, abundance, association and grain sizes useful for mineral processing, across the various UG-2 chromitites and systematically within the stratigraphy.

E.1.1 (continued): Conference Abstract